ABSTRACT

Structural Brain Tissue Abnormalities in Patients with Mild Cognitive Impairment as Assessed by Diffusion Tensor Imaging

Savannah Gosnell

Director: Lea Steele, Ph.D.

The goal of this study was to provide new insights concerning neuroimaging measures that identify early indicators of amnestic mild cognitive impairment (a-MCI). Diffusion tensor imaging (DTI) scans from a previous study of adults age 58-78 were used to compare measures in the cingulum and 11 cortical structures in a-MCI cases (n=13) and age-matched controls (n=15). Fractional anisotropy (FA) and related measures of diffusivity were compared between a-MCI cases and controls using analyses of variance; correlations between DTI measures and measures of verbal memory were evaluated as well. Results showed FA was significantly reduced in the right hemisphere of the cingulum and significantly increased in the sagittal stratum (SS) for a-MCI cases compared to controls. Increased FA for the SS and reduced FA for the anterior segment of the corona radiata were significantly correlated with poorer performance on tests of verbal memory for a-MCI cases. A number of study results were compromised by bias in the application of analysis methods. Overall, however, findings indicate that greater degeneration was not consistently detectable in a-MCI cases as compared to controls.

APPROVED BY DIRECTOR OF HONORS THESIS:

_____

Dr. Lea Steele, Institute of Biomedical Studies

APPROVED BY THE HONORS PROGRAM

_____

Dr. Andrew Wisely, Director of the Honors Program

DATE: _____

STRUCTURAL BRAIN TISSUE ABNORMALITIES IN PATIENTS WITH MILD COGNITIVE IMPAIRMENT AS ASSESSED BY DIFFUSION TENSOR IMAGING

A Thesis Submitted to the Faculty of

Baylor University

In Partial Fulfillment of the Requirements for the

Honors Program

By

Savannah Gosnell

Waco, Texas

May 2014

TABLE OF CONTENTS

LIST OF FIGURES	iii
LIST OF TABLES	iv
CHAPTER ONE: Background, Literature Review and Hypotheses	1
CHAPTER TWO: Methods	26
CHAPTER THREE: Results	59
CHAPTER FOUR: Discussion and Conclusions	77
Appendix	85
References	115

LIST OF FIGURES

Figure 1. Anterior Cingulum: B0 map image 34

Figure 2. Anterior Cingulum: Color map image 35

Figure 3. Anterior Cingulum: Eigenvector1 Map 36

Figure 4. Posterior Cingulum: B0 map image 38

Figure 5. Posterior Cingulum: Color map image 40

Figure 6. Genu of the Corpus Callosum 41

Figure 7. Splenium of the Corpus Callosum 42

Figure 8. Body of the Corpus Callosum 44

Figure 9. Anterior Segment of the Corona Radiata 45

Figure 10: Corticospinal Tract 47

Figure 11. Superior Longitudinal Fasciculus 48

Figure 12. Posterior Segment of the Corona Radiata 49

Figure 13. Forceps Minor 51

Figure 14. External Capsule 52

Figure 15. Forceps Major 53

Figure 16. Sagittal Stratum 54

Figure 17. Average CVLT-II Score for Trials 58

LIST OF TABLES

Table 1. The National Institute on Aging-Alzheimer's Association Criteria for Clinical Diagnosis of Mild Cognitive Impairment 12

Table 2. Cortical Structures Chosen for Analysis 18

Table 3. Previously-Reported Changes in White Matter Integrity in Cortical Structures in Patients with Mild Cognitive Impairment. 23

Table 4. Possible Physiological Significance of Changes in White Matter Integrity Studies 32

Table 5. Participant Demographics and Verbal Memory Data 57

Table 6. Anterior versus Posterior Segments of the Cingulum: Differences in White Matter Integrity 60

Table 7. Interactions between Groups and Hemispheres: Differences in White Matter Integrity in the Cingulum 61

Table 8. Interactions between Positions and Hemispheres: Differences in White Matter Integrity in the Cingulum 62

Table 9. Controls versus Amnestic Mild Cognitive Impairment: Differences in White Matter Integrity in Cortico-cortico Tracts 64

Table 10. Interactions between Groups and Hemispheres: Differences in White Matter Integrity in Anterior Segment of the Corona Radiata 65

Table 11. Bivariate Correlations in the Cingulum with California Verbal Learning Test-Second Edition Scores in Controls 67

Table 12. Bivariate Correlations in Cortico-cortico Tracts with California Verbal Learning Test-Second Edition Scores 70

CHAPTER ONE

Background, Literature Review and Hypotheses

Introductory and Background Material

Dementia encompasses a wide range of debilitating cognitive disorders that plague the aging members of our society, the most common of which is Alzheimer's disease. Once the disease has progressed to its final stage, a person experiences cognitive disabilities so severe that they prevent the person from living a normal life; necessitating dependence on others for daily care and ultimately leading to death (McKhann et al., 2011). Alzheimer's disease is currently the sixth leading cause of death in America. But as the number of senior citizens in America increases, researchers anticipate the number of people affected by Alzheimer's disease will also rise (Miniño, Xu, & Kochanek, 2010). Therefore, Alzheimer's disease is becoming a growing financial and logistical concern for health care providers and care takers of patients with Alzheimer's disease (Bynum, 2009; Silverstein & Maslow, 2006). Currently, there is no cure for Alzheimer's disease and its pathophysiology remains unclear. Unfortunately, the treatments available at best slow disease progression in a subset of those affected (Parsons, Stoffler, & Danysz, 2007). There are no treatments that halt the disease process and no therapies that repair damaged tissue or undo pathology. For these reasons, it is essential to patient care that better treatments and methods for early diagnosis are developed. Currently, researchers are trying to identify pathologic hallmarks of diseases that precede diagnosis of probable Alzheimer's disease. Amnestic MCI (a-MCI) occurs before probable Alzheimer's disease can be diagnosed and before symptoms are severe enough to

interfere with the patient's daily life (Albert et al., 2011). Discovering a pathologic signature in patients with a-MCI through the use of neuroimaging techniques that can distinguish those with a-MCI from healthy individuals would be a vital step toward understanding the progression and functional correlates of the disease.

Defining Dementia and Cognitive Impairment

The symptoms of dementia can be generally defined by the *Diagnostic and Statistical Manual of Mental Disorders, Fourth Edition (DSM-IV)* as impairment of memory and of one or more specified aspects of cognitive functioning. Cognitive functioning is determined to be impaired if the patient exhibits defects in one or more of the following mental abilities: language comprehension (spoken or written) and intelligible speech, recognition of objects, motor functioning (assuming patient is physically capable of performing motor functioning tasks)and executive functioning, such as making reasonable judgments and planning tasks. In order to meet the full *DSM-IV* criteria for dementia, these deficits must adversely impact the daily life of the patient and be caused by permanent neurological damage, as opposed to another mental disorder, hormone or vitamin deficiency, and/or harmful drugs (American Psychiatric Association, 2000). Scientists have defined several different types of dementia, including vascular dementia, mixed dementia, dementia with Lewey bodies, frontotemporal lobar degeneration, Creutzfeldt-Jakob disease, normal pressure hydrocephalous and last but not least, Alzheimer's disease.

Prevalence and Impact of Cognitive Impairment and Alzheimer's Disease in Aging Populations

Alzheimer's disease is the most commonly diagnosed form of dementia, accounting for 60-80 percent of all dementia cases. According to a recent study which utilized the 2000 U.S. census, Alzheimer's disease affects an estimated 13% of Americans ages 65 and older and 45% of Americans ages 85 and older (Hebert, Scherr, Bienias, Bennett, & Evans, 2003). An additional report by the Alzheimer's Association estimates 500,000 Americans under the age of 65 have early indications of dementia (Maslow, 2006). Other prevalence studies on Alzheimer's disease have recorded similar findings, with the variances arising from the operational definitions of Alzheimer's disease used, inclusion and exclusion criteria and the geographical region the sample population was taken from (Plassman et al., 2007; Wilson et al., 2011). With estimates indicating that 5.4 million Americans currently suffer from Alzheimer's disease, this illness represents a serious, growing concern for the rising senior population and their care givers (Plassman et al., 2007; Hebert et al., 2003).

One factor that makes the current prevalence rates even more daunting, is that the senior population is expected to significantly increase in the next few decades. A study based on the 2000 U.S. census predicts that the number of people afflicted with Alzheimer's disease will almost triple by 2050 (Hebert et al., 2003). This poses a huge financial problem as healthcare costs are estimated to increase from 200 billion dollars, as of 2011, to 1.1 trillion dollars in 2050 (Silverstein & Maslow, 2006). The increase in Alzheimer's disease patients will have a large impact on hospice care, hospital care, nursing homes, Medicaid and Medicare, as well as the individuals' families (Bynum, 2009; Silverstein & Maslow, 2006).

Aside from the financial issues the rising incidence of Alzheimer's disease promises to generate, it is also expected that mortality rates will increase. Presently, Alzheimer's disease is the sixth leading cause of death in America (Miniño et al., 2010). However, this is likely to be an underestimate of the true incidence. Including deaths caused by Alzheimer's disease directly and deaths brought on indirectly by this disease, a study showed that 61 percent of Americans diagnosed with Alzheimer's disease at age 70 are predicted to die before age 80, compared with 30 percent of people who at age 70 have not been diagnosed with Alzheimer's disease (Arrighi, Neumann, Lieberburg, & Townsend, 2010). Therefore, it is estimated that in the next few decades Alzheimer's disease will represent an increasing proportion of the causes of death in the U.S.

Diagnostic Criteria for Alzheimer's Disease

The diagnosis of Alzheimer's disease primarily requires that the patient express certain clinically discernible symptoms and demonstrate deficits on neuropsychological exams. According to the 1984 criteria proposed by the National Institute of Neurological and Communicative Disorders and Stroke and the Alzheimer's Disease and Related Disorders Association, the clinical diagnosis of probable Alzheimer's disease must include the confirmation of dementia by clinical examination and documentation with the Mini-Mental Test (Folstein, Folstein, & McHugh, 1975), Blessed Dementia Scale (Erkinjuntti, Hokkanen, Sulkava, & Palo, 1988), or a related test. It requires the existence of impairments in two or more cognitive functions including declines of memory and cognitive function documented by neuropsychological testing, onset between the ages of 45 and 90, and symptoms cannot fit any other diagnosis. There are several other symptoms and laboratory tests which support a probable Alzheimer's

disease diagnosis, but a definite diagnosis cannot be made without a biopsy or autopsy confirmation (McKhann et al., 1984).

In 2011, the National Institute on Aging (NIA) and the Alzheimer's Association proposed two new criteria to supplement the original 1984 criteria. The first alteration is in the characterization of the three accepted stages of Alzheimer's disease which according to the original criteria were denoted as (1) mild/early-stage, (2) moderate/mid-stage and (3) severe/late-stage. However, according to the NIA and Alzheimer's Association, the 2011 criteria suggest that the new first and second stages—preclinical Alzheimer's disease and a-MCI—begin before symptoms become severe enough to affect daily life and before memory loss has definitively developed; that is, before the mild/early stage (Albert et al., 2011; Sperling et al., 2011). This is a marked difference from the original criteria which require symptoms to affect daily life before the diagnosis of probable Alzheimer's disease can be made (McKhann et al., 1984). The third stage of Alzheimer's disease is proposed to be dementia due to Alzheimer's disease and includes all the previously utilized stages of Alzheimer's disease from mild to severe (McKhann et al., 2011).

The second change of criteria is the addition of a biomarker test. Currently, many biomarkers for Alzheimer's disease are still being researched; however, beta-amyloid and tau levels in the cerebrospinal fluid and blood, as well as FDA-approve PET studies that assess amyloid burden are being used to help support diagnosis. The use of these tests prior to the onset of symptoms severe enough to impact daily life, may help to diagnose patients earlier, at a time when potentially beneficial treatments would be most effective (Jack et al., 2011).

Onset and Development of Alzheimer's Disease

The diagnosis of Alzheimer's disease at the earliest possible stage is critical in providing the best treatment, since the neurodegeneration which manifests itself in the disease's debilitating symptoms is irreversible and progresses over a number of decades. It is hypothesized that the underlying causes of Alzheimer's disease do not coincide with the initial presentation of symptoms, but occur years earlier in a stage referred to as preclinical Alzheimer's disease. Curiously, some patients who show signs of preclinical Alzheimer's disease never progress to the later stages of the disease (Sperling et al., 2011); the reason for this is unknown.

The characteristic neurological changes associated with Alzheimer's disease are the formation of amyloid plaques that surround neurons and neurofibrillary tangles which are created by high levels of the protein tau and accumulate inside neurons. Long term, these pathologic signatures of Alzheimer's disease lead to programmed cell death. The amyloid plaques caused by an abnormal increase in the levels of beta-amyloid protein inhibit synaptic communication, while the neurofibrillary tangles prevent intracellular movement of critical substances, such as nutrients (Fields, 2009). Although the exact cause of Alzheimer's disease is unknown, researchers are making progress in their search for explanations of this enigmatic pathophysiology. There have been three genetic mutations found which are predictive of in Alzheimer's disease; however, only a very small percent of Alzheimer's disease cases express these genetic mutations (Żekanowski et al., 2003). Fortunately, other hypotheses exist to explain the pathophysiology of Alzheimer's disease.

Pathophysiology of Alzheimer's Disease: Neuroinflammation

One hypothesis which shows promising results is that the pathophysiology of Alzheimer's disease is integrally related to neuroinflammatory processes. The theory revolves around the finding that there is a great deal of neuroinflammation surrounding the hallmark abnormalities of Alzheimer's disease—the amyloid plaques and neurofibrillary tangles. Most of the explanation for the inflammation hypothesis involves the interaction of these afflicted neurons with glial cells. Glial cells are a part of the central nervous system's (CNS) immune system. It is notable that a risk factor for Alzheimer's disease is systemic infection, because studies have shown that the glia interact with and are affected by the peripheral immune system (Eikelenboom et al., 2012). One type of glia, microglia, roams the CNS searching for foreign bodies and dead or injured cells or debris, which it eliminates through phagocytosis or by releasing certain chemokines and/or cytokines. Large clusters of these microglia can be observed surrounding the amyloid plaques; which makes sense because it is their function to rid the CNS of unhealthy tissues. However, researchers have recently found that when glia malfunction they can contribute to the creation of amyloid plaques and cell death (Fields, 2009). The malfunction of glia may be attributable to the local inflammation surrounding the plaques. In inflamed conditions, the ability of microglia to remove the beta-amyloid protein is impaired. Also, in the presence of beta-amyloid, microglia release neurotoxic factors which contribute to the cell death (Fields, 2009). One of these neurotoxic factors is the pro-inflammatory cytokine interleukin 6 (IL-6) which not only contributes to the toxicity of the environment, but also activates more microglia, furthering the process of inflammation. It is notable that this cytokine is present in abnormally high levels in

patients with Alzheimer's disease (Griffin et al., 1998). It is also noteworthy that studies have shown that under normal conditions microglia aid in neurogenesis; however, under inflammatory conditions they release cytokines and other neurotoxic factors which impair neurogenesis. Therefore, microglia may not only be contributing to cell death, but they may also be preventing other neurons from forming (Gemma, Bachstetter, & Bickford, 2010; Kohman & Rhodes, 2012).

Another type of glial cell which accumulates at the plaque site is the astrocyte. It is also phagocytic and functions to remove waste. Astrocytes have the peculiar ability to create the precursor for the beta-amyloid protein and can thus contribute to the accumulation of the protein at the plaque site. Also, the beta-amyloid protein has a deleterious effect on the astrocyte's ability to generate antioxidants, which leaves the cells open to attack from oxidative stress. In Alzheimer's disease, astrocytes actually contribute to the oxidative stress in the environment by releasing nitric oxide (Fields, 2009). Once activated by the beta-amyloid protein, the astrocyte can lyse and become a part of the amyloid plaque, physically contributing to the amassing plaque formation (Lee, Han, Nam, Oh, & Hong, 2010). Astrocytes also release abnormally high levels of S100beta protein, in patients with Alzheimer's disease, which furthers the process of inflammation (Griffin et al., 1998). In the inflammatory environment, the astrocyte's ability to uptake glutamate is also inhibited and the excess glutamate acts as a further factor contributing to cell death. While glia can still offer some neuroprotective functions in Alzheimer's disease, their overall effect seems to be the exacerbation of the neurotoxicity of the environment surrounding the plaques and facilitation of the spread of the disease within the CNS (Fields, 2009).

Pathophysiology of Alzheimer's Disease: Insights Based on Pharmacological Treatments

Other hypotheses for explaining the pathophysiology of Alzheimer's disease provide the pharmacodynamics basis for the current drugs available for treating Alzheimer's disease. There are currently five FDA approved drugs for the treatment of Alzheimer's disease, four of which are based on the acetylcholine theory of Alzheimer's disease—Galantamine, Rivastigmine, Donapezil and Tacrine (McGleenon, Dynan, & Passmore, 1999). This theory is based on the hypothesis that the symptoms of Alzheimer's disease are caused by a deficiency of acetylcholine and the drugs act as acetylcholinesterase inhibitors in order to prevent the breakdown of acetylcholine in the synapse. The action of the drug works to allow the most acetylcholine possible access to the receptors on the post-synaptic neuron by decreasing its breakdown in the synapse, in the hopes of increasing the amount of synaptic transfer of acetylcholine (McGleenon et al., 1999). The fifth drug available for the treatment of Alzheimer's disease functions as an N-methyl-D-aspartate (NMDA) receptor antagonist Memantine. The NMDA receptor is the binding site for the neurotransmitter glutamate. In excess quantities glutamate causes neuroinflammation and hyperexcitability of neurons both of which can lead to cell death. The drug binds at the NMDA receptor and prevents the glutamate from interacting with the neurons that have NMDA receptors (Parsons et al., 2007). While both of these hypotheses have some merit, it is apparent from the effect of the drugs on Alzheimer's disease patients that they do not entirely explain the pathophysiology of Alzheimer's disease. Unfortunately, the drugs only temporarily slow down the progression of the disease (Parsons et al., 2007). Currently no treatment permanently slows or prevents the neuronal degeneration, nor are there drugs which can reverse neurodegeneration.

Risk Factors for Alzheimer's Disease

While the cause of Alzheimer's disease may still be unknown, several risk factors have been identified. Not surprisingly, age has been identified as the number one risk factor for Alzheimer's disease. Other factors include heredity factors (Fratiglioni, Ahlbom, Viitanen, & Winblad, 1993; Green et al., 2002; Lautenschlager et al., 1996; Mayeux, Sano, Chen, Tatemichi, & Stern, 1991), head trauma (Lye & Shores, 2000; Plassman et al., 2000) and poor cardiovascular health. Some risk factors affecting cardiac health may also apply such as diabetes, lack of exercise, obesity, high blood pressure, and smoking (Anstey, von Sanden, Salim, & O'Kearney, 2007; Hendrie et al., 2006; Pendlebury & Rothwell, 2009; Raji et al., 2010; Solomon, Kivipelto, Wolozin, Zhou, & Whitmer, 2009; Yaffe et al., 2011). Examples of head trauma include concussions, or loss of consciousness and traumatic brain injury (TBI). Several studies have found that almost two-thirds of Alzheimer's disease cases are females; however, after adjusting for the fact that women live longer than men, studies conclude that women are not more likely than men to develop Alzheimer's disease (Hebert, Scherr, McCann, Beckett, & Evans, 2001; Seshadri et al., 1997); therefore, gender was not determined to be a risk factor. However, the influence of sex is still somewhat ambiguous, as one study concluded that women were more likely to present with symptoms of dementia when showing Alzheimer's pathology than men (Barnes et al., 2005). It has also been found that estrogen has neuroprotective effects that shield against the development of Alzheimer's disease; suggesting that women may be less likely to develop Alzheimer's than men (Green, Gridley, & Simpkins, 1996).

Studies have also shown differences in the prevalence of Alzheimer's disease among different races. African Americans are twice as likely as Caucasians to develop AD (Potter et al., 2009) and Hispanics are one and a half times as likely as Caucasians to develop Alzheimer's disease (Gurland et al., 1999). Genetic factors were not found to explain racial differences in these studies (Chin, Negash, & Hamilton, 2011). Some studies show the increase in additional risk factors in both African Americans and Hispanics, as compared to Caucasians, may explain the increased risk (Kukull et al., 2002; Plassman et al., 2007). These risk factors include socioeconomic class, heart disease, diabetes and high blood pressure (Plassman et al., 2007). One other risk factor is the development of a-MCI which is predictive of a progression to Alzheimer's disease, but is not causal or definitive (Albert et al., 2011; Sperling et al., 2011).

It has also been noted in the Alzheimer's Association report that people of higher education are less at risk for Alzheimer's disease than less educated people (Hebert, Scherr, McCann, Beckett, & Evans, 2001; Seshadri et al., 1997). Some researchers attribute this to confounding variables, such as the lack of a sufficient level of health care for those in lower socioeconomic classes (McDowell, Xi, Lindsay, & Tierney, 2007). However, other researchers think higher levels of education equate to higher levels of baseline intelligence which provide the patient with a "cognitive reserve " (Roe, Xiong, Miller, & Morris, 2007; Stern, 2006). For example, if the symptoms of Alzheimer's disease were measured by an I.Q. test and two patients both lost the same number of I.Q. points due to neurodegeneration caused by Alzheimer's disease, the person with the highest I.Q. when not affected by the disease would perhaps now be considered of

average intelligence, while a person with a baseline of average I.Q. would now be considered of below average I.Q.—or impaired

Mild Cognitive Impairment: Definition and Diagnostic Criteria

The NIA and Alzheimer's Association provided diagnostic criteria for a-MCI as a part of the new criteria for Alzheimer's disease in 2011 (Table 1). It is important to track the progression of a-MCI symptoms because patients who experience progressive decline and especially those with memory impairments are most likely to develop Alzheimer's disease (Ganguli et al., 2011). Those patients diagnosed with MCI where memory deficits are the major complaint are categorized as having a-MCI (Petersen et al., 1999). Notably, not all patients with a-MCI progress to Alzheimer's disease. Some remain stable and others improve (Ganguli et al., 2011). According to a study by Hänninen and colleagues the prevalence of a-MCI among seniors ages 60-76 was found to be 5.3 percent; however, another larger study showed prevalence among seniors 75 years and younger to be 19 percent (Hänninen, Hallikainen, Tuomainen, Vanhanen, & Soininen, 2002; Lopez et al., 2003). Disturbingly, half of those patients who contact their doctor because they are experiencing MCI symptoms will be diagnosed with dementia in the next three to four years after their initial consultation (Petersen et al., 1999).

Table 1. The National Institute on Aging-Alzheimer's Association Criteria for Clinical Diagnosis of Mild Cognitive Impairment

- Change in cognition which causes concern
- One or more cognitive impairments
- The impairment does not alter the patient's daily life or functional abilities
- Not demented

Source: Albert et al., 2011

Neuroimaging

Magnetic Resonance Imaging of Brain Tissue

Other developments in this research involve the use of Magnetic Resonance Imaging (MRI) which commonly utilizes radio-frequency waves to cause hydrogen to flip off of its axis. When hydrogen returns to its original position this emits energy which can be analyzed based on our knowledge of the nature of radio frequency excitation in different types of tissues to provide an evaluation of the identity of the tissue. Hydrogen is found in abundance in most tissues, therefore it is often used for identification and evaluation of tissues in MRI, although other molecules can emit distinct waves due to varying radiofrequencies as well. The varying amounts of hydrogen (water) present in tissues are used to differentiate the types of tissues found in the brain and to create a three-dimensional image from this information on tissue conformation (Meyer, 2013). These images are formed by measuring relaxation times of the hydrogen molecules which are excited by radio frequencies. T2 relaxation time (spin-spin relaxation time) is the amount of time it takes a resonance signal to reach 37% of its original value or, in other terms, the time the hydrogen molecules spend knocked out of their spin. Whereas T1 relaxation time also known as spin-lattice relaxation time is a measurement of the time it takes a component of the magnetization vector to return to thermodynamic equilibrium, that is, the time it takes for the hydrogen to return to its normal spin position (Pooley, 2005). Another MRI sequence used to increase MRI contrast and sensitivity is fluid attenuated inversion recovery (FLAIR). FLAIR uses a traditionally long echo time; meaning there is a long time between the initiation of the radio frequency pulse and the maximal signal induced by the pulse. It is a type of T2 weighted image that increases T2

relaxation time and particularly increases cerebrospinal fluid contrast (Hajnal et al., 1992).

The current study used single shot echo planar imaging (EPI) to analyze the tissue. Single shot EPI involves using a single radio frequency to initiate one T2 relaxation with multiple gradient echoes (Hashemi, Bradley, & Lisanti, 2010). These gradient echoes are created by the frequency encoding oscillations of the radio frequency as it moves quickly back in forth from positive to negative amplitudes. The gradients are represented in the k space which is a graphic matrix of all magnetic resonance data that is used to create the image (Poustchi-Amin, Mirowitz, Brown, McKinstry, & Li, 2001). Multiple shot EPI also exists, but single shot EPI is the fastest (Hashemi et al., 2010) and it also has the advantage of being able to image transient physiological processes and reduce motion artifact (Poustchi-Amin et al., 2001).

Diffusion Tensor Imaging of Brain Tissue

Diffusion tensor imaging (DTI) is another type of MRI which shows the diffusion of water in tissue. Water diffuses in predictable patterns around and through cells. For example, heavy concentrations of myelin or axon sheaths slow the diffusion of water and intracellular fluid limits its movement. When water diffuses in unexpected patterns the tissue is perceived to be compromised. For instance, when necrosis of tissue occurs, there are fewer obstacles to impede water and so diffusivity increases. The diffusion patterns allow the magnitude, degree and orientation of the diffusional anisotropy to be analyzed. Anisotropy is a directional measure, indicating the water diffusion is parallel to the tissue. This type of parallel diffusion is observed in fibrous tissue, such as white matter. Another classification of directional diffusivity is isotropy in which water is free

to diffuse in many or all directions; this can be found in grey matter and cerebrospinal fluid. The directional diffusivity of water is determined by mathematical equations which provide what are called eigenvalues. There are three axes along which diffusion is measured. The longest axis is termed the primary eigenvalue, the second longest is termed the secondary eigenvalue and the shortest is the tertiary eigenvalue. The proportions of these eigenvalues are used to determine the three eigenvectors—the measures of directional diffusivity. The relative proportions of the eigenvectors determine the direction of diffusion, if there is one. When these proportions are roughly equivalent, the diffusion is said to be isotropic and when they are significantly different the diffusion is said to be anisotropic (Alexander, Lee, Lazar, & Field, 2007).

The common measures used in DTI are based on eigenvalues. Three eigenvectors are obtained from the eigenvalues which represent directional diffusivities. Eigenvectors are used to determine the other measures of white matter integrity listed below. Some of the commonly used measures include fractional anisotropy (FA), the mean diffusivity (MD), radial diffusivity (RD) and axial diffusivity (AD). FA is highly sensitive, but because all DTI measures are non-specific it can be compared to other measures in order to more conclusively determine what the FA value illustrates about the nature of the tissue. It is also susceptible to error when measuring areas of tissue in which white matter fibers crossover repeatedly, a fault which may be corrected by diffusion spectrum imaging (DSI). MD is just an average of the eigenvalues (Alexander et al., 2007) and decreases when anything is present to obstruct the flow of water, such as cell membranes (Gold, Johnson, Powell, & Smith, 2012). It changes when there are alterations in white matter integrity. RD and AD are other useful measures, which assist in ascertaining

tissue integrity. Variations in RD are suggestive of alterations in myelination because it characterizes the degree of diffusion along the axis that is perpendicular to the primary diffusion direction. Changes in AD are more indicative of alterations in axonal tissue and are characterized by the degree of diffusion that runs in parallel to the primary diffusion direction (Alexander et al., 2007).

Diffusion Tensor Imaging in Alzheimer's Disease Patients

There have been several studies which have utilized DTI to attempt to distinguish which parts of the brain may be predictive of Alzheimer's disease and indicative of a-MCI. According to a review by Gold et al., (2012) studies show demyelination in the parahippocampus, the cingulum, the inferior fronto-occipital fasciculus, the fronto-occipital uncinate fasciculus and the corpus callosum to be predictive of the development of Alzheimer's disease. It is notable that these white matter tracts link gray matter that have functions in episodic memory such as the posterior cingulate cortex with the entorhinal cortex and hippocampus (Gold et al., 2012) and that several studies have correlated compromises in white matter integrity of tracts that connect with these structures with cognitive dysfunction (Fellgiebel & Yakushev, 2011; Madden et al., 2012). Fellgiebel and Yakushev (2011) have supporting results which show the increased MD values in the anterior hippocampus to be correlated with patients who suffer from impairments in episodic memory. High MD values are indicative of neurdegeneration (Alexander et al., 2007; Fellgiebel & Yakushev, 2011). Consistent with these findings, other studies have shown high MD values of the hippocampus to be present in patients with a-MCI (Wang et al., 2012).

Other measures have also been used to determine tissue loss of the hippocampus, such as FA and RD; however, the FA values are inconsistent. One study showed an increase in FA (Wang et al., 2012) and another showed a decrease (Zhang et al., 2007) in the hippocampus. Interestingly, MRI studies show that FA is known to decrease throughout the white matter tracts and especially in the frontal and prefrontal cortices in normal aging and is an indicator of general white matter integrity (Schulze et al., 2011). Altered measures of AD have also been noted (Wang et al., 2012), though, it is generally not considered to be an effective measure of demyelination (Alexander et al., 2007). This is an example of why more research needs to be done in imaging to determine the neurological indicators of a-MCI. There are other areas of inconsistency in this research, as well, such as whether or not hippocampal volume loss is an indicator of a-MCI (Fellgiebel & Yakushev, 2011; Zhang et al., 2007). Unfortunately, DTI currently does not offer the necessary specificity and sensitivity to be used in clinical diagnosis of a-MCI, but with further research this can change (Little & Holloway, 2007).

Overview of Current Study

The data evaluated for the present study were collected by researchers at the University of Illinois College of Medicine, as part of a larger project funded by a grant awarded to Dr. Deborah Little and colleagues by the National Institutes of Health (NIH). The initial project included MRI acquisition, DTI acquisition and neuropsychological testing for a total of 36 subjects who met inclusion and exclusion criteria. This study evaluated the DTI data for 28 of the original subjects and obtained measures of FA, MD, AD and RD for the cingulum bundle and 11 cortical structures. Refer to Table 2 for an overview of the regions evaluated in this study.

Table 2. Cortical Structures Analyzed for the Current Study

Cortical Structures	**Function**	**Location**
Anterior Segment of the Corona Radiata	Relays information within the cerebral cortex [1]	Fibers connect the internal capsule with areas of the cerebral cortex [1]
Body of the Corpus Callosum	Relays information across hemispheres [2]	Fibers extend from posterior frontal and parietal lobes [2]
Corticopinal Tract	Motor functions [2]	Fibers radiate from the primary motor cortex to the spinal cord [2]
Superior Longitudinal Fasciculus	Somatosensory and motor functions (attention and language) [2]	Connects association cortex in the frontal, temporal and parietal lobes intrahemispherically [2]
Posterior Segment of the Corona Radiata	Relays information within the cerebral cortex [1]	Fibers connect the internal capsule with areas of the cerebral cortex [1]
Forceps Minor	Relays information intrahemispherically and across corpus callosum [2]	Fibers extend from the medial frontal lobe [2]
Genu of the Corpus Callosum	Relays information across hemispheres [2]	Fibers extend from the medial frontal lobe hemispheres [2]
External Capsule	Contain association fibers that make connections across hemispheres [5]	This tract is located between the genu and splenium of the corpus callosum; near the claustrum and lentiform nuclei [5]
Cingulum	It has been associated with cognitive functions such as attention, speech, consciousness and memory [4]	The anterior cingulum is located anterior to the genu of the corpus callosum and the posterior is located laterally from the brainstem and proximal to the hippocampus.
Splenium of the Corpus Callosum	Relays information across hemispheres [2]	Fibers extend from parietal, temporal and occipital lobes [2]
Forceps Major	Relays information intrahemispherically and across corpus callosum [2]	Fibers extend from the parietal lobe [2]
Sagittal Stratum	Relays information from the occipital lobe to other areas of the cerebral cortex [3]	The sagittal stratum is made up of the inferior fronto-occipital fasciculus, the inferior longitudinal fasciculus, and posterior thalamic radiation [3]

References: [1]Corona Radiata. *Merriam-Webster*. Retrieved from http://www.merriam-webster.com/medical/corona%2520radiata. [2]Hermoye, L., Wakana, S., Laurent, J., Jiang, H., Cosnard, G., Van Zigl, P., & Mori, S. *White matter atlas*. Retrieved from http://www.dtiatlas.org/. [3]Jellisona, B., J., Fielda, A. S., Medowb, J., Lazarc, M., Salamatd, M. S., & Alexander, A. L. (2004). Diffusion tensor imaging of cerebral white matter: A pictorial review of physics, fiber tract anatomy, and tumor imaging patterns. *American Journal of Neuroradiology, 25*, 356-369. [4]*What is the Cingulum?* Retrieved from http://www.wisegeek.com/what-is-the-cingulum.htm. [5]*What is the External Capsule?* Retrieved from http://www.wisegeek.com/what-is-the-external-capsule.htm.

The goal of this study was to compare patients diagnosed with a-MCI with healthy controls, in order to determine if any pathological signatures are predictably present in a-MCI. Imaging was used to determine the presence of neurodegeneration and demyelination in regions of interest. The presence of degeneration in patients with a-MCI was compared to those of the controls—who only showed the normal tissue transformations involved in aging—to establish if loss of white matter integrity in the cingulum or cortical structures analyzed could be considered indicative of the pathogenesis of a-MCI. A neuropsychological test evaluating verbal memory—the California Verbal Learning Test, second edition (CVLT-II)—was also used to evaluate correlations of a specific aspect of cognitive functioning with measures of white matter integrity. Based on a review of findings in studies using DTI to evaluate differences in white matter integrity between a-MCI cases and controls, several hypotheses were formulated to establish the methodology and predict the results of this study.

Increases in neuronal tissue loss were assessed using the primary measure of FA. This is a non-specific measure of tissue loss which could represent tissue degeneration caused by the loss of axonal tissue, demyelination or both. Measures of MD, RD and AD were also analyzed for the cingulum bundle and each cortical structure in order to provide information on what factors affected FA. RD has been shown to measure the integrity of myelin in several animal studies, while AD is a measure of axonal diffusivity and is thought to measure the degree of axonal degeneration (Song et al., 2003; Sun, Liang, Cross, & Song, 2008; Sun et al., 2006; Sun et al., 2005).

Significance of Demyelination in Amnestic Mild Cognitive Impairment

Based on the literature, it was suggested that any degeneration found in the a-MCI cases could be due to neuroinflammation. As discussed above, inflammatory processes have been indicated in Alzheimer's disease (Minghetti, 2005) and recent studies have shown that inflammatory processes can be assessed as a change in diffusivity in DTI (Samann et al., 2003). Several studies have shown white matter changes in Alzheimer's disease (Bozzali et al., 2002; Medina et al., 2006; Minghetti, 2005; Rose et al., 2000; Takahashi et al., 2002) and it is possible that these changes are due to inflammation and are a measure of demyelination (Minghetti, 2005). It is also possible that demyelination could be caused by Wallerian degeneration, an interruption in the neuronal pathways due to neurofibrillary tangles and amyloid plaques or by normal aging processes (Bronge, Bogdanovic, & Wahalund, 2002; Brun & Englund, 1986; Siger, Schuff, Zhu, Miller, & Weiner; 2009; Zhang et al., 2008). However, the pathology of Alzheimer's disease suggests demyelination is a part of the disease course. Studies have found that demyelination in Alzheimer's disease occurs in a pattern that begins with the structures which form late in development and progresses throughout the disease course to structures that form earlier in development (Bartzokis, 2011; Filippi & Agosta, 2011; Reisberg et al., 2002; Stricker et al., 2009). There has been some research to support the hypothesis that degeneration has already begun in white matter tracts in the a-MCI stage (Medina et al., 2006; Parente et al., 2008). Based on supporting literature (Bosch et al., 2012; Stenset et al., 2011) indicating there would be a greater degree of demyelination in the a-MCI cases compared to controls, any significant differences between groups in RD

was of particular interest in this study—as RD is the measure that is most indicative of changes in myelin integrity.

Hypotheses

Hypothesis 1: Participants with amnestic mild cognitive impairment will exhibit significantly greater loss of white matter integrity in the cingulum bundle compared to controls as assessed by measures of white matter integrity.

The region of particular interest in this study was the cingulum. Several studies have shown changes in the cingulum bundle fiber in early Alzheimer's disease (Zhang et al., 2007; O'Dwyer et al, 2011). This is significant because of the functional relevance of the cingulum; it projects from the entorhinal cortex, temporal and parietal lobes to the frontal cortex, carrying information critical for cognitive functioning of memory (Derflinger et al. 2011). Therefore, it was predicted that the cingulum would show significantly more degeneration in a-MCI cases compared to controls as assessed by FA.

Hypothesis 2: Participants with amnestic mild cognitive impairment will exhibit significantly greater neuronal tissue loss in the posterior cingulum compared to the anterior cingulum as assessed by measures of white matter integrity

The cingulum was also analyzed in both the posterior and the anterior regions of the tract. Several studies support degeneration of the posterior cingulum in Alzheimer's disease and in a-MCI as measured by significant changes in diffusivity (Medina et al. 2006; Parente et al. 2008, Fellgiebel et al. 2005, Zhang et al. 2009). Delono-Wood et al. (2012) have also shown that the posterior cingulum has significantly more changes in diffusivity than the anterior cingulum. This is supported by what is known about the progression of Alzheimer's disease since the posterior cingulum has projections to the entorhinal cortex which as previously stated has been shown to degenerate early in

Alzheimer's disease and connects the parahippocampal tract to the prefrontal cortex. The parahippocampal tract is also known to experience degeneration early in Alzheimer's disease (Echa´varri et al., 2011) and its connections with the prefrontal cortex have functional significance in types of episodic memory which are impaired in Alzheimer's disease (Acosta-Cabronero, Williams, Pengas & Nestor, 2010; Salat et al., 2010; Seeley, Crawford, Zhou, Miller & Greicius, 2009; Maguire, 2001; Fellgiebel et al. 2005). Therefore, the anterior and posterior cingulum was compared in this analysis to determine if our results would support the findings in the literature.

Hypothesis 3: Participants with amnestic mild cognitive impairment will exhibit significantly greater neuronal tissue loss in the anterior and posterior segment of the corona radiata, body, genu and splenium of the corpus callosum, superior longitudinal fasciculus, forceps minor, external capsule and sagittal stratum compared to controls as assessed by measures of white matter integrity

Refer to Table 3 for a review of significant findings from the literature on changes in diffusivity for a-MCI cases compared to controls for cortical regions that were analyzed in this study. The hypothesis for these structures was based on this literature review. The cortical structures—forceps major and corticospinal tract—that have not been found to be affected by the pathology of a-MCI were chosen for analysis based on their location and function. The forceps major has projections which extend from the parietal lobe; an area that has been shown to be affected early in Alzheimer's pathology (Thompson et al., 2001; Thompson et al., 2003). And the corticospinal tract was included because it functions in motor movements which are impaired later in Alzheimer's disease (Thompson et al., 2001; Thompson et al., 2003).

Table 3. Previously-Reported Changes in White Matter Integrity in Cortical Structures in Patients with Mild Cognitive Impairment.

Cortical Structures	FA	MD	AD	RD
Anterior Segment of the Corona Radiata	Decrease[3], Decrease[4]	Increase[4], Increase[7]		
Body of the Corpus Callosum	Decrease[3]	Increase[1]		
Corticopinal Tract				
Superior Longitudinal Fasciculus	Decrease[3], Decrease[4], Decrease[6]	Increase[1], Increase[4]		
Posterior Segment of the Corona Radiata	Decrease[3], Decrease[4]	Increase[4], Increase[7]		
Forceps Minor			Increase[5]	
Genu of the Corpus Callosum	Decrease[3]	Increase[2], Increase[7]		
External Capsule	Decrease[4]	Increase[4]		
Splenium of the Corpus Callosum	Decrease[3], Decrease[6], Decrease[8]	Increase[7]		Increase[8]
Forceps Major				
Sagittal Stratum	Decrease[4]	Increase[4]		

FA: fractional anisotropy, MD: mean diffusivity; AD: axial diffusivity; RD: radial diffusivity

References: [1]Bosch, B., Arenaza-Urquijo, E. M., Rami, L., Sala-Llonch, R., Junqué, C., Padullésa, C., … Bartrés-Faz, D. (2012). Multiple DTI index analysis in normal aging, amnestic MCI and AD. Relationship with neuropsychological performance. *Neurobiology of Aging*, *33*, 61-74. [2]Chen, T., Chen, Y., Cheng, T., Hua, M. Liu, H., & Chiu, M. (2009). Executive dysfunction and periventricular diffusion tensor changes in amnesic mild cognitive impairment and early Alzheimer's disease. *Human Brain Mapping*, *30*, 3826-3836. [3]Duffy, S. L., Paradise, M., Hickie, I. B., Lewis, S. J. G., Naismith, S. L., Lagopoulos, J. (2014). Cognitive impairment with and without depression history: An analysis of white matter microstructure. *Journal of Psychiatry and Neuroscience*, *39*(2), 135-43. [4]Liu, J., Yin, C., Xia, S., Jia, L., Guo, Y., Zhao, Z., … Jia, J. (2013). White matter changes in patients with amnestic mild cognitive impairment detected by diffusion tensor imaging. *PLoS ONE, 8(*3), e59440. [5]O'Dwyer, L., Lamberton, F., Bokde, A. L. W., Ewers, M., Faluyi, Y. O., Tanner, C., … Hampel, H. (2011). Multiple indices of diffusion identifies white matter damage in mild cognitive impairment and Alzheimer's disease. *PLoS ONE, 6*(6), e21745. [6]Parente, D. B., Gasparetto, E. L., Hygino da Cruz, L. C., Domingues, R. C., Baptista, A. C., Carvalho, A. C. P., & Domingues, R. C. (2008). Potential Role of Diffusion Tensor MRI in the Differential Diagnosis of Mild Cognitive Impairment and Alzheimer's Disease. *American Journal of Roentgenology*, *190*, 1369-1374. [7]Thillainadesan, S., Wen, W., Zhuang, L., Crawford, J., Kochan, N., Reppermund, S., … Sachdev, P. (2012). Changes in mild cognitive impairment and its subtypes as seen on diffusion tensor imaging. *International Psychogeriatric*, *24*(9), 1483-93. [8]Zhang, Y., Schuff, N., Camacho, M., Chao, L. L., Fletcher, T. P. Yaffe, K., … Weiner, W. (2013). MRI markers for mild cognitive impairment: Comparisons between white matter integrity and gray matter volume measurements. PLoS ONE, 8(6), e66367.

Hypothesis 4: Poorer verbal memory, as assessed by the CVLT-II, will correlate with findings of increased degeneration as assessed by measures of white matter integrity

Correlations between measures of white matter integrity and a functional measure of verbal memory (California Verbal Learning Test(CVLT-II), second edition (Dellis, Kramer, Kaplan, & Ober, 1986)) were included because verbal memory is known to be impaired in Alzheimer's disease and has also been shown to be detrimentally affected in a-MCI (Greenway et al., 2006). Also the CVLT-II requires the use of semantic clustering—a technique used to aid recall—which is conducted using the frontal lobes; an area that is affected in a-MCI and Alzheimer's (Thompson et al., 2001; Thompson et al., 2003). The cingulum bundle was of particular interest in this analysis because degeneration in the cingulum has been shown to correlate with poor performance on the CVLT-II in a-MCI cases (Zhang et al., 2013). Therefore, it was predicted that poorer performance on the CVLT-II would be correlated with degeneration in the cingulum as measured by FA, MD, AD and RD. Correlations between FA and number of items recalled on the CVLT-II were also analyzed to assess the cognitive effects of degeneration in the other cortical structures.

CHAPTER TWO

Methods

This study utilized existing neuroimaging data including diffusion tensor imaging (DTI) scans and neuropsychological testing from a previously-completed study, to determine whether white matter loss in the cingulum and 11 cortical structures is significantly greater in a-MCI cases compared to similarly aged healthy control subjects. Additional analyses evaluated correlations between imaging data and neuropsychological measures of verbal memory function.

Study Design

This case-control study compared a clinical population of 13 senior adults who met diagnostic criteria for a-MCI with 15 matched controls who had no measurable cognitive impairment.

Data Collection

All data utilized for the present study was collected by researchers at the University of Illinois College of Medicine, as part of a larger project funded by a grant awarded to Dr. Deborah Little and colleagues by the National Institutes of Health (NIH). For the current project, no personal identifiers or clinical data were provided and diagnosis was blinded until all analyses were completed.

Neuropsychological testing was used to assess cognitive function, confirm diagnosis of a-MCI and to ensure controls did not have any form of cognitive

impairment. Magnetic Resonance Imaging (MRI) scans were also performed to provide measures of brain structures and white matter integrity.

Participants

For the original study, a total of 36 subjects—18 cases and 18 controls—who met all study and matching criteria were recruited from an outpatient clinic in the suburbs of Chicago that specializes in the screening and diagnosis of a-MCI and other forms of dementia. For the current study, eight of the participants were excluded; due to the discovery that they possessed lesions or signs of atrophy and in one case because the background noise level chosen invalidated the measures. Prior to recruitment, a waiver of consent was received to review medical records including physician progress notes. Patients were approached if they had a primary diagnosis of a-MCI as defined by CPT code (780.93 (Memory loss). 294.8 (Dementia), had completed neuropsychological testing to confirm the diagnosis within the past 12 months, had at least one follow up visit, and had a diagnostic note signed by the physician.

All subjects were 58 – 78 years of age, with 9 males and 6 females in the control group and 8 males and 5 females in the a-MCI group. Neuropsychological testing was used to confirm reductions in memory and to confirm the diagnosis of MCI. Case and control subjects were matched for age, sex, race, socioeconomic status, and premorbid I.Q. Subjects were also specifically matched on years of educational attainment, as well as educational levels of their mothers. This is because the level of parental education has been shown to affect I.Q. (Rowe, Jacobson, & van den Oord, 1999). Overall, subjects were highly educated, averaging 16.68 years of formal education. Additionally, all subjects were required to be right handed because evidence exists which suggests

handedness may be a risk factor in AD (de Leon et al., 1986) and may bias measures of cerebral white matter (Westerhausen et al., 2004). Inclusion criteria also included the subject's indication of English as a primary spoken language and ability to sign an informed consent. Participants who spoke English as a second language were not included because the neuropsychological tests were given in English and an imperfect understanding of the language could negatively bias their results.

Exclusionary Criteria

Subjects were excluded from the study for any major psychiatric or medical health problem. Exclusions included any form of dementia including meeting criteria for probable Alzheimer's disease, major depression, and neurological disease. Subjects with uncontrolled diseases of the cardiovascular system were also excluded. This included any potential participant who had undergone cardiac surgery, had a history of stroke or had been given a diagnosis of diabetes. Subjects were not excluded, however, if they had one of either high cholesterol or hypertension—that was medically controlled for at least one year. Subjects were also excluded if they were using any medication to treat AD at the time of testing. However, other forms of medication were acceptable as long as the patient had been stable in their use of the medication for the past six months. Other exclusionary criteria included illicit drug use with the exception of recreational marijuana use for six months or less, not exceeding once per month. Subjects with a history of neurological illnesses or injury including traumatic brain injury, concussions, sexually transmitted diseases, meningitis, or other illnesses that cause inflammation of the central nervous system were also excluded.

Exclusion criteria also included any contraindications for undergoing an MRI scan including participant safety factors. These included contraindicated implanted medical devices or metal fragments (e.g., cardiac pacemakers, aneurysm clips, cochlear implants, shrapnel, history of metal fragments in eyes, neuro-simulators, permanent makeup or large tattoos located on the head and neck or tattoos done by non-licensed tattoo artists). Participants were screened for weight and excluded if their weight exceeded 225 pounds. Individuals who were potentially unable to undergo a sustained MRI session due to claustrophobia and/or the inability to lie comfortably for an hour were also excluded.

Amnestic Mild Cognitive Impairment Case Criteria

Case subjects were classified as having a-MCI for the present study based on guidelines published by an expert consensus panel convened by the National Institute of Neurological Disorders and Stroke (NINDS) (Portet et al., 2006). Briefly, subjects were determined to be eligible if their primary presentation complaint was memory function. Also, daily living must have only been mildly impaired, if at all. Criteria also included a progressive onset with sustained memory concerns. The a-MCI diagnosis was characterized by a hippocampal type of amnestic syndrome which entails poor performance on free-recall tests due to impaired cuing and/or recognition mechanisms with intact encoding mechanisms (Portet et al., 2006).

Neuropsychological Testing

The test of primary interest for assessing cognitive function in relation to neuroimaging measures for the present project evaluated verbal learning and memory.

The California Verbal Learning Test-Second Edition (CVLT-II), (Delis, Kramer, Kaplan, & Ober, 2000) is a commonly used and generally accessible tool for the assessment of memory, and has been specifically noted for its association with white matter loss in the cingulum bundle in a-MCI patients (Zhang et al., 2013). The CVLT-II consists of five trials during which a list of 16 words from four related categories is read aloud. Subjects are asked to recall as many items as possible after each trial and obtain a point for each item recalled from the list. The total score is calculated by adding up the total number of items recalled across all five trials (with 80 representing perfect recall on all 5 trials) (Delis, Kramer, Kaplan, & Ober, 2000). As a free recall test, the test measures the participants' ability to learn new information. Participants' performance is expected to get better with each trial as the participant has more time and opportunity to encode the information. Also because the list generally includes some words that are similar to one another, participants use semantic clustering to improve their ability to recall. The ability to place items into categories based on their meanings is an important aspect of verbal memory. The CVLT-II has also been identified as an accurate predictor of preclinical AD (Albert, Moss, Tanzi, & Jones, 2001).

Diffusion Tensor Imaging Acquisition

Pre-Processing of Diffusion Tensor Imaging

Standard structural MRI—T1-weighted, T2-weighted, FLAIR, and Diffusion Tensor Imaging (DTI)—studies were performed on both case and control subjects on a 3.0T whole body GE scanner (Excite 2.0; GEMS, Milwaukee, Wisconsin) using the 8-channel phase array head coil. A customized diffusion tensor imaging (DTI) pulse

sequence based on a single-shot EPI pulse sequence was used for image reconstruction and analysis of white matter structural integrity. This dynamically modified the imaging gradient waveforms in order to correct for eddy currents created by diffusion gradients. All images were obtained axially and the electrostatic repulsion model proposed by Jones et al. (1999) was used for creating diffusion-weighting orientations (TR = 5000-6000ms, TE = minimum (81ms), b-values = 750 s/mm2, diffusion gradient directions = 27, FOV = 22cm, Matrix = 128x128, slice thickness = 5mm, gap = 1.5mm, ramp-sampling = on, NEX = 2, total acquisition time = 5:46). A background noise level of 75 (MR units) was selected prior to calculation of FA, MD and the eigenvalues which were interpolated using standard linear regression. The background noise level was selected for all subjects because the noise level can bias measures of white matter integrity and can reduce the signal to noise ratio. The background noise level was chosen by reviewing individual diffusion tensor images for each subject and determining that the background noise level selected did not exclude white matter tissue.

The primary measure was FA which is calculated from the eigenvalues $\lambda_1, \lambda_2, \lambda_3$ using the equation:

$$FA = \sqrt{\frac{1}{2}} \frac{\sqrt{(\lambda_1 - \lambda_2)^2 + (\lambda_2 - \lambda_3)^2 + (\lambda_3 - \lambda_1)^2}}{\sqrt{\left(\lambda_1{}^2 + \lambda_2{}^2 + \lambda_3{}^2\right)}}$$

The resulting values from this equations are between zero and one, where zero represents complete isotropy—water can flow in all directions—and one represents anisotropy in which water flows almost entirely in one direction. Free diffusion of water would be expected when nothing is present to block the flow of water. In contrast, anisotropy occurs when the tract is intact and the water is forced to flow in one direction parallel to

the tract. Because most tissues are not entirely impermeable to water and not perfectly intact even in healthy brains, anisotropy values will never be exactly zero or one, but somewhere between the two; where lower values represent a more isotropic flow—flow in many directions—which can be interpreted as a loss of white matter integrity. Another non-specific measure is mean diffusivity (MD) which can be calculated by taking the average of the eigenvalues:

$$MD = \frac{\left(\lambda_1{}^2 + \lambda_2{}^2 + \lambda_3{}^2\right)}{3}$$

In order to provide information on what factors affected FA, other measures were calculated from the eigenvalues—axial diffusivity (AD) and radial diffusivity (RD). AD is characteristic of axonal degeneration in general (Table 4) and is defined as the diffusivity that is measured in parallel with the fiber or tract.

$$AD = \lambda_1$$

RD is more specifically suggestive of demyelination (Table 4) and is the average diffusivity that is measured perpendicularly to the fiber or tract.

$$RD = \frac{(\lambda_1{}^2 + \lambda_2{}^2)}{2}$$

Overall, a growing body of studies conducted in animals has demonstrated that these DTI measures are associated with significant alterations in white matter, as summarized in Table 4.

Table 4. Possible Physiological Significance of Changes in White Matter Integrity in Animal Studies

White Matter Changes	Physiological Interpretation
Decreases in FA	Indicative of general tissue loss[1, 2, 3, 10]
Increases in MD	Indicative of general increases in water diffusion[6]
Decreases in AD	Suggests the presence of axonal degeneration[4, 5, 7, 8, 9]
Increases in RD	Specifically suggestive of demyelination[4, 5, 7, 8, 9]

References: [1]Boska, M. D., Hasan, K. M., Kibuule, D., Banerjee, R., McIntyre, E., Nelson, J. A., … Mosley, R. L. (2007). Quantitative diffusion tensor imaging detects dopaminergic neuronal degeneration in a murine model of Parkinson's disease. *Neurobiology of Disease, 26*(3), 590-596. [2]Bennet, R. E., MacDonald, C. L., & Brody, D. L. (2012). Diffusion tensor imaging detects axonal injury in a mouse model of repetitive closed-skull traumatic brain injury. *Neuroscience Letters, 513*(2), 160-165. [3]Ruest, T., Holmes, W. M., Barrie, J. A., Griffiths, I. R., Anderson, T. J., Dewar, D., & Edgar, J. M. (2011). High-resolution diffusion tensor imaging of fixed brain in a mouse model of Pelizaeus–Merzbacher disease: comparison with quantitative measures of white matter pathology. *NMR in Biomedicine, 24*(10), 1369-1379. [4]Song, S., Sun, S., Ju, S., Lin, S., Cross, A. H., & Neufeld, A. H. (2003). Diffusion tensor imaging detects and differentiates axon and myelin degeneration in mouse optic nerve after retinal ischemia. *NeuroImage, 20*, 1714-722. [5]Sun, S., Liang, H., Cross, A. C., & Song, S. (2008). Evolving Wallerian degeneration after transient retinal ischemia in mice characterized by diffusion tensor imaging. *Neuroimage, 40*(1), 1-10. [6]Shu, X., Qin, Y., Zhang, S., Jiang, J., Zhang, Y., Zhao, L., … & Zhu, W. (2013). Voxel-based diffusion tensor imaging of an app/ps1 mouse model of Alzheimer's disease. *Molecular Biology, 48*, 78-83. [7]Sun, S., Liang, H., Le, T. Q., Armstrong, R. C., Cross, A. C., & Song, S. (2006). Differential sensitivity of in vivo and ex vivo diffusion tensor imaging to evolving optic nerve injury in mice with retinal ischemia. *NeuroImage, 32*, 1195-1204. [8]Sun, S., Liang, H., Schmidt, R. E., Cross, A. C., & Song, S. (2007). Selective vulnerability of cerebral white matter in a murine model of multiple sclerosis detected using diffusion tensor imaging. *Neurobiology of Disease, 28*(1), 30-38. [9]Sun, S., Song, S. Harms, M. P., Lin, A., Holtzman, D., Merchant, K. M., & Kotyk, J. J. (2005). Detection of age-dependent brain injury in a mouse model of brain amyloidosis associated with Alzheimer's disease using magnetic resonance diffusion tensor imaging. *Neuroimage, 191*(1), 77-85. [10]Tyszka, J. M., Readhead, C., Bearer, E. L., Pautler, R. G., & Jacobs, R. E. (2006). Statistical diffusion tensor histology reveals regional dysmyelination effects in the shiverer mouse mutant. *NeuroImage, 29*(4), 1058-1065.

Regions of Interest Analysis (ROI) Measures and Analysis

A detailed examination of the cingulum bundle fiber and 11 cortico-cortico tracts was performed. Regions of interest were localized using DTI and hand drawn using DTI Studio and by utilizing anatomical landmarks and the white matter atlas. Tissue integrity was assessed by several measures including fractional anisotropy FA, MD, RD and AD.

The structures that were analyzed included the anterior cingulum, posterior cingulum, genu of the corpus callosum, splenium of the corpus callosum, the body of the corpus callosum, anterior segment of the corona radiata, corticospinal tract, superior longitudinal fasciculus, posterior segment of the corona radiata, forceps minor, external capsule, forceps major and the sagittal stratum.

White Matter Tracts Evaluated in Analyses

Anterior Cingulum

Slice identification began with the inferior most slice using the B0 image and moved superiorly through the slices until the slice was found in which the genu and splenium of the corpus callosum (CC) were visible in the anterior and posterior midline respectively, forming arch-like shapes. The genu of the CC should form a U-like shape and the splenium of the CC should resemble an upside down U-like shape. If the slice was chosen too inferiorly the splenium of the CC will not be visible and if the slice was choen too superiorly the arches will become V-like shaped. For reference, the anterior horn of the lateral ventricle is located posteriorly to the genu and the lateral ventricle body should be located anteriorly to the splenium. These are notable markers because the cerebrospinal fluid in the ventricles has a significantly different appearance than that of the surrounding structures on the B0 image (Figure 1).

Figure 1. This figure shows the three regions of interest placed bilaterally within the anterior cingulum on the B0 map. The regions of interest are represented by the white circles and the red arrow points to the right anterior cingulum.

Figure 1. Anterior Cingulum: B0 map image

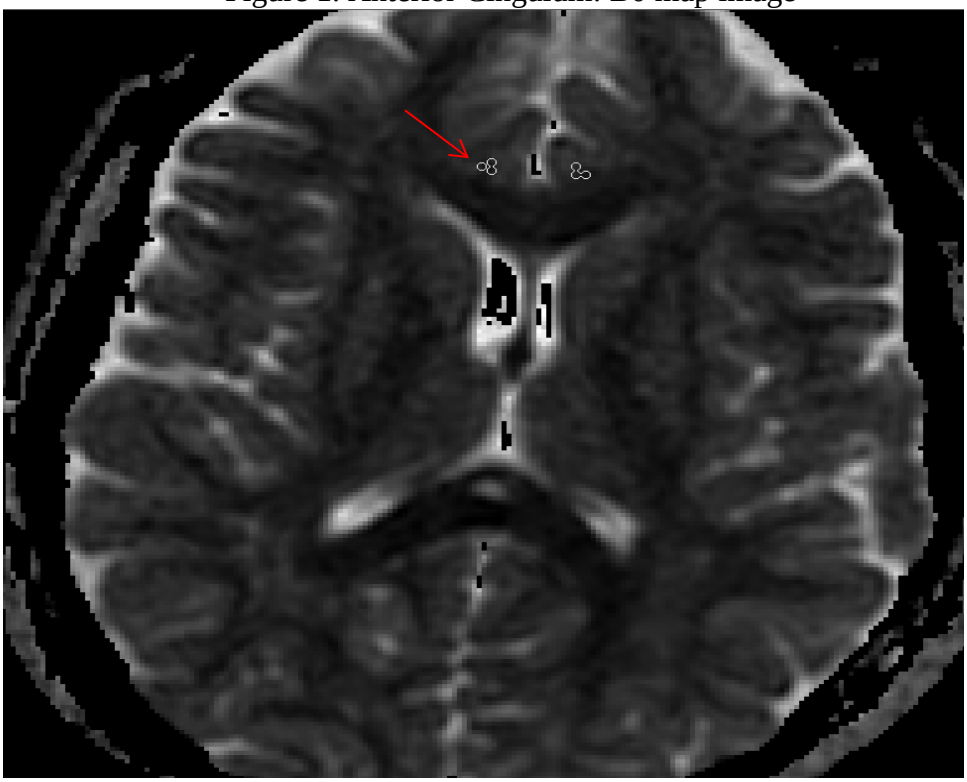

If there was more than one slice that met the above criteria, then the Color map was used to better visualize the CC regions more clearly. The slice in which the arches that constitute the genu and splenium were clearly rounded and not pointed in the center was chosen. The center of the arch should be more transversely oriented than the legs of the arch which should appear to be obliquely oriented. If the slices were still ambiguous then the slice that had the fornix visible in the near exact center of the slice was chosen. The fornix should be clearly identified by its inferior-superior orientation and should be anteriorly and posteriorly surrounded by ventricular space. The ROI was 16.78 mm^3 with each voxel being 1.28 mm and each ROI being 2 voxels in diameter. Three ROIs were placed on the left and right cingulum each. The cingula on this slice represent the most

anterior hemispheric crossing of the cingula and are located anteriorly and bilaterally on the lateral portions of the genu. The cingula are identifiable by their inferior-superior orientation. The first ROI was placed on the left anterior cingulum using the Color map (Figure 2) where the highest superior-inferior value was in the top right corner of the voxel.

Figure 2. This figure shows the three regions of interest placed bilaterally within the anterior cingulum on the Color map. The regions of interest are represented by the white circles and the red arrow points to the right anterior cingulum.

Figure 2. Anterior Cingulum: Color map image

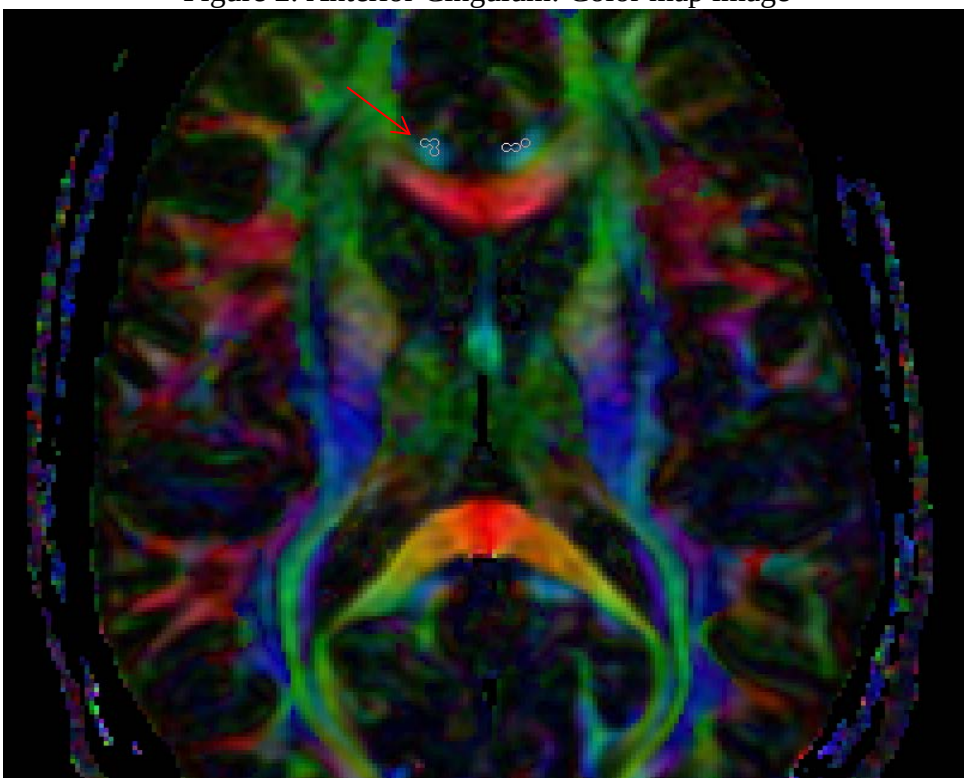

The Eigenvector1 map (Figure 3) was then used to move the first ROI away from the corpus callosum by at least one row laterally and posteriorly. The second ROI was then placed using the Color map in the location proximal to the first ROI, flush but not touching that had the highest average superior-inferior values on the Color map not

including the posterior location. The Eigenvector1 map was then used to move the second ROI away from the corpus callosum by at least one row laterally and posteriorly. If there was room for a third ROI in to be placed in the cingulum, it was placed in the same manner as the second except it could be anterior, medial or lateral to the first or second ROI on the Color map. The Eigenvector1 map was then used to move the second ROI away from the corpus callosum by at least one row laterally and posteriorly. If the only location the third ROI would fit within the cingulum was posteriorly to the first or second ROI then it was placed there. However if there was no room for a third ROI, then the superior slice was chosen and the third ROI was placed there in the same manner as the first was placed on the inferior slice. Rarely only the first ROI fit in the cingulum on the ideal slice. In this case, the slice superior was chosen for the second and first ROI and they were placed the same way the first ROI and second ROI would be placed on the inferior slice respectively.

Figure 3. This figure shows the three regions of interest placed bilaterally within the anterior cingulum on the Eigenvector1 map. The regions of interest are represented by the white circles and the red arrow points to the right anterior cingulum.

Figure 3. Anterior Cingulum: Eigenvector1 Map

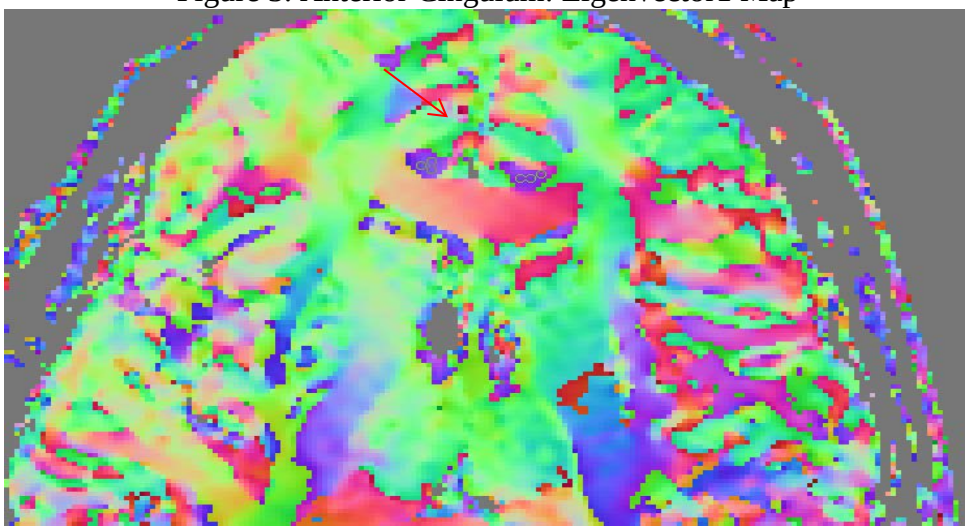

Posterior Cingulum

Beginning with the superior most slice using the B0 image, we moved inferiorly through the slices until the slice was found in which the hippocampus is visible at the CA1 region in the right and left hemispheres. The hippocampal region was identified using several anatomical markers. The hippocampi on this slice appear to be roughly circular regions of grey matter structure and are particularly defined by the inferior horn of the lateral ventricle that circumscribes the anterior and anterior-medial portions of the structure. This is a notable marker because the cerebrospinal fluid in the lateral ventricle has a significantly different appearance than that of the surrounding grey matter on the B0 image. Another significant anatomical marker on this slice is the midbrain which is located in the center of the slice medial to both hippocampi and forms a unique butterfly shape (parts of the midbrain visible on this slice include crus cerebri, substantia nigra and medial lemniscus. The parahippocampal gyri should also be visible on the B0 image posterior to the hippocampi (Figure 4).

Figure 4. This figure shows the three regions of interest placed bilaterally within the posterior cingulum on the B0 map. The regions of interest are represented by the white circles and the red arrow points to the right posterior cingulum.

Figure 4. Posterior Cingulum: B0 map image

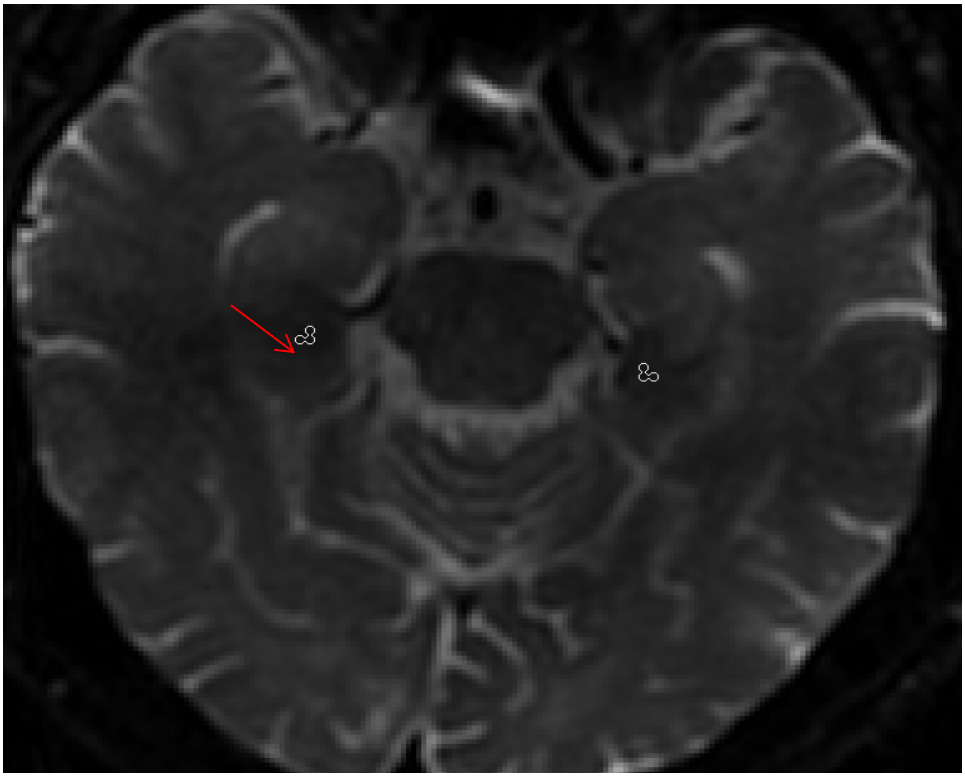

After identifying this slice, the Color map was used to find the cingulum in the right and left hemispheres. For reference, the butterfly shape should still be visible in the center of the slice and the visible structures which make it up should include the cerebral peduncle, midbrain and superior cerebral peduncle and sometimes the decussation of the superior cerebral peduncle which crosses in transverse orientation through this slice. The cerebellar hemisphere should also be visible and is located posteriorly to the midbrain and has an orientation partly between lateral-medial and inferior-superior. The cerebellar hemisphere also has a distinct X-like shape with its branches curving anteriorly toward the midbrain. The cingulum is located bilaterally in the left and right hemispheres. The

cingulum is located medially and slightly posteriorly to the hippocampus which appears to be a dark semi-spherical region on the Color map (Figure 5). The parahippocampal gyrus is located medially to the cingulum and also appears as dark space on the Color Map. The cingulum is located laterally to the cerebral peduncle which makes up the portion of the midbrain that appears to be the butterfly's upper wing. If there appeared to be more than one slice with a butterfly shape, then the slice in which the middle cerebral peduncle was chosen was chosen. If no butterfly shaped midbrain showed the middle cerebral peduncle on its anterior portion then the slice where the decussation of the superior cerebral peduncle was visible was chosen. The cingulum is identifiable by its predominantly inferior-superior orientation. The slice that met all of the above criteria was chosen and three regions of interest (ROIs) on the left and then the right cingulum were placed. The ROI was 16.78 mm^3 with each voxel being 1.28 mm and each ROI being 2 voxels in diameter. Using the Color map the first ROI was placed in the center of the cingulum. The second ROI was placed posteriorly to the first, flush but not overlapping. The third ROI was placed laterally to the second, flush but not overlapping. If the cingulum was small, so that the second and third ROI would be positioned outside the cingulum or extremely proximal to its edge, then the first ROI was moved anteriorly in the cingulum. In this way the second and third ROI would be placed within the cingulum.

Figure 5. This figure shows the three regions of interest placed bilaterally within the posterior cingulum on the Color map. The regions of interest are represented by the white circles and the red arrow points to the right posterior cingulum.

Figure 5. Posterior Cingulum: Color map image

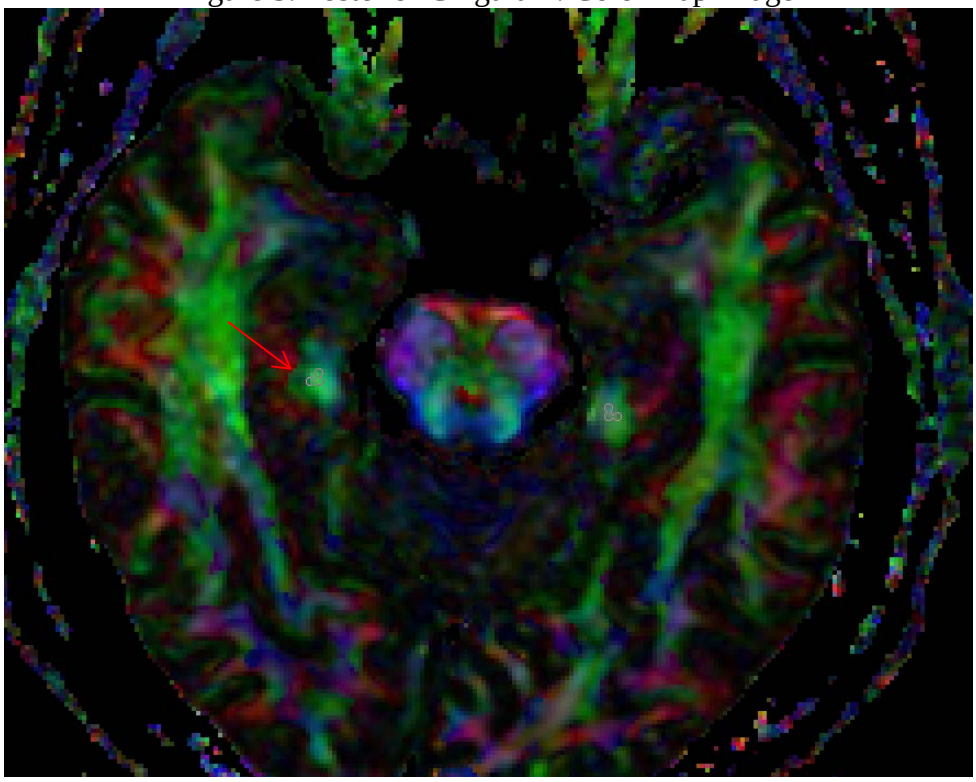

Genu of the Corpus Callosum

We began with the superior most slice of the brain and moved inferiorly using the Color map until there was a clear visualization of the genu of the corpus callosum (gCC). The ideal slice was considered to be the one in which the gCC was visible as a "U"-like shape in the anterior medial portion of the slice. The fornix was also preferentially in the medial midpoint of the slice. It appeared to be a small superiorly-inferiorly oriented or anteriorly-posteriorly oriented oval shaped region. However, in some subjects no fornix was visible. If there were multiple slices in which the gCC was visible and the fornix was also present, the slice with the clearest transverse orientation and visibility of the gCC was chosen. The gCC can be further identified by its location relative to the ACR.

It is flush with the ACR which is located laterally to the structure bilaterally. The ROI was 262.14 mm^3 with each voxel being 1.28 mm and each ROI being 5 voxels in diameter. A single ROI was placed in the midline portion of the gCC in the center of the structure (Figure 6).

Figure 6. This figure shows the region of interest placed centrally within the genu of the corpus callosum on the Color map. The region of interest is represented by the white circle and the red arrow points to the center of the genu of the corpus callosum.

Figure 6. Genu of the Corpus Callosum

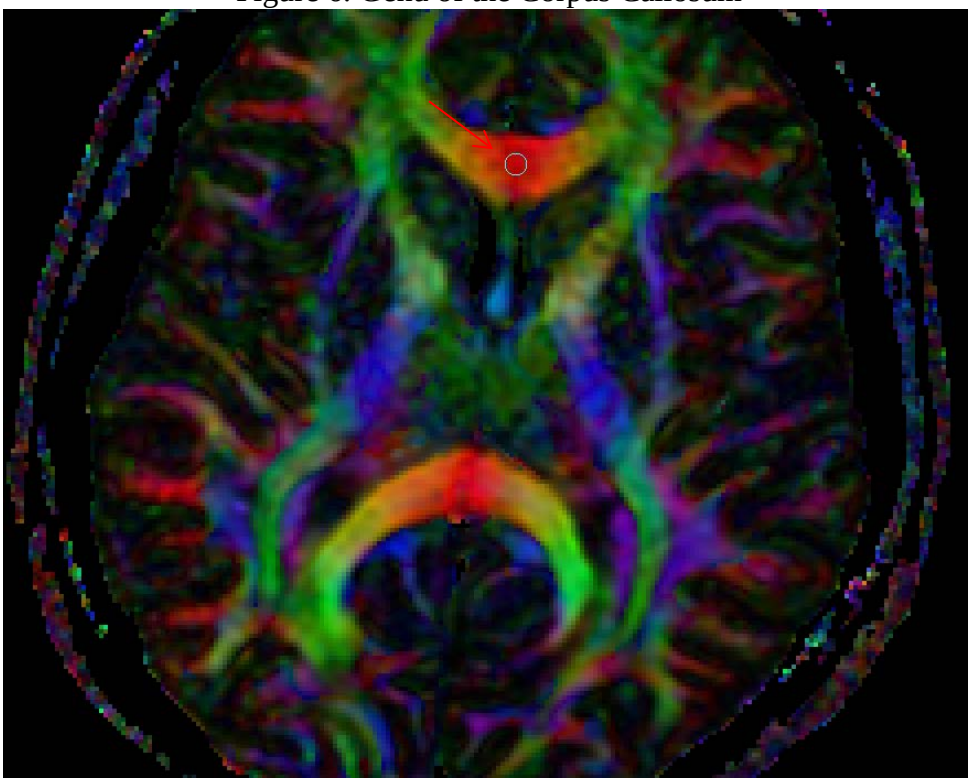

Splenium of the Corpus Callosum

Slice identification began with the superior most slice of the brain and moved inferiorly using the Color map until there was a clear visualization of the sCC. The ideal slice was considered to be the one in which the sCC was visible as an arch-like shape in the posterior medial portion of the slice; with its peak in the anterior most portion of the

structure. The fornix was also preferentially in the medial midpoint of the slice. It appeared to be a small superiorly-inferiorly oriented or anteriorly-posteriorly oriented oval shaped region. However, in some subjects no fornix was visible. If there were multiple slices in which the sCC was visible and the fornix was also present, the slice with the clearest transverse orientation and visibility of the sCC was chosen. The sCC can be further identified by its location relative to the posterior thalamic radiation (PTR). It is flush with the PTR which is located laterally to the structure bilaterally. The ROI was 262.14 mm^3 with each voxel being 1.28 mm and each ROI being 5 voxels in diameter. A single ROI was placed in the midline portion of the sCC in the center of the structure (Figure 7).

Figure 7. This figure shows the region of interest placed centrally within the splenium of the corpus callosum on the Color map. The region of interest is represented by the white circle and the red arrow points to the center of the splenium of the corpus callosum.

Figure 7. Splenium of the Corpus Callosum

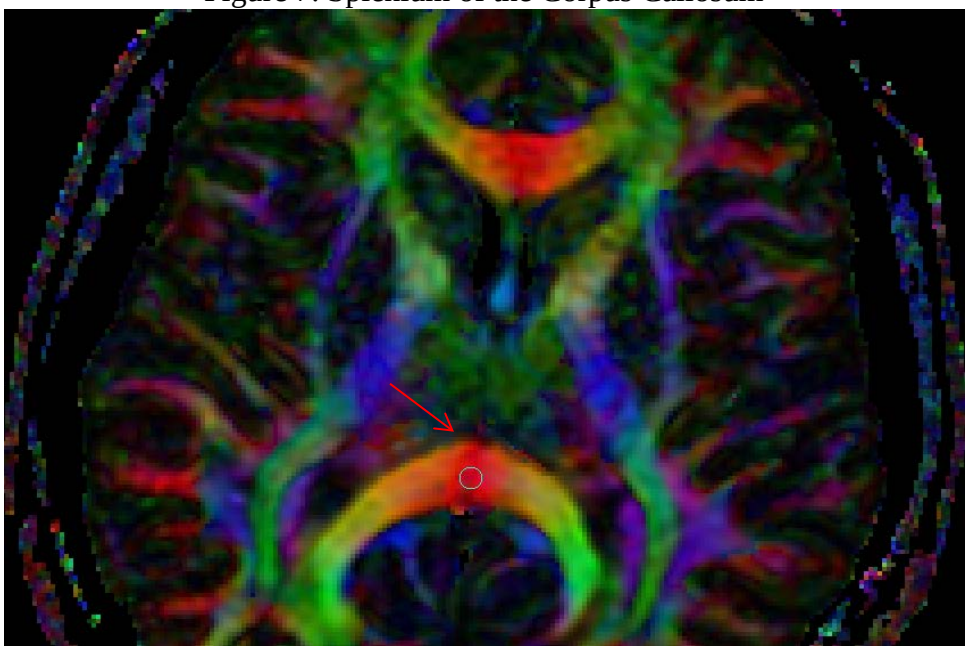

Body of the Corpus Callosum

Slice identification began with the superior most slice of the brain and moved inferiorly using the Color map until there was a clear visualization of the bCC. The ideal slice was considered to be the one in which the bCC was located in the center of the brain, arching with its peak in the most medial midpoint location on the slice and with its branches extending laterally; one anteriorly and the other posteriorly into the splenium of the corpus callosum (sCC). This configuration was visible bilaterally, with the left and right bCCs barely crossing each other at the midline. For reference, the superior corona radiata was also visible extending bilaterally from the tips of the anterior lateral branches of the bCCs to the sCC in a straight line. The ROI was 262.14 mm^3 with each voxel being 1.28 mm and each ROI being 5 voxels in diameter. One ROI was placed at the peak of the left bCC (Figure 8). This constituted its most medial portion. The bCC was further identified by its transverse orientation. The ROI was placed preferentially lateral to the midline while still remaining within the medial portion of the bCC in order to avoid the crossing fibers of the left and right bCCs located at the midline. An additional ROI was then placed on the right bCC using the same criteria for identification as the left bCC.

Figure 8. This figure shows the regions of interest placed bilaterally within the body of the corpus callosum on the Color map. The regions of interest are represented by the white circles and the red arrow points to the center of the right body of the corpus callosum.

Figure 8. Body of the Corpus Callosum

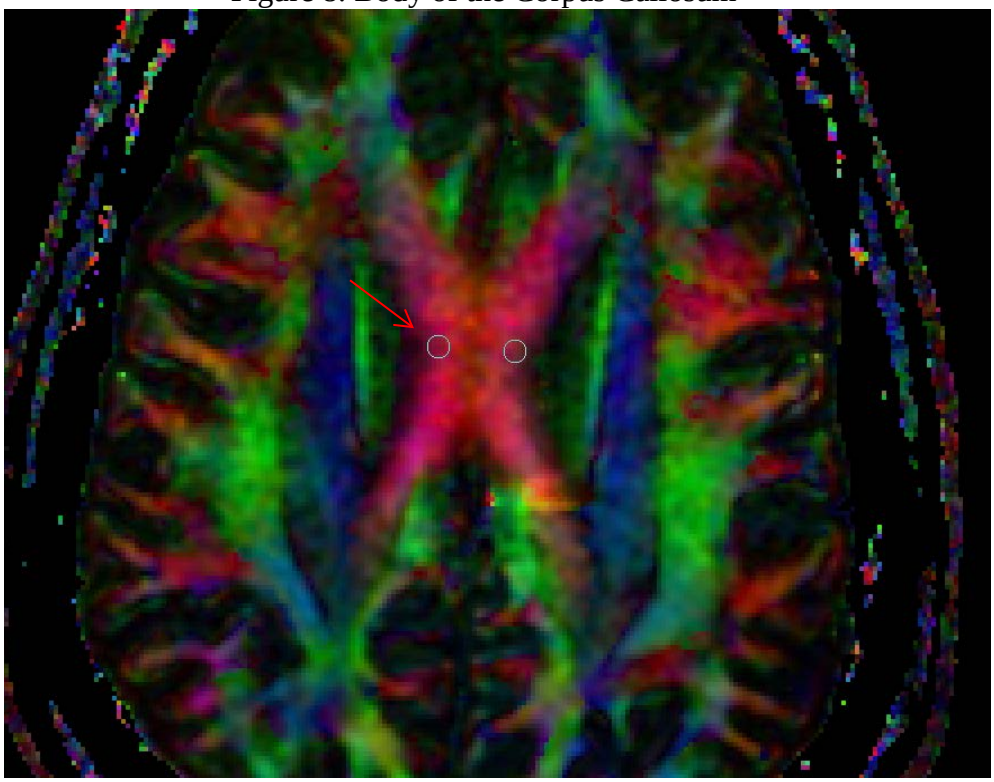

Anterior Segment of the Corona Radiata

Slice identification began with the superior most slice of the brain and moved inferiorly using the Color map until there was a clear visualization of the body of the corpus callosum (bCC). The ideal slice was considered to be the one in which the bCC was located in the center of the brain, arching with its peak in the most medial midpoint location on the slice and with its branches extending laterally; one anteriorly and the other posteriorly into the splenium of the corpus callosum (sCC). This configuration was visible bilaterally, with the left and right bCCs barely crossing each other at the midline. With some subjects, it was necessary to move a slice inferior or superior to the slice described above in order to get the optimal view of the anterior segment of the corona

radiata (ACR). The region of interest (ROI) was 262.14 mm^3 with each voxel being 1.28 mm and each ROI being 5 voxels in diameter. One ROI was placed just anteriorly and slightly laterally to the most anterior portion of the left bCC (Figure 9). For additional reference, the ROI was positioned anteriorly and medially to the superior corona radiata and anteriorly and laterally to the anterior cingulum. The ACR was further identified by its anterior-posterior and superior-inferior orientation. An additional ROI was then placed on the right ACR using the same criteria for identification as the left ACR.

Figure 9. This figure shows the regions of interest placed bilaterally within the anterior segment of the corona radiata on the Color map. The regions of interest are represented by the white circles and the red arrow points to the center of the right anterior segment of the corona radiata.

Figure 9. Anterior Segment of the Corona Radiata

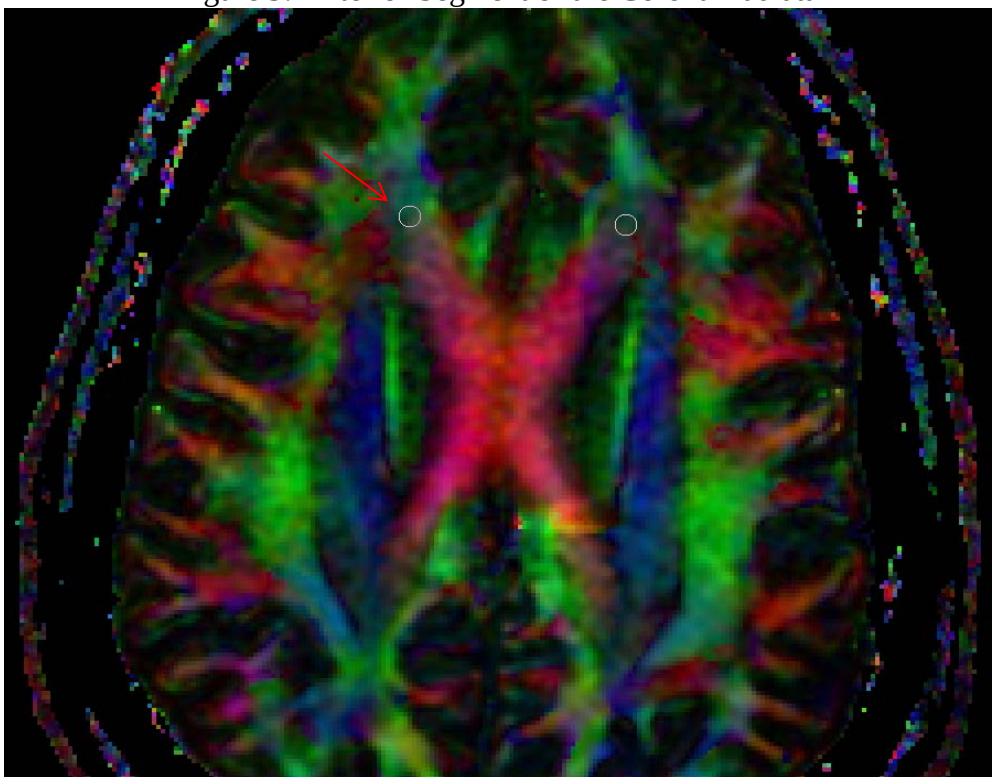

Corticospinal Tract

Slice identification began with the superior most slice of the brain and moved inferiorly using the Color map until there was a clear visualization of the bCC. The ideal slice was considered to be the one in which the bCC was located in the center of the brain, arching with its peak in the most medial midpoint location on the slice and with its branches extending laterally; one anteriorly and the other posteriorly into the splenium of the corpus callosum (sCC). This configuration was visible bilaterally, with the left and right bCCs barely crossing each other at the midline. The corticospinal tract (CST) was located within the superior corona radiata which was visible extending bilaterally from the tips of the anterior lateral branches of the bCCs to the sCC in a straight line. It was identified by its superior-inferior orientation. With some subjects it was necessary to move to an inferior or superior slice in order to avoid the transverse orientations of the superior corona radiata. The ROI was 262.14 mm^3 with each voxel being 1.28 mm and each ROI being 5 voxels in diameter. The first ROI was placed in the midpoint of the left superior corona radiata and laterally from the most medial portion of the bCC (Figure 10). An additional ROI was placed on the right CST using the same criteria for the left CST.

Figure 10. This figure shows the regions of interest placed bilaterally within the corticospinal tract on the Color map. The regions of interest are represented by the white circles and the red arrow points to the center of the right corticospinal tract.

Figure 10. Corticospinal Tract

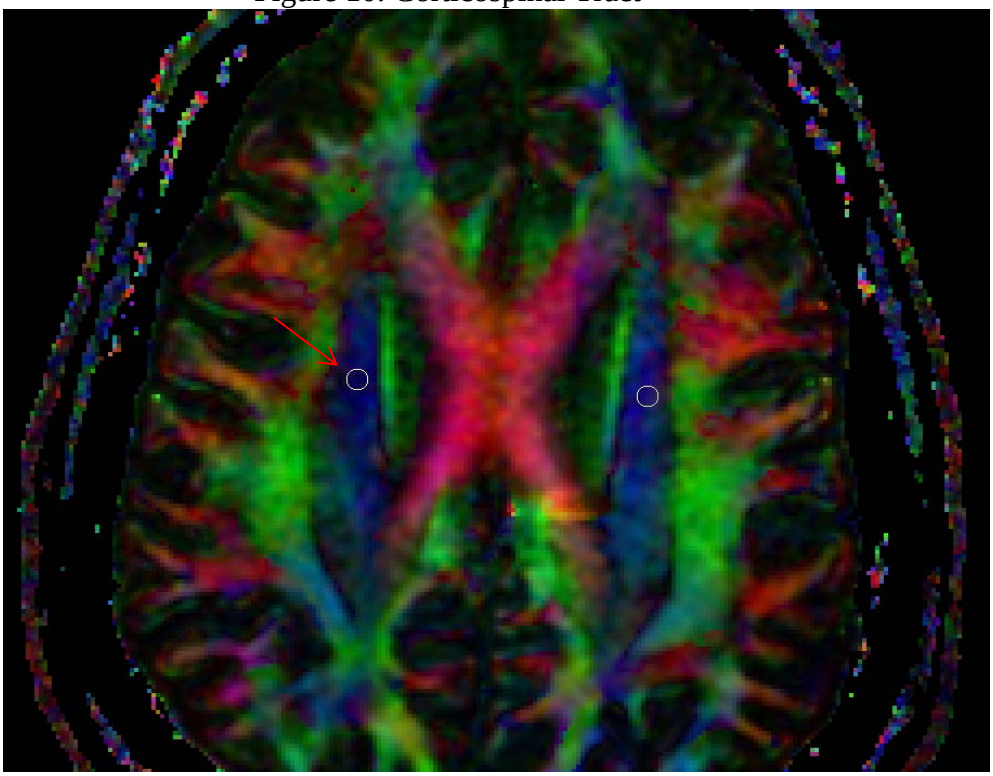

Superior Longitudinal Fasciculus

Slice identification began with the superior most slice of the brain and moved inferiorly using the Color map until there was a clear visualization of the bCC. The ideal slice was considered to be the one in which the bCC was located in the center of the brain, arching with its peak in the most medial midpoint location on the slice and with its branches extending laterally; one anteriorly and the other posteriorly into the splenium of the corpus callosum (sCC). This configuration was visible bilaterally, with the left and right bCCs barely crossing each other at the midline. The superior longitudinal fasciculus (SLF) is located laterally to and flush with the posterior portion of the superior corona radiata bilaterally. It was identified by its anterior-posterior orientation. With some

subjects it was necessary to move to a superior or inferior slice in order to get the best view of the SLF. Often the right and left ROIs were placed on two different slices due to tilting in the images. The optimal slice was chosen based on the visualization of the largest portion of the SLF extending anterior to posterior. The ROI was 262.14 mm^3 with each voxel being 1.28 mm and each ROI being 5 voxels in diameter. The first ROI was placed on the left SLF directly in the center of the structure and the right was then placed similarly (Figure 11).

Figure 11. This figure shows the regions of interest placed bilaterally within the superior longitudinal fasciculus on the Color map. The regions of interest are represented by the white circles and the red arrow points to the center of the right superior longitudinal fasciculus.

Figure 11. Superior Longitudinal Fasciculus

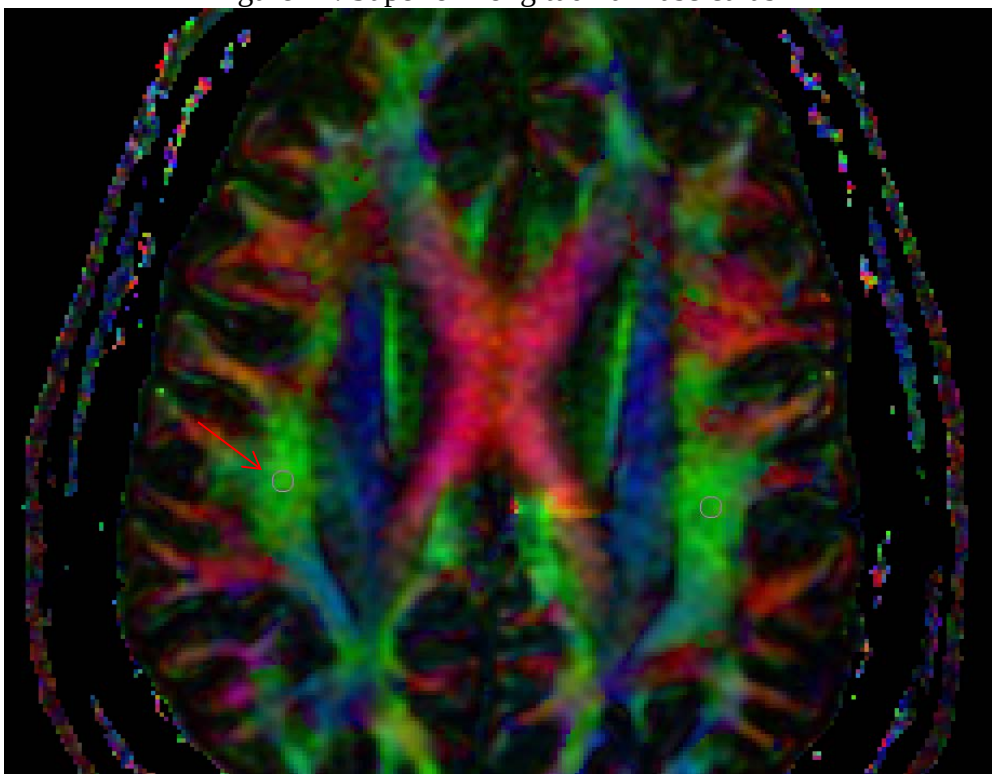

Posterior Segment of the Corona Radiata

Slice identification began with the superior most slice of the brain and moved inferiorly using the Color map until there was a clear visualization of the bCC. The ideal

slice was considered to be the one in which the bCC was located in the center of the brain, arching with its peak in the most medial midpoint location on the slice and with its branches extending laterally; one anteriorly and the other posteriorly into the splenium of the corpus callosum (sCC). This configuration was visible bilaterally, with the left and right bCCs barely crossing each other at the midline. The posterior segment of the corona radiata (PCR) was located posteriorly and slightly medially to the sCC and posteriorly and slightly laterally from the posterior cingulum. It was further identified by its anterior-posterior orientation. In some subjects the PCR was not visible on the described slice and it was necessary to move to a slice inferior or superior in order to locate the PCR. The ROI was 56.62 mm^3 with each voxel being 1.28 mm and each ROI being 3 voxels in diameter. A ROI was placed on the left PCR in its most lateral portion, in the mid-point of the structure. A second ROI was placed on the in the same manner on the right PCR (Figure 12).

Figure 12. This figure shows the regions of interest placed bilaterally within the posterior segment of the corona radiata on the Color map. The regions of interest are represented by the white circles and the red arrow points to the center of the right posterior segment of the corona radiata.

Figure 12. Posterior Segment of the Corona Radiata

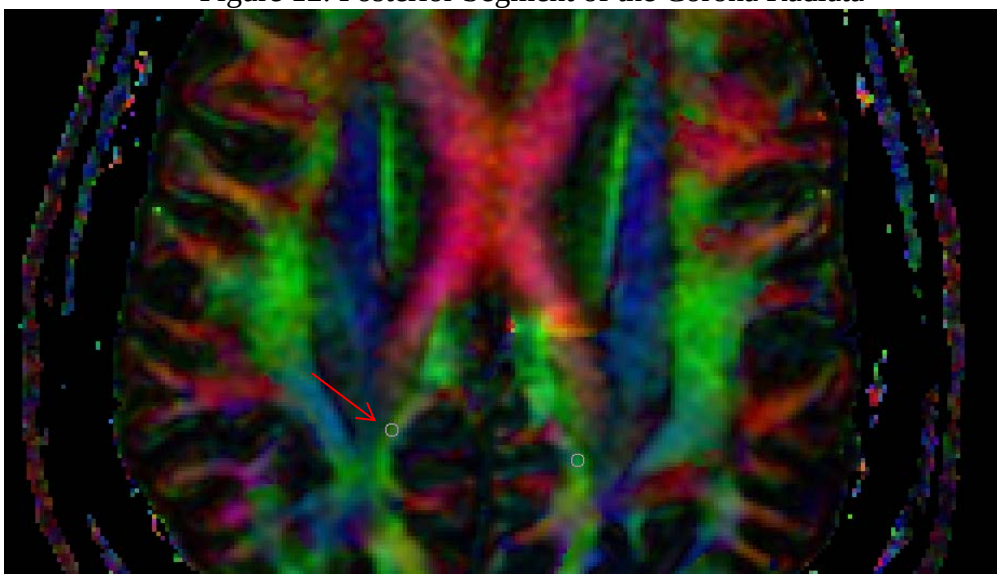

Forceps Minor

Slice identification began with the superior most slice of the brain and moved inferiorly using the Color map until there was a clear visualization of the genu of the corpus callosum (gCC). The ideal slice was considered to be the one in which the gCC was visible as a "U"-like shape in the anterior medial portion of the slice. The fornix was also preferentially in the medial midpoint of the slice. It appeared to be a small superiorly-inferiorly oriented or anteriorly-posteriorly oriented oval shaped region. However, in some subjects no fornix was visible. The forceps minor (fMin) was identified as the region flush with the lateral most parts of the gCC and within the point where the gCC and ACR meet. The fMin was further identified by its anterior-posterior orientation. The ROI was 262.14 mm^3 with each voxel being 1.28 mm and each ROI being 5 voxels in diameter. A ROI was placed on the left fMin just lateral to the lateral most part of the gCC and the second ROI was placed in the same way on the right fMin (Figure 13).

Figure 13. This figure shows the regions of interest placed bilaterally within the forceps minor on the Color map. The regions of interest are represented by the white circles and the red arrow points to the center of the right posterior forceps minor.

Figure 13. Forceps Minor

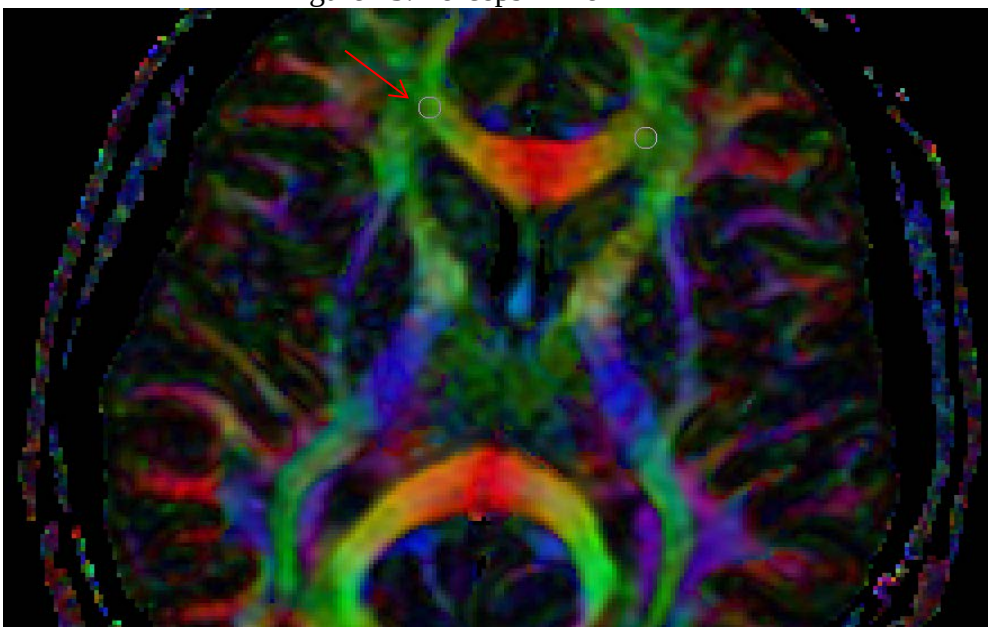

External Capsule

Slice identification began with the superior most slice of the brain and moved inferiorly using the Color map until there was a clear visualization of the genu of the corpus callosum (gCC). The ideal slice was considered to be the one in which the fornix was also preferentially in the medial midpoint of the slice. It appeared to be a small superiorly-inferiorly oriented or anteriorly-posteriorly oriented oval shaped region. However, in some subjects no fornix was visible. In this case the slice with the clearest transverse orientation and visibility of the gCC was chosen. If there was more than one slice with the fornix visible the slice in which the external capsule (ExtCap) was located most laterally was chosen. The ExpCap was defined as the structure connecting anteriorly branching from the ACR and the anterior limb of the internal capsule and posteriorly from the retrolenticular part of the internal capsule. It appears to be a branch

from these structures to form an arch which peaks in the most lateral portion of the structure. It was further defined by its superior-inferior and transverse orientation. The ROI was 56.62 mm^3 with each voxel being 1.28 mm and each ROI being 3 voxels in diameter. The first ROI was placed in the portion of the left ExtCap that was directly laterally to the fornix. If there was no fornix visible, then it was placed in the lateral most part of the structure. The second ROI was placed on the right ExtCap in the same manner (Figure 14).

Figure 14. This figure shows the regions of interest placed bilaterally within the external capsule on the Color map. The regions of interest are represented by the white circles and the red arrow points to the center of the right posterior external capsule.

Figure 14. External Capsule

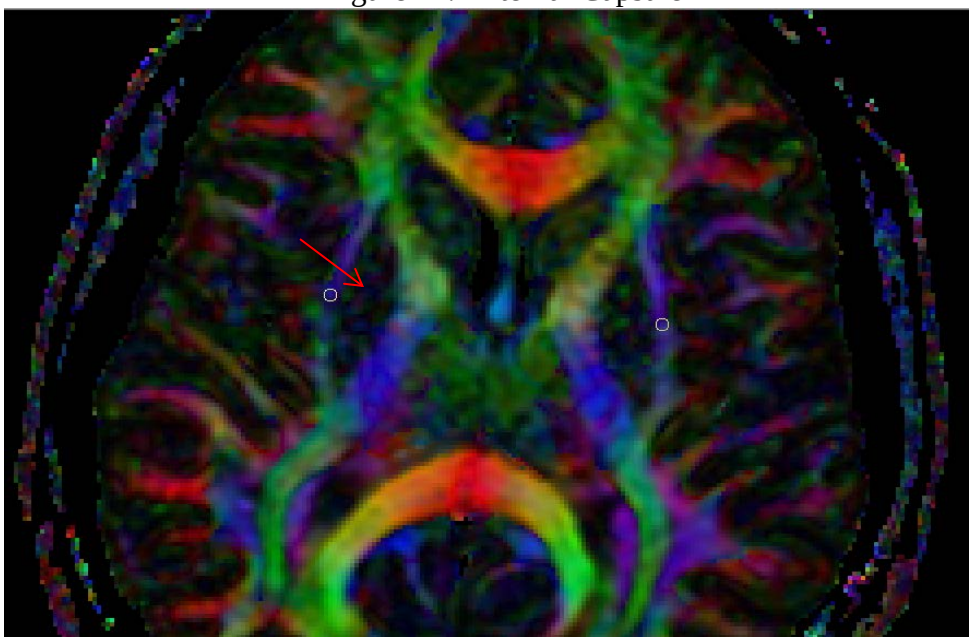

Forceps Major

Slice identification began with the superior most slice of the brain and moved inferiorly using the Color map until there was a clear visualization of the sCC. The ideal slice was considered to be the one in which the sCC was visible as an arch-like shape in the posterior medial portion of the slice; with its peak in the anterior most portion of the

structure. The fornix was also preferentially in the medial midpoint of the slice. It appeared to be a small superiorly-inferiorly oriented or anteriorly-posteriorly oriented oval shaped region. However, the fornix in some subjects was not visible and in a few subjects in the slice where the forceps major (fMaj) was most visible; the sCC was not entirely visible. The fMaj was defined as the location where the sCC and PTR meet. It was further identified by its anterior-posterior orientation. The ROI was 56.62 mm^3 with each voxel being 1.28 mm and each ROI being 3 voxels in diameter. A ROI was placed in this location on the left fMaj and then on the right in the same manner (Figure 15).

Figure 15. This figure shows the regions of interest placed bilaterally within the forceps major on the Color map. The regions of interest are represented by the white circles and the red arrow points to the center of the right posterior forceps major.

Figure 15. Forceps Major

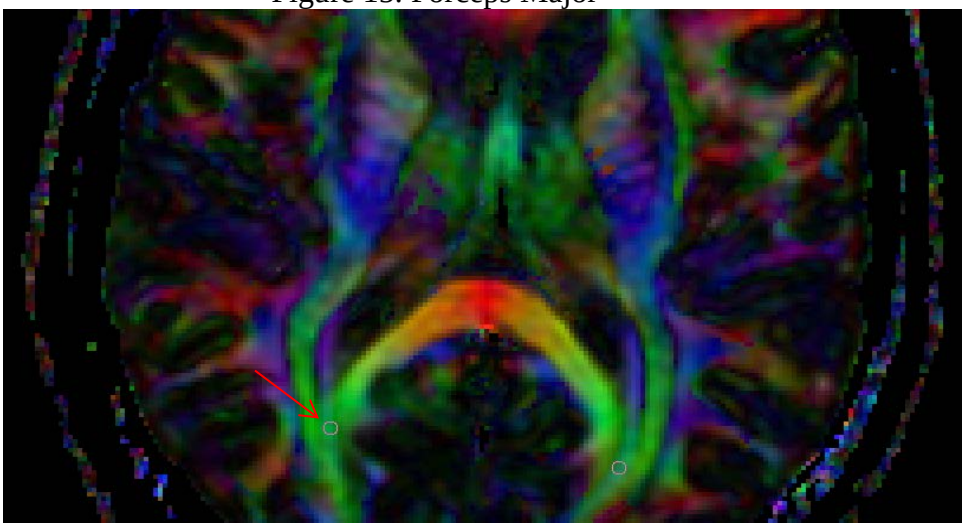

Sagittal Stratum

Slice identification began with the superior most slice of the brain and moved inferiorly using the Color map until there was a clear visualization of the optic tract located medially in the center of the slice running in a lateral-medial direction with a medial-lateral orientation. This structure is found in the same location that the fornix

would be in the superior slices and anterior to the midbrain in inferior slices. In some subjects the midbrain was visible on the ideal slice and in others the sCC or gCC was visible. The sagittal stratum was positioned posteriorly to the ExtCap, extreme capsule and claustrum and anteriorly to the PTR. It was positioned in the lateral portion of the slice and ran in an anterior-posterior direction with an anterior-posterior orientation. The ROI was 262.14 mm^3 with each voxel being 1.28 mm and each ROI being 5 voxels in diameter. A ROI was placed in the portion of the left SS that was directly below where the superior temporal gyrus white matter meets the SS. Then a second ROI was placed in the same manner on the left SS (Figure 16).

Figure 16. This figure shows the regions of interest placed bilaterally within the sagittal stratum on the Color map. The regions of interest are represented by the white circles and the red arrow points to the center of the right posterior sagittal stratum.

Figure 16. Sagittal Stratum

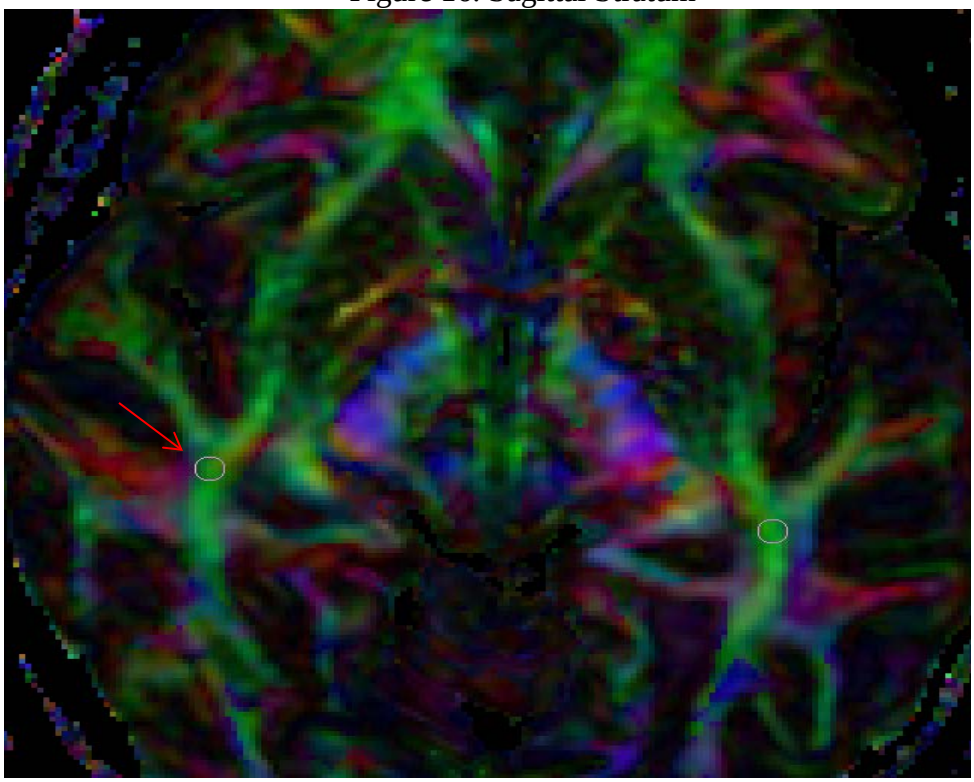

Compromised Results in Some Areas Resulting from Method Used to Assess White Matter Tracts

The background noise level selected in the measures was too high, as determined by the exclusion of white matter tissue in one subject. The high background threshold compromised the findings for all subjects. This is because the background noise level could have excluded white matter tissue from analysis, particularly in areas where the signal to noise ratio was already low. Areas that were especially susceptible to this bias include regions near the cerebrospinal fluid and brainstem. Therefore, the measures of the posterior cingulum—located proximal to cerebrospinal fluid and brainstem—in particular could have been biased by the high background noise level.

Statistical Analysis

A between subjects one-way analysis of variance (ANOVA) test was performed for the genu and splenium of the corpus callosum using FA as the primary dependent measure extracted from the DTI data to assess significant differences in white matter integrity in a-MCI cases versus controls. A mixed design two-way ANOVA test was also performed with one between subjects factor—between groups (a-MCI, controls) and one within subjects factor—between hemispheres (right and left) for those cortico-cortico tracts in which ROIs were placed bilaterally. These included the anterior segment of the corona radiata, the body of the corpus callosum, corticospinal tract, superior longitudinal fasciculus, posterior segment of the corona radiata, forceps minor, external capsule, forceps major and the sagittal stratum. For the anterior and posterior cingulum a mixed design three-way ANOVA was used for comparisons between groups, between hemispheres and between anterior and posterior cingulum. There was one between

subjects factor—between groups (a-MCI, controls) and two within subjects factors—between hemispheres (right and left) and between positions (anterior and posterior). Additional analyses determined Pearson's correlation coefficients to evaluate correlations of FA, MD, AD and RD values within the cingulum, with verbal memory performance on the CVLT-II. Correlations were determined between groups (collapsing across positions and hemispheres) in the cingulum, and also between groups for positions (collapsing across hemispheres). Correlations were also evaluated between FA values in the 11 cortico-cortico tracts and verbal memory performance on the CVLT-II. Correlations in the cortico-cortico tracts in which bilateral regions of interest had been placed were evaluated between groups (collapsing across hemispheres) and between groups for hemispheres.

CHAPTER THREE

Results

Measures extracted from diffusion tensor imaging (DTI) were used to assess differences in white matter integrity in the cingulum and 11 cortical tracts in a-MCI cases compared to controls. The primary measure of white matter integrity was fractional anisotropy (FA); however, other measures of diffusivity were calculated as well—mean diffusivity (MD), axial diffusivity (AD) and radial diffusivity (RD)—in order to provide information on what factors affected FA.

Participants

A total of 15 controls and 13 a-MCI cases were included in the analysis. The two groups were roughly matched for gender—Controls: 6 females and 9 males; a-MCI cases: 5 females and 8 males, with no significant differences in age, pre-morbid I.Q., or education level (Table 5).

Table 5. Participant Demographics and Verbal Memory Data

	Controls (n = 15)		a-MCI (n = 13)			
	M	SEM	M	SEM	F value	p value
Demographics Variables						
Age	72.33	0.49	72.00	0.47	0.24	.631
Pre-morbid I.Q.	115.40	2.50	108.77	3.58	2.40	.133
Education Level	16.73	0.53	16.62	0.58	0.02	.882
Verbal Memory Variable						
Total CVLT-II Total Score	57.40	1.78	53.46	2.11	2.06	.160

*p < .050

Note: a-MCI: amnestic mild cognitive impairment; M: mean; SEM: standard error of mean; CVLT-II: California Verbal Learning Test-second edition.

Neuropsychological Testing: CVLT-II

The CVLT-II (California Verbal Learning Test-second edition) is a measure of verbal memory. Although controls recalled on average 4 more words total than the a-MCI (refer to Table 5 above for means) there was no statistically significant difference between groups, $F(1,26) = 2.06$, $p = .163$. As depicted in Figure 17 below, there was a trend for better performance by controls on Trials 2-5 relative to the a-MCI but this was not found to be significantly different, nor did group membership affect the scores on any of the trials.

Figure 17. Average CVLT-II Score for Trials

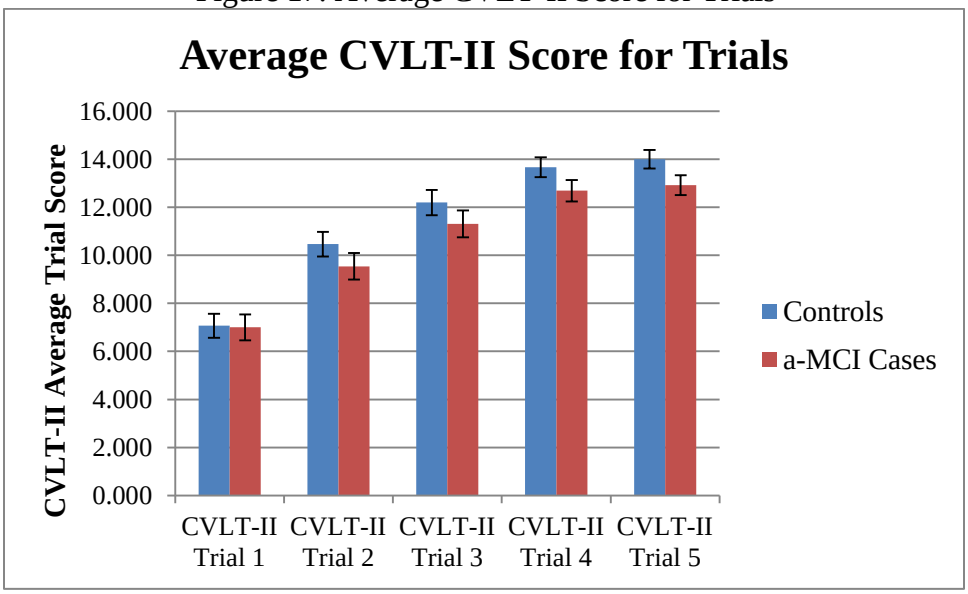

Results for the Analysis of the Cingulum

Statistical Assessment of Cingulum Integrity

For the anterior and posterior cingulum, a mixed design three-way analysis of variance (ANOVA) was used for comparisons between groups (controls, a-MCI), and within groups for the comparisons between hemispheres (left, right) and between

locations along the fiber bundle (anterior, posterior). The omnibus interaction was between groups, hemispheres and positions, but two way interactions and main effects were also evaluated for comparisons between factors or for each factor. FA was used as the primary dependent measure but the same analyses were also used to examine differences on MD, AD and RD. Findings that are relevant to the hypotheses investigated in this study and that were found to be significant or to approach significance are reported in this chapter; however, for a full report of our findings refer to the Appendix.

Main Effects Found in the Cingulum

There were no overall differences between controls and a-MCI cases in the cingulum for any DTI measure. Similarly, there were no laterality effects. There was a main effect of position (anterior, posterior) for all measures of white matter integrity. The FA for the anterior cingulum (M = .485, SEM = .014) was lower than that of the posterior cingulum (M = .613, SEM = .012; $F(1,26) = 47.21$, $p < .001$), and corresponded to an increase in MD in the anterior portion; ($M = 2.60*10^{-3}$, SEM = $3.58*10^{-5}$; $M = 2.50*10^{-3}$, SEM = $3.98*10^{-5}$), $F(1,26) = 6.94$, $p = .014$. Within this anterior region of interest, there was also a decrease (relative to the posterior region) in AD, $F(1,26) = 17.07$, $p < .001$ and an increase in RD, $F(1,26) = 37.12$, $p < .001$. The combination of findings suggests that FA of the anterior segment is lower than the posterior due in part to both degree of myelination (RD) and axonal length or density (AD) (Table 6). However, these results may have been compromised by the methods used to analyze the data. The posterior measures in particular were subject to bias from the background noise level that was chosen.

Table 6. Anterior versus Posterior Segments of the Cingulum: Differences in White Matter Integrity

	Anterior Cingulum		Posterior Cingulum			
Measures of WM Integrity	M	SEM	M	SEM	F value	p value
FA	0.485	0.014	0.613	0.012	42.21	<0.001**
MD	$2.60x10^{-3}$	$3.58x10^{-5}$	$2.50x10^{-3}$	$3.98x10^{-5}$	6.94	0.014**
AD	$1.39x10^{-3}$	$1.98x10^{-5}$	$1.50x10^{-3}$	$2.04x10^{-5}$	17.07	<0.001**
RD	$6.12x10^{-4}$	$1.67x10^{-5}$	$4.98x10^{-4}$	$1.79x10^{-5}$	37.12	<0.001**

**p< .050 for significant values;
*.050 < p < 0.10 for near significant values
Note: M: mean; SEM: standard error of mean; FA: fractional anisotropy; MD: mean diffusivity; AD: axial diffusivity; RD: radial diffusivity; WM: white matter

Alterations in Laterality within the Cingulum Fiber Bundle

There were significant interactions between group membership and hemisphere found for FA in the cingulum. The FA for controls in the right hemisphere (M = .561, SEM = .018) was higher than that of the left hemisphere (M = .552, SEM = .013) and the FA for a-MCI cases in the right hemisphere (M = .513, SEM = .019) was lower than that of the left hemisphere (M = .571, SEM = .014). The interaction was found to be significant, $F(1, 26)= 5.09$, $p = .033$). There was also an interaction between group membership and hemisphere found in the cingulum for RD, $F(1, 26)= 5.53$, $p = .027$. This suggests that for the controls there was lower FA in the left hemisphere and in the a-MCI cases there was lower FA in the right hemisphere due in part to degree of myelination (RD) (Table 7).

Table 7. Interactions between Groups and Hemispheres: Differences in White Matter Integrity in the Cingulum

		Right Hemisphere		Left Hemisphere			
	Measures of WM Integrity	M	SEM	M	SEM	F value	p value
Controls (n = 15)	FA	0.561	0.018	0.552	0.013		
	RD	$5.39x10^{-4}$	$2.23x10^{-5}$	$5.45x10^{-4}$	$1.70x10^{-5}$		
a-MCI (n = 13)	FA	0.513	0.019	0.571	0.014	5.09	0.033**
	RD	$6.01x10^{-4}$	$2.40x10^{-5}$	$5.33x10^{-4}$	$1.83x10^{-5}$	5.53	0.027**

**p< .050 for significant values;
*.050 < p < 0.10 for near significant values
Note: F values and p values represent interaction effects between groups and hemispheres. a-MCI: amnestic mild cognitive impairment; M: mean; SEM: standard error; FA: fractional anisotropy; RD: radial diffusivity. WM: white matter

There were no significant interactions between group membership and positions found for FA or any other measure of diffusivity in the cingulum. There were significant interactions between positions and hemispheres found for FA in the cingulum. The FA for anterior cingulum in the right hemisphere (M = .486, SEM = .017) was slightly higher than that of the left hemisphere (M = .485, SEM = .019) and the FA for the posterior cingulum in the right hemisphere (M = .588, SEM = .016) was lower than that of the left hemisphere (M = .638, SEM = .012; F(1, 26)= 4.67, p = .040). There was also an interaction between positions and hemispheres found in the cingulum for RD, F(1, 26) = 4.35, p = .047. This suggests that the posterior cingulum had lower FA in the right hemisphere and that there was little asymmetry in the anterior cingulum between hemispheres, due in part to the degree of myelination (RD) (Table 8).

There were no significant interactions found between group membership, positions and hemispheres for FA or any other measure of white matter integrity in the cingulum.

Table 8. Interactions between Positions and Hemispheres: Differences in White Matter Integrity in the Cingulum

	Measures of WM Integrity	Right Hemisphere M	Right Hemisphere SEM	Left Hemisphere M	Left Hemisphere SEM	F value	p value
Ant. Cing.	FA	0.486	0.017	0.485	0.019		
	RD	$6.12x10^{-4}$	$1.65x10^{-5}$	$6.11x10^{-4}$	$2.26x10^{-5}$		
Post. Cing.	FA	0.588	0.016	0.638	0.012	4.67	0.040*
	RD	$5.49x10^{-4}$	$2.12x10^{-5}$	$4.66x10^{-4}$	$1.37x10^{-5}$	4.35	0.047*

**p< .050 for significant values;
*.050 < p < 0.10 for near significant values
Note: F values and p values represent interaction effects between positions and hemispheres. Ant. Cing.: Anterior Cingulum; Post. Cing.: Posterior Cingulum; M: mean; SEM: standard error; FA: fractional anisotropy; RD: radial diffusivity. WM: white matter

Results for the Analysis of the Cortico-cortico Tracts

Overview of Results

A between subjects one-way ANOVA test was performed for the genu and splenium of the corpus callosum to assess significant differences in white matter integrity in a-MCI cases versus controls. A mixed design two-way ANOVA test was also performed with one between subjects factor—between groups (a-MCI, controls)—and one within subjects factor—between hemispheres (right, left)—for those cortico-cortico tracts in which ROIs were placed bilaterally; these included the anterior segment of the corona radiata (ACR), the body of the corpus callosum (bCC), corticospinal tract (CST), superior longitudinal fasciculus (SLF), posterior segment of the corona radiata (PCR), forceps minor (fMin), external capsule (ExCap), forceps major (fMaj) and the sagittal stratum (SS). Main effects were analyzed for group differences and across hemispheres. Interactions between group membership and hemispheres were analyzed as well. FA was

used as the primary dependent measure. Significant findings of main effects of group membership for FA were only found in the SS. Significant findings of main effects of hemisphere were found for FA in the CST and ExCap. No effects of interaction were found for FA in any of the cortico-cortico tracts.

Effects of Amnestic Mild Cognitive Impairment on White Matter Integrity Measures in the Cortico-cortico Tracts

There was a main effect for group differences found in the SS. The a-MCI cases (M = .582, SEM = .013) had significantly higher FA than the controls (M = .528, SEM = .012), $F(1,26) = 9.24$, $p = .005$. This suggested that the cases had a greater degree of white matter integrity in this structure. The a-MCI cases also ($M = 2.49*10^{-3}$, $SEM = 6.36*10^{-5}$) showed higher MD than the controls ($M = 2.66*10^{-3}$, $SEM = 5.92*10^{-5}$) which approached significance, $F(1,26) = 3.87$, $p = .060$. In contrast to the findings from the FA analysis, the increase in MD for a-MCI cases suggests more degeneration is present in this structure for a-MCI cases than controls. There was also a decrease in RD ($F(1,26) = 6.94$, $p = .014$) for a-MCI cases relative to controls in the SS. This finding suggests that the lower FA for controls is due in part to degree of myelination (RD). The only other cortical structure that approached significance in FA was the PCR. The a-MCI cases (M = .466, SEM = .014) had lower FA than the controls (M = .499, SEM = .013), although this difference only approached significance, $F(1,26) = 3.21$, $p = .085$. Refer to Table 9 for significant findings and findings that approached significance. No other main effects were found for group membership in any of the other cortico-cortico tracts.

Table 9. Controls versus Amnestic Mild Cognitive Impairment: Differences in White Matter Integrity in Cortico-cortico Tracts

Measures of WM Integrity	Cortico-cortico Tracts	Controls (n = 15) M	Controls (n = 15) SEM	a-MCI (n = 13) M	a-MCI (n = 13) SEM	F value	p value
FA	PCR	0.499	0.013	0.466	0.014	3.21	0.085*
	SS	0.528	0.012	0.582	0.013	9.24	0.005**
AD	SS	$2.66x10^{-3}$	$5.92x10^{-5}$	$2.49x10^{-3}$	$6.36x10^{-5}$	3.87	0.06*
MD	SS	$5.96x10^{-4}$	$2.00x10^{-5}$	$5.19x10^{-4}$	$2.15x10^{-5}$	6.94	0.014**
RD	SS	$5.96x10^{-4}$	$2.00x10^{-5}$	$5.19x10^{-4}$	$2.15x10^{-5}$	6.94	0.014**

**p< .050 for significant values;
*.050 < p < 0.10 for near significant values
Note: a-MCI: amnestic mild cognitive impairment; M: mean; SEM: standard error; FA: fractional anisotropy; MD: mean diffusivity; RD: radial diffusivity; WM: white matter; PCR: posterior segment of the corona radiata

Main Effects across Hemispheres for White Matter Integrity Measures in the Cortico-cortico Tracts

A main effect of hemisphere was found for FA in the CST and in the ExCap and both had significantly decreased FA in the right hemisphere. Other measures of diffusivity corroborated these findings as decreased AD and increased RD were found in the right hemisphere for both CST and Ex Cap. These findings suggest the right hemisphere for the CST and Ex Cap had greater axonal degeneration and demyelination. No other main effects were found across hemispheres in any of the other cortico-cortico tracts for FA. However, several of the other cortico-cortico tracts showed significant differences in measures of diffusivity across hemispheres.

Effects of Interaction between Groups and Hemispheres for Measures of White Matter Integrity in the Cortico-cortico Tracts

There were no significant interactions between group membership and hemisphere found for FA in any of the cortico-cortico tracts. However, interactions

between groups and hemispheres in the ACR approached significance for FA and were significant for RD. The mean FA value for the control group in the right hemisphere (M = .384, SEM = .019) was higher than that of the left hemisphere (M = .355, SEM = .018) and the mean FA value for the a-MCI group in the right hemisphere (M = .357, SEM = .020) was lower than that of the left hemisphere (M = .368, SEM = .019). This interaction was not quite significant, $F(1, 26) = 3.73$, $p = .065$. For RD, interactions between groups and hemispheres in the ACR were found to be significant, $F(1, 26) = 5.56$, $p = .026$. These findings suggest that both the controls and a-MCI cases showed asymmetry of hemisphere in the ACR. It also suggests that for the controls there was lower FA in the left hemisphere, while in the a-MCI cases there was lower FA in the right hemisphere; in part due to degree of myelination (RD) (Table 10).

Table 10. Interactions between Groups and Hemispheres: Differences in White Matter Integrity in Anterior Segment of the Corona Radiata

		Right Hemisphere		Left Hemisphere			
	Measures of WM Integrity	M	SEM	M	SEM	F value	p value
Controls (n = 15)	FA	0.384	0.019	0.355	0.018		
	RD	6.36×10^{-4}	1.94×10^{-5}	6.66×10^{-4}	1.77×10^{-5}		
a-MCI (n = 13)	FA	0.357	0.020	0.368	0.019	3.73	0.065*
	RD	6.64×10^{-4}	2.09×10^{-5}	6.50×10^{-4}	1.90×10^{-5}	5.56	0.026**

**p< .050 for significant values;
*.050 < p < 0.10 for near significant values
Note: F values and p values represent interaction effects between positions and hemispheres. a-MCI: amnestic mild cognitive impairment; M: mean; SEM: standard error; FA: fractional anisotropy; RD: radial diffusivity; WM: white matter

Correlations between Measures of White Matter Integrity and Verbal Memory

Overview

Analyses were performed to determine if performance on the CVLT-II was correlated with changes in white matter integrity in the cingulum. Since the CVLT-II was used as a measure of verbal memory and measures of white matter integrity are evaluated as representations of tissue integrity, the goal of this analysis was to determine if impairments in verbal memory were correlated with decreases in white matter integrity. Analysis of the cingulum included FA as the primary measure and MD, AD and RD as secondary measures of diffusivity. There were no significant correlations between the cingulum and the CVLT-II scores for a-MCI cases; however, there were significant correlations for controls between the cingulum, collapsing across hemispheres and positions, the anterior cingulum and the posterior cingulum and the CVLT-II scores for secondary measures. For the cortico-cortico tracts, analysis only included FA. Significant positive correlations were found between lower FA in the ACR for a-MCI and poorer performance on the CVLT-II. Significant negative correlations were found between higher FA in the SS for a-MCI and poorer performance on the CVLT-II. Significant negative correlations were also found between lower FA in the ExCap and SS for controls and better performance on the CVLT-II. Therefore, only the FA for the ACR supported the hypothesis that loss of white matter integrity would correlate with an assessment of poorer verbal memory.

Significant Bivariate Correlations in the Cingulum with CVLT-II scores

There were no significant correlations between the cingulum and the CVLT-II scores for a-MCI cases.

There were, however, several correlations between the controls and the CVLT-II scores. There was a significant correlation between trial two and FA in the cingulum collapsing across hemispheres and positions (cingulum) ($r = .569$, $p = .027$) and the anterior cingulum collapsing across hemispheres (anterior cingulum) ($r = .591$, $p = .020$). There was a significant correlation between MD in the cingulum and the total CVLT-II scores ($r = .566$, $p = .028$). There was also a significant correlation for MD between the posterior cingulum collapsing across hemispheres (posterior cingulum) and trial four ($r = .560$, $p = .030$) and approaching significance for trial five ($r = .513$, $p = .051$). There was a significant correlation between AD in the cingulum and the total CVLT-II scores ($r = .543$, $p = .036$). There were also significant correlations for AD between the posterior cingulum and trial four ($r = .653$, $p = .008$) and trial five ($r = .782$, $p = .001$). There were also a significant correlations for RD between trial two and the cingulum ($r = .609$, $p = .016$) and the anterior cingulum ($r = .595$, $p = .019$) (Table 11).

Table 11. Significant (and near-significant) Bivariate Correlations between Measures of Cingulum White Matter Integrity and Verbal Memory in Controls

Measures of WM Integrity	ROI	Total Score	Trial 1	Trial 2	Trial 3	Trial 4	Trial 5
FA	Cingulum			0.569**			
	Ant. Cingulum			0.591**			
MD	Cingulum	0.566**					
	Post. Cingulum					0.560**	0.513*
AD	Cingulum	0.543**					
	Post. Cingulum					0.653**	0.782**
RD	Cingulum			0.600**			
	Ant. Cingulum			0.595**			

**p< .050 for significant values;
*.050 < p < 0.10 for near significant values
Note: ROI: region of interest; FA: fractional anisotropy; MD: mean diffusivity; AD: axial diffusivity; RD: radial diffusivity; Post. Cingulum: Posterior Cingulum; Ant. Cingulum: anterior cingulum; WM: white matter

Significant Bivariate Correlations in the Cortico-cortico Tracts with CVLT-II scores

Additional analyses were performed on each cortical structure to determine correlations between FA and CVLT-II scores. Significant positive correlations were found for a-MCI cases between the ACR collapsing across hemispheres and trial three ($r = .577$, $p = .039$) and trial four ($r = .593$, $p = .033$). Significant positive correlations were found for a-MCI cases between the right ACR and trial three ($r = .554$, $p = .050$) and trial four ($r = .646$, $p = .017$). These correlations suggest there is a relationship between decreased white matter integrity in the ACR and poorer performance on the CVLT-II. A positive correlation approaching significance was found for a-MCI cases between the decreased FA in the left PCR and poorer performance on trial one ($r = .552$, $p = .056$). This suggests there may be a relationship between decreased white matter integrity in the PCR and poorer performance on the CVLT-II. A negative correlation

approaching significance was found for a-MCI between the increased FA in the ExCap collapsing across hemispheres and poorer performance on trial one ($r = .537$, $p = .058$). This suggests there may be a relationship between increased white matter integrity in the ExCap and poorer performance on the CVLT-II. A significant correlation was found for a-MCI cases between the SS collapsing across hemispheres and trial four ($r = .608$, $p = .028$). A significant correlation was also found for a-MCI between the left SS and trial four ($r = .613$, $p = .026$). These findings suggest that increases in white matter integrity in the SS were correlated with poorer performance on the CVLT-II (Table 12).

A correlation approaching significance was found for controls between the right CST and trial two ($r = .510$, $p = .052$). A significant correlation was found for controls between the ExCap collapsing across hemispheres and the total CVLT-II score ($r = .691$, $p = .004$). A significant correlation was found for controls between the left ExCap and the total CVLT-II score ($r = .608$, $p = .016$). A significant correlation was also found for controls between the right ExCap and the total CVLT-II score ($r = .556$, $p = .031$). Significant correlations were found for controls between the ExCap collapsing across hemispheres and trial three ($r = .563$, $p = .029$), trial four ($r = .754$, $p = .001$) and trial five ($r = .584$, $p = .022$). Significant correlations were found for controls between the left ExCap and trial three ($r = .525$, $p = .044$), trial four ($r = .649$, $p = .009$) and trial five ($r = .565$, $p = .028$). A significant correlation was found for controls between the right ExCap and trial four ($r = .629$, $p = .012$). A correlation approaching significance was found for controls between the ExCap collapsing across hemispheres and trial two ($r = .511$, $p = .051$). A significant correlation was found for controls between the SS collapsing across hemispheres and the total CVLT-II score ($r = .560$, $p = .030$). A

significant correlation was found for controls between the left SS and trial four (r = .598, p = .019). A correlation approaching significance was found for controls between the left SS and trial three (r = .487, p = .066). A correlation approaching significance was found for controls between the right SS and trial one (r = .511, p = .052) (Table 13). All of these cortico-cortico tracts for which significant (and near significant) findings are listed had decreased FA as compared to a-MCI cases. Contrary to what was expected, these correlations suggest that the decrease in white matter integrity within these regions correlates with better verbal memory.

Table 12. Bivariate Correlations in Cortico-cortico Tracts with California Verbal Learning Test-Second Edition Scores

	Hemi-sphere	ROI	Total Score	Trial 1	Trial 2	Trial 3	Trial 4	Trial 5
a-MCI (n = 13)		ACR				0.577**	0.593**	
	Right	ACR				0.554**	0.646**	
	Left	PCR		0.552*				
		ExCap		0.537*				
		SS					0.608**	
	Left	SS					0.613**	
Controls (n = 15)	Right	CST			0.510*			
		ExCap	0.691**		0.511*	0.563**	0.754**	0.584**
	Left	ExCap	0.608**			0.525**	0.649**	0.565**
	Right	ExCap	0.556**				0.629**	
		SS	0.560**					
	Left	SS				0.487*	0.598**	
	Right	SS		0.511*				

**p< .050 for significant values;
*.050 < p < 0.10 for near significant values
Note: a-MCI: amnestic mild cognitive impairment; ROI: region of interest; FA: fractional anisotropy; MD: mean diffusivity; AD: axial diffusivity; RD: radial diffusivity; ACR: anterior segment of the corona radiata; PCR: posterior segment of the corona radiata; CST: corticospinal tract; ExCap: external capsule; SS: sagittal stratum

CHAPTER FOUR

Discussion and Conclusions

The purpose of this study was to identify physiological signatures of a-MCI by assessing measures of white matter integrity in the cingulum bundle and eleven cortico-cortico tracts. However, our overall results did not identify a physiological signature of a-MCI, nor were most of our findings consistent with previous literature.

Significance of Group Differences Found in White Matter

The literature suggested that a-MCI cases would exhibit significant reductions of FA in the cingulum (Zhang et al., 2007) anterior segment of the corona radiata (ACR) (Duffy et al., 2014; Liu et al., 2013), body of the corpus callosum (bCC) (Duffy et al., 2014), genu of the corpus callosum (gCC) (Duffy et al., 2014), splenium of the corpus callosum (sCC) (Duffy et al., 2014; Parente et al., 2008; Zhang et al., 2013), superior longitudinal fasciculus (SLF) (Duffy et al., 2014; Liu et al., 2013; Parente et al., 2008), posterior segment of the corona radiata (PCR) (Duffy et al., 2014; Liu et al., 2013), external capsule (ExCap) (Liu et al., 2013) and the sagittal stratum (SS) (Liu et al., 2013) compared to healthy controls. However, no significant reductions in FA were found in any of the cortico-cortico tracts or the cingulum for a-MCI cases as compared to controls.

The lack of significant findings in our results could be due to biases introduced in the methodology of the analysis. A high background noise threshold was chosen for the analysis of the DTI data, which zeroed out voxels in certain areas and reduced our ability to detect effects. The high background noise threshold biased our results, in some cases making even strong effects difficult to detect. The posterior cingulum in particular is

located near the brainstem and cerebrospinal fluid which have low signal to noise ratios; therefore, this region is particularly biased. The only significant case/control group differences for cortico-cortico tracts were decreased FA in the SS for controls as compared to a-MCI cases. As indicated by several murine studies (Bennet, MacDonald, & Brody, 2012; Boska et al., 2007; Ruest et al., 2011; Tyszka, Readhead, Bearer, Pautler & Jacobs, 2006), FA reductions for controls in the SS suggests that the controls had greater general tissue loss than did the a-MCI cases in this region.

The literature suggests that significant increases in MD would be associated with decreases in FA in the ACR (Liu et al., 2013; Thillainadesan et al., 2012), bCC (Bosch et al., 2012), gCC (Chen et al., 2009; Thillainadesan et al., 2012), sCC (Thillainadesan et al., 2012), SLF (Bosch et al., 2012; Liu et al., 2013;), PCR (Liu et al., 2013; Thillainadesan et al., 2012), ExCap (Liu et al., 2013) and the SS (Liu et al., 2013) for a-MCI cases compared to controls. However, there were no significant findings for MD for group comparisons in any of the cortico-cortico tracts analyzed. O'Dwyer et al. (2011) found increased AD independent of FA changes in the forceps minor for a-MCI cases compared to controls; however in the present study, no significant findings for AD for group comparisons in any of the cortico-cortico tracts analyzed were found. Zhang et al. (2013) found decreases in FA to be associated with increased RD in the sCC for a-MCI compared to controls. In contrast, in our analyses the only significant finding for RD in any of the cortico-cortico tracts analyzed was an increase in RD for controls versus a-MCI cases in the SS. According to several murine studies (Song et al., 2003; Sun, Liang, Cross, & Song, 2008; Sun et al., 2006; Sun, Liang, Schmidt, Cross, & Song, 2006; Sun et al., 2005) an increase in RD is suggestive of demyelination. Therefore, our results

suggest that the controls present with more demyelination in the SS than do the a-MCI cases. Again, the lack of other significant findings could be due to biases introduced in the methodology of the analysis. Our overall findings, which are limited by these methodological biases, did not identify greater degeneration in a-MCI cases as compared to controls for the cingulum or the cortico-cortico tracts analyzed.

Significance of Effects of Interaction Found in White Matter

Significant effects of interaction between groups and hemispheres were found for the cingulum. For controls the FA was decreased in the left hemisphere and for a-MCI cases FA was decreased in the right hemisphere. This finding suggests that both the controls and a-MCI cases showed asymmetry of hemisphere in the cingulum, although additional analyses would be required to conclude if these were significant. It also suggests that for the controls there was more tissue loss in the left hemisphere and in the a-MCI cases there was more tissue loss in the right hemisphere. An effect of interactions between group and hemisphere was also found for RD in the cingulum. For controls, the RD was increased in the left hemisphere and for a-MCI cases RD was increased in the right hemisphere. This suggests that for the controls there was more demyelination in the left hemisphere and in the a-MCI cases there was more demyelination in the right hemisphere.

Although there were significant hemispheric differences for several of the cortico-cortico tracts, only the RD in the ACR showed significant effects of interaction between case/control group and hemispheres. For controls, the RD was increased in the left hemisphere and for a-MCI cases RD was increased in the right hemisphere. This finding suggests that both the controls and a-MCI cases showed asymmetry of hemisphere in the

ACR. It also suggests that for the controls there was more demyelination in the left hemisphere while in the a-MCI cases there was more demyelination in the right hemisphere.

Delono-Wood et al. (2012) have shown that the posterior cingulum has reduced FA in a-MCI, while the anterior cingulum does not. In the present study, however, no significant effects of interaction were found between groups (cases vs. controls) and positions (anterior vs. posterior); nor were there any significant effects of interaction between the groups, positions and hemispheres. There were, however, interactions between the positions and hemispheres in the cingulum. The findings suggest that the posterior cingulum had increased white matter loss and demyelination in the right hemisphere and that there was little asymmetry in the anterior cingulum between hemispheres. Therefore, according to our overall results, at this stage of a-MCI, degeneration is not detectable by measuring for degeneration near the structures that are known to be affected early in the progression of the disease—namely, the hippocampus and entorhinal cortex. In fact, because the posterior cingulum was found to show degeneration in the right hemisphere across groups, it may be proposed that degeneration in the cingulum may be due to normal processes of aging. However, there are caveats to this postulate, as previous results would indicate degeneration in the left hemisphere as compared to the right for early stages of Alzheimer's disease (Loewenstein et al., 1989). Because left hemispheric degeneration was not a prominent finding in our study, our results are not consistent with this hypothesis of disease progression. Once again, these findings were compromised by bias in the application of analysis methods and this could explain why results are not consistent with previous findings.

Significance of Correlations Found between White Matter Integrity and Verbal Memory Assessment

Increased FA in the cingulum and anterior cingulum as compared to controls was correlated with better performance on trial two. Decreased MD for the cingulum was found to be significantly correlated with better performance on the CVLT-II (total score) for controls. Decreased MD for the posterior cingulum was found to be significantly correlated with better performance on the CVLT-II (trials four and five) for controls. According to a murine study by Shu et al. (2013), decreases in MD are thought to suggest decreases in overall water diffusivity which would signify less degeneration. Therefore, the decreases in MD correlated with better verbal memory performance are expected. Decreased AD for the cingulum was found to be significantly correlated with better performance on the CVLT-II (total score) for controls. Decreased AD for the posterior cingulum was found to be significantly correlated with better performance on the CVLT-II (trials four and five) for controls. According to several murine study findings, decreased AD signifies greater degeneration (Song et al., 2003; Sun, Liang, Cross, & Song, 2008; Sun et al., 2006; Sun, Liang, Schmidt, Cross, & Song, 2006; Sun et al., 2005). Therefore, it was not expected that decreases in AD would correlate with a better verbal memory assessment. Decreased RD for the cingulum and posterior cingulum were found to be significantly correlated with better performance on the CVLT-II (trial two) for controls. Because an increase in RD is thought to represent greater degeneration, it would follow that decreased RD should be correlated with better performance on the CVLT-II. From these results it cannot be concluded that measures of CVLT-II can accurately predict degeneration in a-MCI cases as assessed by DTI measures of FA and diffusivity.

Decreased FA for the ACR and right ACR were found to be significantly correlated with poorer performance on the CVLT-II (trials three and four) for MCI cases. Increased FA for the SS and left SS were found to be significantly correlated with poorer performance on the CVLT-II (trials three and four) for MCI cases. The decreased FA in the ACR and right ACR should correspond to increased degeneration; therefore, it was expected that the subjects would perform more poorly on the verbal memory test. However, the poorer performance of the subjects with increased FA in the SS and left SS is contrary to predictions. Decreased FA for the ExCap and left ExCap was found to be significantly correlated with better performance on the CVLT-II (total score and trials three, four and five) for controls. Also, decreased FA for right ExCap was found to be significantly correlated with better performance on the CVLT-II (total score and trial four) for controls. Decreased FA for the SS was found to be significantly correlated with better performance on the CVLT-II (total score) for controls. Decreased FA for the left SS was found to be significantly correlated with better performance on the CVLT-II (trial four) for controls. The better performance of the subjects with decreased FA is contrary to predictions that the presence of less degeneration will correlate with better performance on verbal memory tests.

Limitations of This Study

As described, results of our study were compromised due to the high background noise threshold selected for the analysis of the DTI data. This biased against significant findings for areas with lower signal to noise ratio particularly in the posterior cingulum. However, we cannot be confident that measures and findings in other brain areas were

not also affected by this problem, diminishing our ability to detect significant differences between a-MCI cases and healthy controls, as well as other comparisons.

Another limitation of this study was the small sample size. A larger sample size is required to get a more accurate evaluation of degeneration in a-MCI cases. Unfortunately, the original study collected data using spectroscopy which required that the subjects have less atrophy in order to provide accurate evaluations of the data. Therefore, only participants with limited atrophy were included in this study. This means, overall, that the general population of a-MCI patients has more atrophy than our sample population. The reduced level of atrophy in our case subjects may have contributed to the lack of significant findings. It is also notable that although the a-MCI cases and controls were not significantly different for premorbid I.Q., they were most likely even more closely matched because assessments of pre-morbid I.Q. are generally biased toward lower overall scores. Another limitation to the study was that the multiple regions of interest for the anterior cingulum were not placed with consistency, so this prevented a four-way mixed design analysis of variance comparing groups, hemispheres, positions and regions of interest. Therefore, it could not be evaluated if a certain region within the fiber bundle showed greater degeneration than another and no conclusions could be drawn concerning varying amounts of degeneration in different locations within the region. It should also be noted that because regions of interests in the different cortico-cortico tracts were not all the same size, the measures for these regions are not directly comparable.

Directions for Further Study

This study could be improved upon by obtaining a larger sample size and by selecting a lower threshold for detecting signal vs. noise in the analysis of diffusion tensor images to avoid biasing against atrophied tissue. It could also use more than one region of interest placed with consistency in the cingulum and the cortico-cortico tracts. This would allow for a more detailed assessment of the cingulum and structures. That is, several different regions could be separately analyzed and compared to the cingulum and each cortical structure so that specific areas of degeneration could be evaluated. Further analysis is needed to make significant conclusions concerning the progression and severity of degeneration in a-MCI cases.

Conclusions

Based on the overall findings, greater degeneration was not detectable in a-MCI cases as compared to controls for the cingulum or the cortico-cortico tracts analyzed. Also it cannot be concluded that the a-MCI cases showed more cortical asymmetry than the controls, nor that greater degeneration in the left hemisphere was present, as would be consistent with the progression of the disease. Measures of CVLT-II showed very weak if any correlations with DTI measures of FA and diffusivity from the results of this study. Some findings, however, were compromised by bias in the application of analysis methods, rendering it difficult to draw clear conclusions from our results, particularly in relation to cingulum measures. Additional analyses should be conducted to determine if any pathological signatures are evident in a-MCI. Establishing the presence of these signatures is critical for understanding the pathophysiology of the disease and could be useful for understanding the initial progression of Alzheimer's disease. Consistent

identification of these signatures could also be beneficial in the diagnosis of a-MCI and Alzheimer's disease.

APPENDIX

APPENDIX

Full Report of Findings

Table 1. Controls versus Amnestic Mild Cognitive Impairment Cases: Differences in White Matter Integrity within the Cingulum.

	Controls (n = 15)		a-MCI (n = 13)			
Measures of WM Integrity	M	SEM	M	SEM	F value	p value
FA	0.556	0.012	0.542	0.013	0.646	0.429
MD	$2.51x10^{-3}$	$4.34x10^{-5}$	$2.58x10^{-3}$	$4.65x10^{-5}$	1.35	0.256
AD	$1.43x10^{-3}$	$2.07x10^{-5}$	$1.46x10^{-3}$	$2.23x10^{-5}$	0.635	0.433
RD	$5.42x10^{-4}$	$1.67x10^{-5}$	$5.67x10^{-4}$	$1.79x10^{-5}$	1.03	0.319

**p< .050 for significant values; *.050 < p < 0.10 for near significant values

Note: a-MCI: amnestic mild cognitive impairment; M: mean; SEM: standard error of mean; FA: fractional anisotropy; MD: mean diffusivity; AD: axial diffusivity; RD: radial diffusivity; WM: white matter

Table 2. Right versus Left Hemisphere: Differences in White Matter Integrity in the Cingulum

	Right Hemisphere		Left Hemisphere			
Measures of WM Integrity	M	SEM	M	SEM	F value	p value
FA	0.537	0.013	0.561	0.010	2.71	0.107
MD	$2.58x10^{-3}$	$4.14x10^{-5}$	$2.52x10^{-3}$	$3.34x10^{-5}$	2.39	0.134
AD	$1.45x10^{-3}$	$2.00x10^{-5}$	$1.45x10^{-3}$	$1.96x10^{-5}$	0.000	0.997
RD	$5.70x10^{-4}$	$1.64x10^{-5}$	$5.39x10^{-4}$	$1.24x10^{-5}$	3.97	0.057

**p< .050 for significant values; *.050 < p < 0.10 for near significant values

Note: M: mean; SEM: standard error of mean; FA: fractional anisotropy; MD: mean diffusivity; AD: axial diffusivity; RD: radial diffusivity; WM: white matter

Table 3. Anterior versus Posterior Segments of the Cingulum: Differences in White Matter Integrity

Measures of WM Integrity	Anterior Cingulum		Posterior Cingulum			
	M	SEM	M	SEM	F value	p value
FA	0.485	0.014	0.613	0.012	42.21	<0.001**
MD	2.60×10^{-3}	3.58×10^{-5}	2.50×10^{-3}	3.98×10^{-5}	6.94	0.014**
AD	1.39×10^{-3}	1.98×10^{-5}	1.50×10^{-3}	2.04×10^{-5}	17.07	<0.001**
RD	6.12×10^{-4}	1.67×10^{-5}	4.98×10^{-4}	1.79×10^{-5}	37.12	<0.001**

**p< .050 for significant values; *.050 < p < 0.10 for near significant values

Note: M: mean; SEM: standard error of mean; FA: fractional anisotropy; MD: mean diffusivity; AD: axial diffusivity; RD: radial diffusivity; WM: white matter

Table 4. Interactions between Groups and Hemispheres:
Differences in White Matter Integrity in the Cingulum

	Measures of WM Integrity	Right Hemisphere M	Right Hemisphere SEM	Left Hemisphere M	Left Hemisphere SEM	F value	p value
Controls (n = 15)	FA	0.561	0.018	0.552	0.013		
	MD	$2.51x10^{-3}$	$5.64x10^{-5}$	$2.51x10^{-3}$	$4.56x10^{-5}$		
	AD	$1.44x10^{-3}$	$2.73x10^{-5}$	$1.43x10^{-3}$	$2.67x10^{-5}$		
	RD	$5.39x10^{-4}$	$2.23x10^{-5}$	$5.45x10^{-4}$	$1.70x10^{-5}$		
a-MCI (n = 13)	FA	0.513	0.019	0.571	0.014	5.09	0.033**
	MD	$2.65x10^{-3}$	$6.07x10^{-5}$	$2.52x10^{-3}$	$4.74x10^{-5}$	2.76	0.109*
	AD	$1.45x10^{-3}$	$2.93x10^{-5}$	$1.46x10^{-3}$	$2.87x10^{-5}$	0.082	0.777*
	RD	$6.01x10^{-4}$	$2.40x10^{-5}$	$5.33x10^{-4}$	$1.83x10^{-5}$	5.53	0.027**

**p< .050 for significant values;

*.050 < p < 0.10 for near significant values

Note: F values and p values represent interaction effects between groups and hemispheres. a-MCI: amnestic mild cognitive impairment; M: mean; SEM: standard error of mean; FA: fractional anisotropy; MD: mean diffusivity; AD: axial diffusivity; RD: radial diffusivity; WM: white matter

Table 5. Interactions between Groups and Positions:
Differences in White Matter Integrity in the Cingulum

	Measures of WM Integrity	Anterior Cingulum M	Anterior Cingulum SEM	Posterior Cingulum M	Posterior Cingulum SEM	F value	p value
Controls (n = 15)	FA	0.501	0.019	0.612	0.016		
	MD	$2.57x10^{-3}$	$4.88x10^{-5}$	$2.46x10^{-3}$	$5.42x10^{-5}$		
	AD	$1.39x10^{-3}$	$2.70x10^{-5}$	$1.48x10^{-3}$	$2.78x10^{-5}$		
	RD	$5.93x10^{-4}$	$2.26x10^{-5}$	$4.91x10^{-4}$	$1.93x10^{-5}$		
a-MCI (n = 13)	FA	0.469	0.021	0.614	0.017	0.822	0.373*
	MD	$2.64x10^{-3}$	$5.24x10^{-5}$	$2.53x10^{-3}$	$5.83x10^{-5}$	0.000	0.983*
	AD	$1.39x10^{-3}$	$2.90x10^{-5}$	$1.53x10^{-3}$	$2.99x10^{-5}$	1.04	0.318*
	RD	$6.31x10^{-4}$	$2.42x10^{-5}$	$5.04x10^{-4}$	$2.08x10^{-5}$	0.454	0.506*

**p< .050 for significant values;

*.050 < p < 0.10 for near significant values

Note: F values and p values represent interaction effects between groups and positions. a-MCI: amnestic mild cognitive impairment; M: mean; SEM: standard error of mean; FA: fractional anisotropy; MD: mean diffusivity; AD: axial diffusivity; RD: radial diffusivity; WM: white matter

Table 6. Interactions between Positions and Hemispheres:
Differences in White Matter Integrity in the Cingulum

		Anterior Cingulum		Posterior Cingulum			
Groups	Measures of WM Integrity	M	SEM	M	SEM	F value	p value
Controls (n = 15)	FA	0.501	0.019	0.612	0.016		
	MD	0.486	0.017	0.485	0.019		
	AD	2.60×10^{-3}	4.31×10^{-5}	2.61×10^{-3}	4.85×10^{-5}		
	RD	1.39×10^{-3}	3.26×10^{-5}	1.40×10^{-3}	2.58×10^{-5}		
a-MCI (n = 13)	FA	0.588	0.016	0.638	0.012	4.67	0.040**
	MD	2.56×10^{-3}	6.07×10^{-5}	2.43×10^{-3}	4.74×10^{-5}	1.78	0.193*
	AD	1.50×10^{-3}	2.75×10^{-5}	1.50×10^{-3}	2.91×10^{-5}	0.044	0.835*
	RD	5.49×10^{-4}	2.12×10^{-5}	4.66×10^{-4}	1.37×10^{-5}	4.35	0.047**

**$p < .050$ for significant values;

*$.050 < p < 0.10$ for near significant values

Note: F values and p values represent interaction effects between positions and hemispheres. M: mean; SEM: standard error of mean; FA: fractional anisotropy; MD: mean diffusivity; AD: axial diffusivity; RD: radial diffusivity; WM: white matter

Table 7A. Interactions between Groups, Positions and Hemispheres:
Differences in White Matter Integrity in the Cingulum

	Controls (n = 15)							
	Anterior Cingulum				Posterior Cingulum			
Measures of WM Integrity	Right Hemisphere		Left Hemisphere		Right Hemisphere		Left Hemisphere	
	M	SEM	M	SEM	M	SEM	M	SEM
FA	0.552	0.023	0.480	0.025	0.600	0.021	0.624	0.017
MD	$2.53x10^{-3}$	$5.87x10^{-5}$	$2.60x10^{-3}$	$6.61x10^{-5}$	$2.49x10^{-3}$	$8.27x10^{-5}$	$2.43x10^{-3}$	$6.45x10^{-5}$
AD	$1.41x10^{-3}$	$4.45x10^{-5}$	$1.38x10^{-3}$	$3.52x10^{-5}$	$1.47x10^{-3}$	$3.74x10^{-5}$	$1.48x10^{-3}$	$3.96x10^{-5}$
RD	$5.70x10^{-4}$	$2.25x10^{-5}$	$6.16x10^{-4}$	$3.08x10^{-5}$	$5.09x10^{-4}$	$2.89x10^{-5}$	$4.47x10^{-4}$	$1.87x10^{-5}$

**p< .050 for significant values;

*.050 < p < 0.10 for near significant values

Note: M: mean; SEM: standard error of mean; FA: fractional anisotropy; MD: mean diffusivity; AD: axial diffusivity; RD: radial diffusivity; WM: white matter

Table 7B. Interactions between Groups, Positions and Hemispheres:
Differences in White Matter Integrity in the Cingulum

a-MCI (n = 13)

Measures of WM Integrity	Anterior Cingulum				Posterior Cingulum					
	Right Hemisphere		Left Hemisphere		Right Hemisphere		Left Hemisphere			
	M	SEM	M	SEM	M	SEM	M	SEM	F Value	p value
FA	0.449	0.025	0.489	0.027	0.576	0.023	0.653	0.018	1.20	0.318
MD	$2.66x10^{-3}$	$6.31x10^{-5}$	$2.62x10^{-3}$	$7.10x10^{-5}$	$2.64x10^{-3}$	$8.88x10^{-5}$	$2.43x10^{-3}$	$6.93x10^{-5}$	0.036	0.852
AD	$1.37x10^{-3}$	$4.78x10^{-5}$	$1.41x10^{-3}$	$3.78x10^{-5}$	$1.54x10^{-3}$	$4.02x10^{-5}$	$1.51x10^{-3}$	$4.25x10^{-5}$	0.697	0.412
RD	$6.54x10^{-4}$	$2.41x10^{-5}$	$6.09x10^{-4}$	$3.31x10^{-5}$	$5.49x10^{-4}$	$3.10x10^{-5}$	$4.59x10^{-4}$	$2.01x10^{-5}$	0.424	0.521

**p< .050 for significant values;
*.050 < p < 0.10 for near significant values
Note: a-MCI: amnestic mild cognitive impairment; M: mean; SEM: standard error of mean; FA: fractional anisotropy; MD: mean diffusivity; AD: axial diffusivity; RD: radial diffusivity; WM: white matter

Table 8A. Controls versus Amnestic Mild Cognitive Impairment:
Differences in White Matter Integrity in Cortico-cortico Tracts

		Controls (n = 15)		a-MCI (n = 13)			
Measures of WM Integrity	Cortico-cortico Tracts	M	SEM	M	SEM	F value	p value
FA	Body of the CC	0.682	0.018	0.685	0.019	0.382	0.542
	Genu of the CC	0.775	0.012	0.785	0.011	0.373	0.547
	Splenium of the CC	0.851	0.015	0.822	0.018	1.70	0.204
	Anterior Segment Corona Radiata	0.370	0.017	0.363	0.018	0.079	0.781
	Corticospinal Tract	0.427	0.017	0.452	0.018	0.981	0.331
	Superior Longitudinal Fasciculus	0.539	0.009	0.523	0.009	1.42	0.245
	Posterior Segment Corona Radiata	0.499	0.013	0.466	0.014	3.21	0.085*
	Forceps Minor	0.493	0.021	0.515	0.023	0.526	0.475
	External Capsule	0.447	0.014	0.455	0.015	0.159	0.693
	Forceps Major	0.563	0.029	0.620	0.031	1.73	0.200
	Sagittal Stratum	0.528	0.012	0.582	0.013	9.24	0.005**

**p< .050 for significant values;
*.050 < p < 0.10 for near significant values
Note: a-MCI: amnestic mild cognitive impairment; M: mean; SEM: standard error of mean; FA: fractional anisotropy; MD: mean diffusivity; AD: axial diffusivity; RD: radial diffusivity; WM: integrity; CC: Corpus Callosum

Table 8B. Controls versus Amnestic Mild Cognitive Impairment:
Differences in White Matter Integrity in Cortico-cortico Tracts

Measures of WM Integrity	Cortico-cortico Tracts	Controls (n = 15)		a-MCI (n = 13)			
		M	SEM	M	SEM	F value	p value
MD	Body of the CC	$3.15x10^{-3}$	$1.84x10^{-5}$	$3.17x10^{-3}$	$1.97x10^{-5}$	0.011	0.917
	Genu of the CC	$2.42x10^{-3}$	$1.67x10^{-4}$	$2.32x10^{-3}$	$1.26x10^{-4}$	0.164	0.689
	Splenium of the CC	$2.34x10^{-3}$	$6.07x10^{-5}$	$2.34x10^{-3}$	$6.26x10^{-5}$	0.001	0.976
	Anterior Segment Corona Radiata	$2.46x10^{-3}$	$4.40x10^{-5}$	$2.46x10^{-3}$	$4.72x10^{-5}$	0.001	0.975
	Corticospinal Tract	$2.34x10^{-3}$	$4.42x10^{-5}$	$2.23x10^{-3}$	$4.75x10^{-5}$	2.73	0.111
	Superior Longitudinal Fasciculus	$2.28x10^{-3}$	$3.24x10^{-5}$	$2.34x10^{-3}$	$3.48x10^{-5}$	1.31	0.263
	Posterior Segment Corona Radiata	$2.31x10^{-3}$	$4.37x10^{-5}$	$2.35x10^{-3}$	$4.70x10^{-5}$	0.409	0.528
	Forceps Minor	$2.57x10^{-3}$	$5.48x10^{-5}$	$2.54x10^{-3}$	$5.89x10^{-5}$	0.122	0.730
	External Capsule	$2.39x10^{-3}$	$5.64x10^{-5}$	$2.37x10^{-3}$	$6.05x10^{-5}$	0.060	0.809
	Forceps Major	$2.60x10^{-3}$	$6.49x10^{-5}$	$2.60x10^{-3}$	$6.98x10^{-5}$	0.004	0.949
	Sagittal Stratum	$2.66x10^{-3}$	$5.92x10^{-5}$	$2.49x10^{-3}$	$6.36x10^{-5}$	3.87	0.060*

**p< .050 for significant values;
*.050 < p < 0.10 for near significant values
Note: a-MCI: amnestic mild cognitive impairment; M: mean; SEM: standard error of mean; FA: fractional anisotropy; MD: mean diffusivity; AD: axial diffusivity; RD: radial diffusivity; WM: integrity; CC: Corpus Callosum

Table 8C. Controls versus Amnestic Mild Cognitive Impairment:
Differences in White Matter Integrity in Cortico-cortico Tracts

Measures of WM Integrity	Cortico-cortico Tracts	Controls (n = 15)		a-MCI (n = 13)			
		M	SEM	M	SEM	F value	p value
AD	Body of the CC	$2.01x10^{-3}$	$8.15x10^{-5}$	$2.00x10^{-3}$	$8.76x10^{-5}$	0.010	0.920
	Genu of the CC	$1.85x10^{-3}$	$3.08x10^{-5}$	$1.82x10^{-3}$	$2.97x10^{-5}$	0.501	0.485
	Splenium of the CC	$1.84x10^{-3}$	$3.44x10^{-5}$	$1.78x10^{-3}$	$6.02x10^{-5}$	0.716	0.405
	Anterior Segment Corona Radiata	$1.16x10^{-3}$	$2.14x10^{-5}$	$1.15x10^{-3}$	$2.30x10^{-5}$	0.123	0.729
	Corticospinal Tract	$1.16x10^{-3}$	$2.37x10^{-5}$	$1.13x10^{-3}$	$2.54x10^{-5}$	0.809	0.377
	Superior Longitudinal Fasciculus	$1.26x10^{-3}$	$3.48x10^{-5}$	$1.22x10^{-3}$	$3.74x10^{-5}$	0.592	0.448
	Posterior Segment Corona Radiata	$1.21x10^{-3}$	$3.01x10^{-5}$	$1.20x10^{-3}$	$3.21x10^{-5}$	0.101	0.753
	Forceps Minor	$1.37x10^{-3}$	$2.87x10^{-5}$	$1.39x10^{-3}$	$3.08x10^{-5}$	0.237	0.630
	External Capsule	$1.19x10^{-3}$	$2.53x10^{-5}$	$1.18x10^{-3}$	$2.72x10^{-5}$	0.105	0.748
	Forceps Major	$1.49x10^{-3}$	$4.33x10^{-5}$	$1.59x10^{-3}$	$4.65x10^{-5}$	2.49	0.127
	Sagittal Stratum	$1.47x10^{-3}$	$2.56x10^{-5}$	$1.45x10^{-3}$	$2.75x10^{-5}$	0.189	0.667

**p< .050 for significant values;
*.050 < p < 0.10 for near significant values
Note: a-MCI: amnestic mild cognitive impairment; M: mean; SEM: standard error of mean; FA: fractional anisotropy; MD: mean diffusivity; AD: axial diffusivity; RD: radial diffusivity; WM: integrity; CC: Corpus Callosum

Table 8D. Controls versus Amnestic Mild Cognitive Impairment:
Differences in White Matter Integrity in Cortico-cortico Tracts

Measures of WM Integrity	Cortico-cortico Tracts	Controls (n = 15) M	Controls (n = 15) SEM	a-MCI (n = 13) M	a-MCI (n = 13) SEM	F value	p value
RD	Body of the CC	$5.69x10^{-4}$	$5.32x10^{-5}$	$5.90x10^{-4}$	$5.71x10^{-5}$	0.071	0.793
	Genu of the CC	$3.66x10^{-4}$	$1.46x10^{-5}$	$3.46x10^{-4}$	$1.86x10^{-5}$	0.761	0.391
	Splenium of the CC	$2.49x10^{-4}$	$2.34x10^{-5}$	$2.78x10^{-4}$	$2.06x10^{-5}$	0.856	0.363
	Anterior Segment Corona Radiata	$6.51x10^{-4}$	$1.75x10^{-5}$	$6.57x10^{-4}$	$1.88x10^{-5}$	0.059	0.810
	Corticospinal Tract	$5.88x10^{-4}$	$1.73x10^{-5}$	$5.51x10^{-4}$	$1.86x10^{-5}$	2.20	0.150
	Superior Longitudinal Fasciculus	$5.13x10^{-4}$	$1.18x10^{-5}$	$5.38x10^{-4}$	$1.27x10^{-5}$	2.10	0.160
	Posterior Segment Corona Radiata	$5.52x10^{-4}$	$1.41x10^{-5}$	$5.80x10^{-4}$	$1.51x10^{-5}$	1.78	0.194
	Forceps Minor	$5.97x10^{-4}$	$2.40x10^{-5}$	$5.72x10^{-4}$	$2.58x10^{-5}$	0.494	0.488
	External Capsule	$1.49x10^{-3}$	$6.02x10^{-5}$	$1.59x10^{-3}$	$5.97x10^{-5}$	0.024	0.127
	Forceps Major	$1.49x10^{-3}$	$4.33x10^{-5}$	$1.59x10^{-3}$	$4.65x10^{-5}$	2.49	0.877
	Sagittal Stratum	$5.96x10^{-4}$	$2.00x10^{-5}$	$5.19x10^{-4}$	$2.15x10^{-5}$	6.94	0.014**

**p< .050 for significant values;
*.050 < p < 0.10 for near significant values
Note: a-MCI: amnestic mild cognitive impairment; M: mean; SEM: standard error of mean; FA: fractional anisotropy; MD: mean diffusivity; AD: axial diffusivity; RD: radial diffusivity; WM: integrity; CC: Corpus Callosum

Table 9A. Right Versus Left Hemisphere: Differences in White Matter Integrity in Cortico-cortico Tracts

Measures of WM Integrity	Cortico-cortico Tracts	Right Hemisphere M	Right Hemisphere SEM	Left Hemisphere M	Left Hemisphere SEM	F value	p value
FA	Body of the CC	0.675	0.012	0.672	0.018	0.042	0.839
	Anterior Segment Corona Radiata	0.370	0.014	0.362	0.013	0.676	0.418
	Corticospinal Tract	0.406	0.013	0.473	0.015	27.43	<0.001**
	Superior Longitudinal Fasciculus	0.524	0.013	0.538	0.010	0.518	0.478
	Posterior Segment Corona Radiata	0.478	0.012	0.487	0.012	0.357	0.556
	Forceps Minor	0.516	0.019	0.493	0.015	2.41	0.133
	External Capsule	0.413	0.010	0.488	0.014	34.33	<0.001**
	Forceps Major	0.594	0.021	0.589	0.026	0.058	0.812
	Sagittal Stratum	0.542	0.010	0.569	0.013	2.87	0.102

**p< .050 for significant values;

*.050 < p < 0.10 for near significant values

Note: M: mean; SEM: standard error of mean; FA: fractional anisotropy; MD: mean diffusivity; AD: axial diffusivity; RD: radial diffusivity; WM: integrity; CC: Corpus Callosum

Table 9B. Right Versus Left Hemisphere: Differences in White Matter Integrity in Cortico-cortico Tracts

Measures of WM Integrity	Cortico-cortico Tracts	Right Hemisphere M	Right Hemisphere SEM	Left Hemisphere M	Left Hemisphere SEM	F value	p value
MD	Body of the CC	$3.07x10^{-3}$	$1.15x10^{-4}$	$3.25x10^{-3}$	$1.66x10^{-4}$	3.71	0.065*
	Anterior Segment Corona Radiata	$2.47x10^{-3}$	$3.54x10^{-5}$	$2.45x10^{-3}$	$3.24x10^{-5}$	0.541	0.469
	Corticospinal Tract	$2.29x10^{-3}$	$3.93x10^{-5}$	$2.29x10^{-3}$	$3.10x10^{-5}$	0.001	0.982
	Superior Longitudinal Fasciculus	$2.31x10^{-3}$	$3.60x10^{-5}$	$2.31x10^{-3}$	$2.69x10^{-5}$	0.042	0.840
	Posterior Segment Corona Radiata	$2.32x10^{-3}$	$3.94x10^{-5}$	$2.35x10^{-3}$	$3.69x10^{-5}$	0.450	0.508
	Forceps Minor	$2.56x10^{-3}$	$4.23x10^{-5}$	$2.54x10^{-3}$	$4.26x10^{-5}$	1.00	0.326
	External Capsule	$2.42x10^{-3}$	$4.28x10^{-5}$	$2.35x10^{-3}$	$5.62x10^{-5}$	1.37	0.252
	Forceps Major	$2.59x10^{-3}$	$5.46x10^{-5}$	$2.60x10^{-3}$	$5.02x10^{-5}$	0.022	0.884
	Sagittal Stratum	$2.60x10^{-3}$	$3.76x10^{-5}$	$2.56x10^{-3}$	$5.93x10^{-5}$	0.665	0.422

**p< .050 for significant values;

*.050 < p < 0.10 for near significant values

Note: M: mean; SEM: standard error of mean; FA: fractional anisotropy; MD: mean diffusivity; AD: axial diffusivity; RD: radial diffusivity; WM: integrity; CC: Corpus Callosum

Table 9C. Right Versus Left Hemisphere: Differences in White Matter Integrity in Cortico-cortico Tracts

Measures of WM Integrity	Cortico-cortico Tracts	Right Hemisphere		Left Hemisphere			
		M	SEM	M	SEM	F value	p value
AD	Body of the CC	$1.96x10^{-3}$	$5.70x10^{-5}$	$2.05x10^{-3}$	$6.92x10^{-5}$	4.27	0.049**
	Anterior Segment Corona Radiata	$1.17x10^{-3}$	$1.84x10^{-5}$	$1.14x10^{-3}$	$1.59x10^{-5}$	4.66	0.040**
	Corticospinal Tract	$1.11x10^{-3}$	$4.56x10^{-5}$	$1.18x10^{-3}$	$1.74x10^{-5}$	17.42	<0.001**
	Superior Longitudinal Fasciculus	$1.21x10^{-3}$	$1.84x10^{-5}$	$1.26x10^{-3}$	$2.02x10^{-5}$	1.10	0.304
	Posterior Segment Corona Radiata	$1.19x10^{-3}$	$2.71x10^{-5}$	$1.22x10^{-3}$	$2.32x10^{-5}$	1.54	0.225
	Forceps Minor	$1.15x10^{-3}$	$1.97x10^{-5}$	$1.22x10^{-3}$	$2.79x10^{-5}$	4.71	0.039**
	External Capsule	$6.32x10^{-4}$	$1.47x10^{-5}$	$5.66x10^{-4}$	$1.90x10^{-5}$	14.73	0.001**
	Forceps Major	$1.54x10^{-4}$	$3.43x10^{-5}$	$1.51x10^{-4}$	$3.99x10^{-5}$	0.001	0.979
	Sagittal Stratum	$1.46x10^{-4}$	$2.15x10^{-5}$	$1.471x10^{-4}$	$2.45x10^{-5}$	0.169	0.685

**p< .050 for significant values;

*.050 < p < 0.10 for near significant values

Note: M: mean; SEM: standard error of mean; FA: fractional anisotropy; MD: mean diffusivity; AD: axial diffusivity; RD: radial diffusivity; WM: integrity; CC: Corpus Callosum

Table 9D. Right Versus Left Hemisphere: Differences in White Matter Integrity in Cortico-cortico Tracts

Measures of WM Integrity	Cortico-cortico Tracts	Right Hemisphere		Left Hemisphere			
		M	SEM	M	SEM	F value	p value
RD	Body of the CC	$5.57x10^{-4}$	$3.13x10^{-5}$	$6.02x10^{-4}$	$5.08x10^{-5}$	1.96	0.173
	Anterior Segment Corona Radiata	$6.50x10^{-4}$	$1.43x10^{-5}$	$6.58x10^{-4}$	$1.30x10^{-5}$	0.696	0.412
	Corticospinal Tract	$5.87x10^{-4}$	$1.46x10^{-5}$	$5.53x10^{-4}$	$1.36x10^{-5}$	7.92	0.009**
	Superior Longitudinal Fasciculus	$5.30x10^{-4}$	$1.49x10^{-5}$	$5.22x10^{-4}$	$1.19x10^{-5}$	0.151	0.701
	Posterior Segment Corona Radiata	$5.67x10^{-4}$	$1.20x10^{-5}$	$5.65x10^{-4}$	$1.37x10^{-5}$	0.019	0.893
	Forceps Minor	$5.79x10^{-4}$	$2.02x10^{-5}$	$5.90x10^{-4}$	$1.68x10^{-5}$	0.846	0.366
	External Capsule	$6.32x10^{-4}$	$1.47x10^{-5}$	$5.66x10^{-4}$	$1.90x10^{-5}$	14.73	0.001**
	Forceps Major	$5.29x10^{-4}$	$2.49x10^{-5}$	$5.33x10^{-4}$	$2.80x10^{-5}$	0.032	0.859
	Sagittal Stratum	$5.70x10^{-4}$	$1.23x10^{-5}$	$5.45x10^{-4}$	$2.15x10^{-5}$	1.75	0.197

**p< .050 for significant values;

*.050 < p < 0.10 for near significant values

Note: a-MCI: amnestic mild cognitive impairment; M: mean; SEM: standard error of mean; FA: fractional anisotropy; MD: mean diffusivity; AD: axial diffusivity; RD: radial diffusivity; WM: integrity; CC: Corpus Callosum

Table 10A. Interactions between Groups and Hemispheres:
Differences in White Matter Integrity in Cortico-cortico Tracts for FA

		Controls (n = 15)			
		Right Hemisphere		Left Hemisphere	
Measures of WM Integrity	Cortico-cortico Tracts	M	SEM	M	SEM
FA	Body of the CC	0.675	0.016	0.675	0.024
	Anterior Segment Corona Radiata	0.384	0.019	0.355	0.018
	Corticospinal Tract	0.391	0.018	0.463	0.020
	Superior Longitudinal Fasciculus	0.523	0.017	0.554	0.014
	Posterior Segment Corona Radiata	0.496	0.016	0.503	0.016
	Forceps Minor	0.499	0.026	0.488	0.020
	External Capsule	0.412	0.013	0.481	0.019
	Forceps Major	0.564	0.029	0.563	0.035
	Sagittal Stratum	0.520	0.014	0.537	0.018

**p< .050 for significant values;
*.050 < p < 0.10 for near significant values
Note: M: mean; SEM: standard error of mean; FA: fractional anisotropy; MD: mean diffusivity; AD: axial diffusivity; RD: radial diffusivity; WM: integrity; CC: Corpus Callosum

Table 10B. Interactions between Groups and Hemispheres:
Differences in White Matter Integrity in Cortico-cortico Tracts for FA

		a-MCI (n = 13)					
		Right Hemisphere		Left Hemisphere			
Measures of WM Integrity	Cortico-cortico Tracts	M	SEM	M	SEM	F value	p value
FA	Body of the CC	0.675	0.018	0.655	0.026	1.36	0.254
	Anterior Segment Corona Radiata	0.357	0.020	0.368	0.019	3.73	0.065*
	Corticospinal Tract	0.420	0.019	0.483	0.022	0.103	0.751
	Superior Longitudinal Fasciculus	0.525	0.018	0.522	0.015	1.42	0.245
	Posterior Segment Corona Radiata	0.460	0.017	0.472	0.018	0.026	0.874
	Forceps Minor	0.533	0.028	0.498	0.022	0.753	0.393
	External Capsule	0.414	0.014	0.495	0.020	0.225	0.639
	Forceps Major	0.624	0.031	0.615	0.038	0.031	0.862
	Sagittal Stratum	0.564	0.015	0.601	0.020	0.410	0.528

**p< .050 for significant values;
*.050 < p < 0.10 for near significant values
Note: F values and p values represent interaction effects between groups and hemispheres. a-MCI: amnestic mild cognitive impairment; M: mean; SEM: standard error of mean; FA: fractional anisotropy; MD: mean diffusivity; AD: axial diffusivity; RD: radial diffusivity; WM: integrity; CC: Corpus Callosum

Table 11A. Interactions between Groups and Hemispheres:
Differences in White Matter Integrity in Cortico-cortico Tracts for MD

		Controls (n = 15)			
		Right Hemisphere		Left Hemisphere	
Measures of WM Integrity	Cortico-cortico Tracts	M	SEM	M	SEM
MD	Body of the CC	$3.06x10^{-3}$	$1.56x10^{-4}$	$3.23x10^{-3}$	$2.26x10^{-4}$
	Anterior Segment Corona Radiata	$2.45x10^{-3}$	$4.82x10^{-5}$	$2.47x10^{-3}$	$4.42x10^{-5}$
	Corticospinal Tract	$2.34x10^{-3}$	$5.26x10^{-5}$	$2.34x10^{-3}$	$4.23x10^{-5}$
	Superior Longitudinal Fasciculus	$2.28x10^{-3}$	$4.90x10^{-5}$	$2.29x10^{-3}$	$3.66x10^{-5}$
	Posterior Segment Corona Radiata	$2.27x10^{-3}$	$5.37x10^{-5}$	$2.35x10^{-3}$	$5.03x10^{-5}$
	Forceps Minor	$2.59x10^{-3}$	$5.76x10^{-5}$	$2.54x10^{-3}$	$5.80x10^{-5}$
	External Capsule	$2.45x10^{-3}$	$5.83x10^{-5}$	$2.34x10^{-3}$	$7.66x10^{-5}$
	Forceps Major	$2.56x10^{-3}$	$7.44x10^{-5}$	$2.63x10^{-3}$	$6.84x10^{-5}$
	Sagittal Stratum	$2.67x10^{-3}$	$5.12x10^{-5}$	$2.65x10^{-3}$	$8.08x10^{-5}$

**p< .050 for significant values;
*.050 < p < 0.10 for near significant values
Note: a-MCI: amnestic mild cognitive impairment; M: mean; SEM: standard error of mean; FA: fractional anisotropy; MD: mean diffusivity; AD: axial diffusivity; RD: radial diffusivity; WM: integrity; CC: Corpus Callosum

Table 11B. Interactions between Groups and Hemispheres:
Differences in White Matter Integrity in Cortico-cortico Tracts for MD

		a-MCI (n = 13)					
		Right Hemisphere		Left Hemisphere			
Measures of WM Integrity	Cortico-cortico Tracts	M	SEM	M	SEM	F value	p value
MD	Body of the CC	$3.08x10^{-3}$	$1.67x10^{-4}$	$3.26x10^{-3}$	$2.42x10^{-4}$	0.004	0.953
	Anterior Segment Corona Radiata	$2.49x10^{-3}$	$5.17x10^{-5}$	$2.44x10^{-3}$	$4.74x10^{-5}$	2.76	0.108
	Corticospinal Tract	$2.23x10^{-3}$	$5.76x10^{-5}$	$2.24x10^{-3}$	$4.54x10^{-5}$	0.024	0.877
	Superior Longitudinal Fasciculus	$2.35x10^{-3}$	$5.26x10^{-5}$	$2.32x10^{-3}$	$3.94x10^{-5}$	0.239	0.629
	Posterior Segment Corona Radiata	$2.37x10^{-3}$	$5.77x10^{-5}$	$2.34x10^{-3}$	$5.40x10^{-5}$	2.06	0.163
	Forceps Minor	$2.54x10^{-3}$	$6.19x10^{-5}$	$2.53x10^{-3}$	$6.23x10^{-5}$	0.434	0.516
	External Capsule	$2.38x10^{-3}$	$6.27x10^{-5}$	$2.37x10^{-3}$	$8.22x10^{-5}$	0.830	0.371
	Forceps Major	$2.63x10^{-3}$	$7.99x10^{-5}$	$2.57x10^{-3}$	$7.35x10^{-5}$	1.84	0.186
	Sagittal Stratum	$2.52x10^{-3}$	$5.50x10^{-5}$	$2.46x10^{-3}$	$8.68x10^{-5}$	0.083	0.775

**p< .050 for significant values;
*.050 < p < 0.10 for near significant values
Note: F values and p values represent interaction effects between groups and hemispheres. a-MCI: amnestic mild cognitive impairment; M: mean; SEM: standard error of mean; FA: fractional anisotropy; MD: mean diffusivity; AD: axial diffusivity; RD: radial diffusivity; WM: integrity; CC: Corpus Callosum

Table 12A. Interactions between Groups and Hemispheres:
Differences in White Matter Integrity in Cortico-cortico Tracts for AD

		Controls (n = 15)			
		Right Hemisphere		Left Hemisphere	
Measures of WM Integrity	Cortico-cortico Tracts	M	SEM	M	SEM
AD	Body of the CC	$1.95x10^{-3}$	$7.77x10^{-5}$	$2.07x10^{-3}$	$9.43x10^{-5}$
	Anterior Segment Corona Radiata	$1.18x10^{-3}$	$2.51x10^{-5}$	$1.14x10^{-3}$	$2.17x10^{-5}$
	Corticospinal Tract	$1.13x10^{-3}$	$2.51x10^{-5}$	$1.20x10^{-3}$	$2.75x10^{-5}$
	Superior Longitudinal Fasciculus	$1.24x10^{-3}$	$6.21x10^{-5}$	$1.28x10^{-3}$	$2.38x10^{-5}$
	Posterior Segment Corona Radiata	$1.18x10^{-3}$	$3.70x10^{-5}$	$1.24x10^{-3}$	$3.16x10^{-5}$
	Forceps Minor	$1.40x10^{-3}$	$3.41x10^{-5}$	$1.35x10^{-3}$	$3.20x10^{-5}$
	External Capsule	$1.17x10^{-3}$	$2.69x10^{-5}$	$1.21x10^{-3}$	$3.80x10^{-5}$
	Forceps Major	$1.47x10^{-3}$	$4.67x10^{-5}$	$1.50x10^{-3}$	$5.54x10^{-5}$
	Sagittal Stratum	$1.46x10^{-3}$	$2.93x10^{-5}$	$1.47x10^{-3}$	$3.33x10^{-5}$

**p< .050 for significant values;
*.050 < p < 0.10 for near significant values
Note: M: mean; SEM: standard error of mean; FA: fractional anisotropy; MD: mean diffusivity; AD: axial diffusivity; RD: radial diffusivity; WM: integrity; CC: Corpus Callosum

Table 12B. Interactions between Groups and Hemispheres:
Differences in White Matter Integrity in Cortico-cortico Tracts for AD

		a-MCI (n = 13)					
		Right Hemisphere		Left Hemisphere			
Measures of WM Integrity	Cortico-cortico Tracts	M	SEM	M	SEM	F value	p value
AD	Body of the CC	$1.97x10^{-3}$	$8.34x10^{-5}$	$2.02x10^{-3}$	$1.01x10^{-4}$	0.787	0.383
	Anterior Segment Corona Radiata	$1.16x10^{-3}$	$2.69x10^{-5}$	$1.13x10^{-3}$	$2.33x10^{-5}$	0.335	0.568
	Corticospinal Tract	$1.10x10^{-3}$	$2.70x10^{-5}$	$1.17x10^{-3}$	$2.95x10^{-5}$	0.007	0.935
	Superior Longitudinal Fasciculus	$1.19x10^{-3}$	$6.67x10^{-5}$	$1.24x10^{-3}$	$2.55x10^{-5}$	0.007	0.933
	Posterior Segment Corona Radiata	$1.20x10^{-3}$	$3.97x10^{-5}$	$1.19x10^{-3}$	$3.40x10^{-5}$	1.86	0.184
	Forceps Minor	$1.42x10^{-3}$	$3.67x10^{-5}$	$1.37x10^{-3}$	$3.44x10^{-5}$	0.043	0.837
	External Capsule	$1.13x10^{-3}$	$2.88x10^{-5}$	$1.23x10^{-3}$	$4.09x10^{-5}$	0.955	0.337
	Forceps Major	$1.60x10^{-3}$	$5.02x10^{-5}$	$1.60x10^{-3}$	$5.85x10^{-5}$	0.785	0.384
	Sagittal Stratum	$1.45x10^{-3}$	$3.15x10^{-5}$	$1.46x10^{-3}$	$3.58x10^{-5}$	0.012	0.913

**p< .050 for significant values;
*.050 < p < 0.10 for near significant values
Note: F values and p values represent interaction effects between groups and hemispheres. a-MCI: amnestic mild cognitive impairment; M: mean; SEM: standard error of mean; FA: fractional anisotropy; MD: mean diffusivity; AD: axial diffusivity; RD: radial diffusivity; WM: integrity; CC: Corpus Callosum

Table 13A. Interactions between Groups and Hemispheres:
Differences in White Matter Integrity in Cortico-cortico Tracts for RD

		Controls (n = 15)			
		Right Hemisphere		Left Hemisphere	
Measures of WM Integrity	Cortico-cortico Tracts	M	SEM	M	SEM
RD	Body of the CC	$5.57x10^{-4}$	$4.26x10^{-5}$	$5.81x10^{-4}$	$6.92x10^{-5}$
	Anterior Segment Corona Radiata	$6.36x10^{-4}$	$1.94x10^{-5}$	$6.66x10^{-4}$	$1.77x10^{-5}$
	Corticospinal Tract	$6.08x10^{-4}$	$1.99x10^{-5}$	$5.69x10^{-4}$	$1.85x10^{-5}$
	Superior Longitudinal Fasciculus	$5.21x10^{-4}$	$2.03x10^{-5}$	$5.05x10^{-4}$	$1.62x10^{-5}$
	Posterior Segment Corona Radiata	$5.47x10^{-4}$	$1.63x10^{-5}$	$5.57x10^{-4}$	$1.87x10^{-5}$
	Forceps Minor	$5.97x10^{-4}$	$2.75x10^{-5}$	$5.97x10^{-4}$	$2.30x10^{-5}$
	External Capsule	$6.40x10^{-4}$	$2.00x10^{-5}$	$5.63x10^{-4}$	$2.57x10^{-5}$
	Forceps Major	$5.46x10^{-4}$	$3.39x10^{-5}$	$5.63x10^{-4}$	$3.81x10^{-5}$
	Sagittal Stratum	$6.04x10^{-4}$	$1.68x10^{-5}$	$5.89x10^{-4}$	$2.93x10^{-5}$

**p< .050 for significant values;
*.050 < p < 0.10 for near significant values
Note: a-MCI: amnestic mild cognitive impairment; M: mean; SEM: standard error of mean; FA: fractional anisotropy; MD: mean diffusivity; AD: axial diffusivity; RD: radial diffusivity; WM: integrity; CC: Corpus Callosum

Table 13B. Interactions between Groups and Hemispheres:
Differences in White Matter Integrity in Cortico-cortico Tracts for RD

		a-MCI (n = 13)					
		Right Hemisphere		Left Hemisphere			
Measures of WM Integrity	Cortico-cortico Tracts	M	SEM	M	SEM	F value	p value
RD	Body of the CC	$5.57*10^{-4}$	$4.58*10^{-5}$	$6.22*10^{-4}$	$7.44*10^{-5}$	0.419	0.523
	Anterior Segment Corona Radiata	$6.64*10^{-4}$	$2.09*10^{-5}$	$6.50*10^{-4}$	$1.90*10^{-5}$	5.56	0.026*
	Corticospinal Tract	$5.66*10^{-4}$	$2.14*10^{-5}$	$5.35*10^{-4}$	$1.99*10^{-5}$	0.093	0.763
	Superior Longitudinal Fasciculus	$5.38*10^{-4}$	$2.18*10^{-5}$	$5.38*10^{-4}$	$1.74*10^{-5}$	0.157	0.695
	Posterior Segment Corona Radiata	$5.87*10^{-4}$	$1.75*10^{-5}$	$5.72*10^{-4}$	$2.01*10^{-5}$	0.687	0.415
	Forceps Minor	$5.61*10^{-4}$	$2.96*10^{-5}$	$5.83*10^{-4}$	$2.47*10^{-5}$	0.853	0.369
	External Capsule	$6.25*10^{-4}$	$2.15*10^{-5}$	$5.69*10^{-4}$	$2.78*10^{-5}$	0.372	0.547
	Forceps Major	$5.12*10^{-4}$	$3.64*10^{-5}$	$5.02*10^{-4}$	$4.09*10^{-5}$	0.414	0.526
	Sagittal Stratum	$5.36*10^{-4}$	$1.80*10^{-5}$	$5.02*10^{-4}$	$3.14*10^{-5}$	0.249	0.622

**p< .050 for significant values;
*.050 < p < 0.10 for near significant values
Note: F values and p values represent interaction effects between groups and hemispheres. a-MCI: amnestic mild cognitive impairment; M: mean; SEM: standard error of mean; FA: fractional anisotropy; MD: mean diffusivity; AD: axial diffusivity; RD: radial diffusivity; WM: integrity; CC: Corpus Callosum

Table 14. Bivariate Correlations in the Cingulum with California Verbal Learning Test-Second Edition Scores for Amnestic Mild Cognitive Impairment Cases

Measures of WM Integrity	ROI	Total Score	Trial 1	Trial 2	Trial 3	Trial 4	Trial 5
FA							
	Cingulum	0.037	0.452	0.074	0.027	0.098	0.189
	Ant. Cingulum	0.224	0.417	0.310	0.162	0.274	0.297
	Post. Cingulum	0.121	0.249	0.440	0.129	0.140	0.027
MD							
	Cingulum	0.173	0.109	0.027	0.271	0.217	0.253
	Ant. Cingulum	0.155	0.251	0.033	0.301	0.330	0.148
	Post. Cingulum	0.155	0.061	0.016	0.181	0.053	0.308
AD							
	Cingulum	0.209	0.276	0.097	0.199	0.021	0.441
	Ant. Cingulum	0.054	0.084	0.364	0.098	0.030	0.351
	Post. Cingulum	0.323	0.190	0.534	0.199	0.004	0.318
RD							
	Cingulum	0.124	0.256	0.060	0.254	0.274	0.054
	Ant. Cingulum	0.179	0.262	0.235	0.315	0.370	0.066
	Post. Cingulum	0.026	0.185	0.175	0.114	0.086	0.192

**p< .050 for significant values;

*.050 < p < 0.10 for near significant values

Note: ROI: region of interest; FA: fractional anisotropy; MD: mean diffusivity; AD: axial diffusivity; RD: radial diffusivity; Post. Cingulum: Posterior Cingulum; Ant. Cingulum: anterior cingulum; WM: white matter

Table 15. Bivariate Correlations in the Cingulum with California Verbal Learning Test-Second Edition Scores for Controls

Measures of WM Integrity	ROI	Total Score	Trial 1	Trial 2	Trial 3	Trial 4	Trial 5
FA							
	Cingulum	0.338	0.254	0.569**	0.097	0.279	0.121
	Ant. Cingulum	0.106	0.196	0.591**	0.043	0.233	0.213
	Post. Cingulum	0.355	0.134	0.102	0.093	0.125	0.094
MD							
	Cingulum	0.566**	0.373	0.548	0.365	0.564	0.488
	Ant. Cingulum	0.415	0.367	0.486	0.226	0.294	0.218
	Post. Cingulum	0.470	0.236	0.388	0.335	0.560**	0.513
AD							
	Cingulum	0.300	0.175	0.072	0.301	0.403	0.435
	Ant. Cingulum	0.078	0.065	0.304	0.082	0.032	0.108
	Post. Cingulum	0.543**	0.203	0.425	0.379	0.653**	0.782**
RD							
	Cingulum	0.486	0.306	0.609**	0.188	0.469	0.380
	Ant. Cingulum	0.395	0.240	0.595**	0.060	0.322	0.339
	Post. Cingulum	0.294	0.194	0.259	0.216	0.348	0.196

**p< .050 for significant values;
*.050 < p < 0.10 for near significant values

Note: ROI: region of interest; FA: fractional anisotropy; MD: mean diffusivity; AD: axial diffusivity; RD: radial diffusivity; Post. Cingulum: Posterior Cingulum; Ant. Cingulum: anterior cingulum; WM: white matter

Table 16A. Bivariate Correlations in Cortico-cortico Tracts with California Verbal Learning Test-Second Edition Scores for Amnestic Mild Cognitive Impairment Cases

Hemisphere	ROI	Total Score	Trial 1	Trial 2	Trial 3	Trial 4	Trial 5
	bCC	0.159	0.060	0.165	0.151	0.407	0.065
Right	bCC	0.111	0.325	0.040	0.160	0.375	0.102
Left	bCC	0.156	0.085	0.202	0.121	0.355	0.139
	gCC	0.129	0.110	0.362	0.058	0.116	0.108
	sCC	0.208	0.078	0.313	0.243	0.076	0.215
	ACR	0.437	0.325	0.300	0.577**	0.593**	0.415
Right	ACR	0.477	0.229	0.327	0.554**	0.646**	0.455
Left	ACR	0.256	0.320	0.178	0.417	0.351	0.243
	CST	0.271	0.151	0.030	0.273	0.270	0.391
Right	CST	0.215	0.296	0.076	0.214	0.166	0.268
Left	CST	0.277	0.028	0.023	0.282	0.326	0.443
	SLF	0.444	0.219	0.468	0.455	0.490	0.099
Right	SLF	0.141	0.148	0.310	0.163	0.252	0.067
Left	SLF	0.391	0.492	0.189	0.374	0.298	0.223
	PCR	0.162	0.252	0.146	0.258	0.242	0.150
Right	PCR	0.405	0.090	0.344	0.460	0.358	0.290
Left	PCR	0.231	0.542*	0.182	0.137	0.037	0.109

**p< .050 for significant values;

*.050 < p < 0.10 for near significant values

Note: ROI: region of interest; FA: fractional anisotropy; MD: mean diffusivity; AD: axial diffusivity; RD: radial diffusivity; bCC: body of the corpus callosum; gCC: genu of the corpus callosum; sCC: splenium of the corpus callosum; ACR: anterior segment of the corona radiata; CST: corticospinal tract; SLF: Superior Longitudinal Fasciculus; PCR: posterior segment of the corona radiata

Table 16B. Bivariate Correlations in Cortico-cortico Tracts with California Verbal Learning Test-Second Edition Scores for Amnestic Mild Cognitive Impairment Cases

Hemisphere	ROI	Total Score	Trial 1	Trial 2	Trial 3	Trial 4	Trial 5
	fMin	0.280	0.000	0.002	0.356	0.444	0.237
Right	fMin	0.272	0.030	0.056	0.362	0.398	0.322
Left	fMin	0.257	0.053	0.094	0.300	0.468	0.057
	ExCap	0.275	0.537*	0.014	0.184	0.140	0.290
Right	ExCap	0.479	0.482	0.176	0.409	0.339	0.523
Left	ExCap	0.053	0.442	0.110	0.030	0.042	0.044
	fMaj	0.404	0.310	0.216	0.431	0.381	0.246
Right	fMaj	0.286	0.371	0.059	0.316	0.201	0.195
Left	fMaj	0.468	0.214	0.339	0.488	0.506	0.264
	SS	0.376	0.278	0.238	0.439	0.608**⋆**	0.356
Right	SS	0.194	0.076	0.080	0.144	0.276	0.316
Left	SS	0.357	0.328	0.267	0.495	0.613**⋆**	0.212

**p< .050 for significant values;

*.050 < p < 0.10 for near significant values

Note: ROI: region of interest; FA: fractional anisotropy; MD: mean diffusivity; AD: axial diffusivity; RD: radial diffusivity; fMin: forceps minor; ExCap: external capsule; fMaj: forceps major; SS: sagittal stratum

Table 17A. Bivariate Correlations in Cortico-cortico Tracts with California Verbal Learning Test-Second Edition Scores for Controls

Hemisphere	ROI	Total Score	Trial 1	Trial 2	Trial 3	Trial 4	Trial 5
	bCC	0.094	0.225	0.073	0.021	0.223	0.162
Right	bCC	0.154	0.086	0.153	0.168	0.290	0.227
Left	bCC	0.027	0.312	0.013	0.117	0.123	0.074
	gCC	0.057	0.293	0.049	0.024	0.276	0.055
	sCC	0.284	0.084	0.254	0.326	0.224	0.360
	ACR	0.156	0.290	0.138	0.128	0.285	0.115
Right	ACR	0.099	0.273	0.192	0.100	0.227	0.014
Left	ACR	0.198	0.272	0.062	0.142	0.312	0.209
	CST	0.283	0.110	0.447	0.249	0.160	0.125
Right	CST	0.326	0.163	0.510*	0.145	0.233	0.218
Left	CST	0.193	0.049	0.309	0.272	0.074	0.031
	SLF	0.153	0.101	0.198	0.075	0.410	0.149
Right	SLF	0.042	0.081	0.061	0.117	0.347	0.030
Left	SLF	0.145	0.034	0.180	0.231	0.114	0.153
	PCR	0.158	0.019	0.344	0.128	0.285	0.180
Right	PCR	0.110	0.223	0.136	0.042	0.161	0.166
Left	PCR	0.138	0.198	0.381	0.213	0.279	0.127

**p< .050 for significant values;

*.050 < p < 0.10 for near significant values

Note: ROI: region of interest; FA: fractional anisotropy; MD: mean diffusivity; AD: axial diffusivity; RD: radial diffusivity; bCC: body of the corpus callosum; gCC: genu of the corpus callosum; sCC: splenium of the corpus callosum; ACR: anterior segment of the corona radiata; CST: corticospinal tract; SLF: Superior Longitudinal Fasciculus; PCR: posterior segment of the corona radiate

Table 17B. Bivariate Correlations in Cortico-cortico Tracts with California Verbal Learning Test-Second Edition Scores for Controls

Hemisphere	ROI	Total Score	Trial 1	Trial 2	Trial 3	Trial 4	Trial 5
	fMin	0.153	0.060	0.267	0.047	0.006	0.243
Right	fMin	0.365	0.221	0.477	0.193	0.154	0.440
Left	fMin	0.099	0.118	0.009	0.114	0.147	0.014
	ExCap	0.691**	0.488	0.511*	0.563**	0.754**	0.584**
Right	ExCap	0.556**	0.384	0.480	0. 409	0.629	0.394
Left	ExCap	0.608**	0.436	0.403	0.525**	0.649**	0.565**
	fMaj	0.206	0.049	0.163	0.054	0.398	0.482
Right	fMaj	0.092	0.106	0.059	0.057	0.251	0.426
Left	fMaj	0.253	0.004	0.209	0.127	0.431	0.430
	SS	0.560**	0.539	0.296	0.498	0.583	0.393
Right	SS	0.401	0.511*	0.290	0.219	0.209	0.333
Left	SS	0.461	0.372	0.199	0.487*	0.598**	0.294

**p< .050 for significant values;

*.050 < p < 0.10 for near significant values

Note: ROI: region of interest; FA: fractional anisotropy; MD: mean diffusivity; AD: axial diffusivity; RD: radial diffusivity. fMin: forceps minor; ExCap: external capsule; fMaj: forceps major; SS: sagittal stratum

REFERENCES

Acosta-Cabronero, J., Williams, G. B., Pengas, G., Nestor, P. J. (2010). Absolute diffusivities define the landscape of white matter degeneration in Alzheimer's disease. *Brain, 133*, 529-539.

Albert, M. S., DeKosky, S. T., Dickson, D., Dubois, B., Feldman, H. H., Fox, N. C., . . . Petersen, R. C. (2011). The diagnosis of mild cognitive impairment due to Alzheimer's disease: Recommendations from the National Institute on Aging-Alzheimer's Association workgroups on diagnostic guidelines for Alzheimer's disease. *Alzheimer's and Dementia, 7*(3), 270-279.

Albert, M. S., Moss, M. B., Tanzi, R., & Jones, K. (2001). Preclinical prediction of AD using neuropsychological tests. *Journal of the International Neuropsychological Society, 7*, 631-639.

Alexander, A. L., Lee, J. E., Lazar, M., & Field, A. S. (2007). Diffusion tensor imaging of the brain. *Neurotherapeutics, 4*(3), 316-329.

American Psychiatric Association. (2000). *Diagnostic and statistical manual of mental disorders: DSM-IV-TR*: American Psychiatric Publishing, Inc.

Anstey, K. J., von Sanden, C., Salim, A., & O'Kearney, R. (2007). Smoking as a risk factor for dementia and cognitive decline: a meta-analysis of prospective studies. *American Journal of Epidemiology, 166*(4), 367-378.

Arrighi, H. M., Neumann, P. J., Lieberburg, I. M., & Townsend, R. J. (2010). Lethality of Alzheimer disease and its impact on nursing home placement. *Alzheimer Disease & Associated Disorders, 24*(1), 90-95.

Barnes, L. L., Wilson, R. S., Bienias, J. L., Schneider, J. A., Evans, D. A., & Bennett, D. A. (2005). Sex Differences in the Clinical Manifestations of Alzheimer Disease Pathology. *Archives of General Psychiatry, 62*(6), 685-691.

Bartzokis, G. (2011). Alzheimer's disease as homeostatic responses to age-related myelin breakdown. *Neurobiology of Aging, 32*, 1341-1371.

Bennet, R. E., MacDonald, C. L., & Brody, D. L. (2012). Diffusion tensor imaging detects axonal injury in a mouse model of repetitive closed-skull traumatic brain injury. *Neuroscience Letters, 513*(2), 160-165.

Bosch, B., Arenaza-Urquijo, E. M., Rami, L., Sala-Llonch, R., Junqué, C., Padullésa, C., … Bartrés-Faz, D. (2012). Multiple DTI index analysis in normal aging, amnestic MCI and AD. Relationship with neuropsychological performance. *Neurobiology of Aging, 33*, 61-74.

Boska, M. D., Hasan, K. M., Kibuule, D., Banerjee, R., McIntyre, E., Nelson, J. A., … Mosley, R. L. (2007). Quantitative diffusion tensor imaging detects dopaminergic neuronal degeneration in a murine model of Parkinson's disease. *Neurobiology of Disease, 26*(3), 590-596.

Bozzali, M., Falini, A., Franceschi, M., Cercignani, M., Zuffi, M., Scotti, G., … Filippi, M. (2002). White matter damage in Alzheimer's disease assessed in vivo using diffusion tensor magnetic resonance imaging. *Journal of Neurology, Neurosurgery and Psychiatry, 72*, 742-746.

Bronge, L., Bogdanovic, N., & Wahalund, L. O. (2002). Postmortem MRI and histopathology of white matter changes in Alzheimer brains: A quantitative, comparative study. *Dementia and Geriatric Cognitive Disorders, 13*, 205-212.

Brun, A., & Englund, E. (1986). A white matter disorder in dementia of the Alzheimer type: A pathoanatomical study. *Annals of Neurology, 19*, 253-262.

Bynum, J. (2009). Characteristics, Costs and Health Service Use for Medicare Beneficiaries with a Dementia Diagnosis: Report 1: Medicare Current Beneficiary Survey. Dartmouth Institute for Health Policy and Clinical Care, Center for Health Policy Research.

Chen, T., Chen, Y., Cheng, T., Hua, M. Liu, H., & Chiu, M. (2009). Executive dysfunction and periventricular diffusion tensor changes in amnesic mild cognitive impairment and early Alzheimer's disease. *Human Brain Mapping, 30*, 3826-3836.

Chin, A. L., Negash, S., & Hamilton, R. (2011). Diversity and disparity in dementia: The impact of ethnoracial differences in Alzheimer's disease. *Alzheimer Disease and Associated Disorders, 25*(3), 187.

Ching, A. S. C., Kuhnast, B., Damont, A., Roeda, D., Tavitian, B., & Dollé, F. (2012). Current paradigm of the 18-kDa translocator protein (TSPO) as a molecular target for PET imaging in neuroinflammation and neurodegenerative diseases. *Insights Imaging, 3*(1), 111-119.

Corona Radiata. *Merriam-Webster*. Retrieved from http://www.merriam-webster.com/medical/corona%2520radiata.

de Leon, M. J., la Regina, M. E., Ferris, S. H., Gentes, C. I., & Miller, J. D. (1986). Reduced incidence of left-handedness in clinically diagnosed dementia of the Alzheimer type. *Neurobiology of Aging, 7*, 161-164.

Delano-Wood, L., Stricker, N. H., Sorg, S. F., Nation, D. A., Jak, A. J., Woods, S. P., … Boni, M. W. (2012). Posterior cingulum white matter disruption and its associations with verbal memory and stroke risk in mild cognitive impairment. *Journal of Alzheimer's Disease, 29*(3), 589-603.

Delis, D.C., Kramer, J.H., Kaplan, E., & Ober, B.A. (2000). California Verbal Learning Test: Second Edition. San Antonio, TX: Psychological Corporation.

Derflinger, S., Sorg, C., Gaser, C., Myers, N., Arsic, M., Kurz, A., … M¨uhlau, M. (2011). Grey-Matter atrophy in Alzheimer's disease is asymmetric but not lateralized. *Journal of Alzheimer's Disease, 25*, 347-357.

Duffy, S. L., Paradise, M., Hickie, I. B., Lewis, S. J. G., Naismith, S. L., Lagopoulos, J. (2014). Cognitive impairment with and without depression history: An analysis of white matter microstructure. *Journal of Psychiatry and Neuroscience, 39*(2), 135-43.

Echa´varri, C., Aalten, P., Uylings, H. B. M., Jacobs , H. I. L., Visser, P. J., Gronenschild, E. H. B. M., … Burgmans, S. (2011). Atrophy in the parahippocampal gyrus as an early biomarker of Alzheimer's disease. *Brain Structure and Function, 215*, 265-271.

Eikelenboom, P., Hoozemans, J. J., Veerhuis, R., van Exel, E., Rozemuller, A. J., van Gool, W. A. (2012). Whether, when and how chronic inflammation increases the risk of developing late onset Alzheimer's disease. *Alzheimer's Research and Therapy, 4*(3), 15.

Erkinjuntti, T., Hokkanen, L., Sulkava, R., & Palo, J. (1988). The blessed dementia scale as a screening test for dementia. *International Journal of Geriatric Psychiatry, 3*(4), 267-273.

Fellgiebel, A., M¨uller, M. J., Wille, P., Dellani, P. R., Scheurich, A., Schmidt, L. G., & Stoeter, P. (2005). Color-coded diffusion-tensor-imaging of posterior cingulate fiber tracts in mild cognitive impairment. *Neurobiology of Aging, 26*, 1193-1198.

Fellgiebel, A., & Yakushev, I. (2011). Diffusion tensor imaging of the hippocampus in MCI and early Alzheimer's disease. *Journal of Alzheimer's Disease, 26*, 257-262.

Fields, R. D. (2009). *The Other Brain*. New York, NY: Simon & Schuster.

Filippi, M., & Agosta, F. (2011). Structural and functional network connectivity breakdown in Alzheimer's disease studied with magnetic resonance imaging techniques. *Journal of Alzheimer's Disease, 24*, 455-474.

Folstein, M. F., Folstein, S. E., & McHugh, P. R. (1975). Mini-mental state: A practical method for grading the cognitive state of patients for the clinician. *Journal of Psychiatric Research, 12*(3), 189-198.

Fratiglioni, L., Ahlbom, A., Viitanen, M., & Winblad, B. (1993). Risk factors for late-onset Alzheimer's disease: A population-based, case-control study. *Annals of Neurology, 33*(3), 258-266.

Ganguli, M., Snitz, B. E., Saxton, J. A., Chang, C.-C. H., Lee, C.-W., Vander Bilt, J., . . . Petersen, R. C. (2011). Outcomes of mild cognitive impairment by definition: A population study. *Archives of Neurology, 68*(6), 761.

Gemma, C., Bachstetter, A. D., & Bickford, P. C. (2010). Neuron-microglia dialogue and hippocampal neurogenesis in the aged brain. *Aging and disease, 1*(3), 232.

Gold, B. T., Johnson, N. F., Powell, D. K., & Smith, C. D. (2012). White matter integrity and vulnerability to Alzheimer's disease: Preliminary findings and future directions. *Biochimica et Biophysica Acta (BBA)-Molecular Basis of Disease, 1822*(3), 416-422.

Green, R. C., Cupples, L. A., Go, R., Benke, K. S., Edeki, T., Griffith, P. A., . . . Bachman, D. (2002). Risk of dementia among white and African American relatives of patients with Alzheimer disease. *The Journal of the American Medical Association, 287*(3), 329-336.

Green, P. S., Gridley, K. E., & Simpkins, J. W. (1996). Estradiol protects against β-amyloid (25–35)-induced toxicity in SK-N-SH human neuroblastoma cells. *Neuroscience Letters, 218*(3), 165-168.

Greenaway, M. C., Lacritz, L. H., Binegar, D., Weiner, M. F., Lipton, A., & Munro, C. C. (2006). Patterns of verbal memory performance in mild cognitive impairment, Alzheimer disease, and normal aging. *Cognitive and Behavioral Neurology, 19*(2), 79-84.

Griffin, W., Sheng, J., Royston, M., Gentleman, S., McKenzie, J., Graham, D., . . . Mrak, R. (1998). Glial-neuronal interactions in Alzheimer's disease: The potential role of a ‘cytokine cycle’ in disease progression. *Brain Pathology, 8*(1), 65-72.

Gurland, B. J., Wilder, D. E., Lantigua, R., Stern, Y., Chen, J., Killeffer, E. H., & Mayeux, R. (1999). Rates of dementia in three ethnoracial groups. *International Journal of Geriatric Psychiatry, 14*(6), 481-493.

Hajnal, J. V., Bryant, D. J., Kasuboski, L., Pattany, P. M., De Coene, B., Lewis, P. D., … Bydder, G. M. (1992). Use of fluid attenuated inversion recovery (FLAIR) pulse sequences in MRI of the brain. *Journal of Computer Assisted Tomography, 16*(6), 841-844.

Hampel, H., Burger, K., Teipel, S. J., Bokde, A. L., Zetterberg, H., & Blennow, K. (2008). Core candidate neurochemical and imaging biomarkers of Alzheimer's disease. *Alzheimer''s and Dementia, 4*(1), 38.

Hänninen, T., Hallikainen, M., Tuomainen, S., Vanhanen, M., & Soininen, H. (2002). Prevalence of mild cognitive impairment: A population-based study in elderly subjects. *Acta Neurologica Scandinavica, 106*(3), 148-154.

Hashemi, R. H., Bradley, W. G., & Lisanti, C. J. (2010). *MRI: The Basics* (3rd ed.). Philadelphia, PA: Lippincott Williams & Wilkins.

Hebert, L. E., Scherr, P. A., Bienias, J. L., Bennett, D. A., & Evans, D. A. (2003). Alzheimer disease in the US population: Prevalence estimates using the 2000 census. *Archives of Neurology, 60*(8), 1119.

Hebert, L. E., Scherr, P. A., McCann, J. J., Beckett, L. A., & Evans, D. A. (2001). Is the risk of developing Alzheimer's disease greater for women than for men? *American journal of Epidemiology, 153*(2), 132-136.

Hendrie, H. C., Albert, M. S., Butters, M. A., Gao, S., Knopman, D. S., Launer, L. J., . . . Wagster, M. V. (2006). The NIH cognitive and emotional health project: Report of the Critical Evaluation Study Committee. *Alzheimer's and Dementia, 2*(1), 12-32.

Hermoye, L., Wakana, S., Laurent, J., Jiang, H., Cosnard, G., Van Zigl, P., & Mori, S. *White Matter Atlas*. Retrieved from http://www.dtiatlas.org/.

Jack, C. R., Albert, M. S., Knopman, D. S., McKhann, G. M., Sperling, R. A., Carrillo, M. C., . . . Phelps, C. H. (2011). Introduction to the recommendations from the National Institute on Aging-Alzheimer's Association workgroups on diagnostic guidelines for Alzheimer's disease. *Alzheimer's and Dementia, 7*(3), 257-262.

Jellisona, B., J., Fielda, A. S., Medowb, J., Lazarc, M., Salamatd, M. S., & Alexander, A. L. (2004). Diffusion tensor imaging of cerebral white matter: A pictorial review of physics, fiber tract anatomy, and tumor imaging patterns. *American Journal of Neuroradiology, 25*, 356-369.

Jones, D. K., Horsfield, M. A., & Simmons, A. (1999). Optimal strategies for measuring diffusion in anisotropic systems by magnetic resonance imaging. *Magnetic Resonance in Medicine, 42*, 515-525.

Kohman, R. A., & Rhodes, J. S. (2012). Neurogenesis, inflammation and behavior. *Brain, Behavior, And Immunity*, *27*(1), 22-32.

Kukull, W. A., Higdon, R., Bowen, J. D., McCormick, W. C., Teri, L., Schellenberg, G. D., . . . Larson, E. B. (2002). Dementia and Alzheimer disease incidence: A prospective cohort study. *Archives of Neurology, 59*(11), 1737.

Lautenschlager, N., Cupples, L., Rao, V., Auerbach, S., Becker, R., Burke, J., . . . Glatt, S. (1996). Risk of dementia among relatives of Alzheimer's disease patients in the MIRAGE study What is in store for the oldest old? *Neurology, 46*(3), 641-650.

Lee, Y. J., Han, S. B., Nam. S., Oh, K. W., & Hong, J. T. (2010). Inflammation and Alzheimer's Disease. *Archives of Pharmacal Research, 33*(10), 1539-56.

Little, D. M., & Holloway, R. G. (2007). Diffusion tensor imaging Scientific advance, clinical tool, or just a pretty picture? *Neurology, 68*(1), 9-10. Lopez, O. L., Jagust, W. J., DeKosky, S. T., Becker, J. T., Fitzpatrick, A., Dulberg, C., . . . Kawas, C. (2003). Prevalence and classification of mild cognitive impairment in the Cardiovascular Health Study Cognition Study: part 1. *Archives of Neurology, 60*(10), 1385.

Liu, J., Yin, C., Xia, S., Jia, L., Guo, Y., Zhao, Z., … Jia, J. (2013) White matter changes in patients with amnestic mild cognitive impairment detected by diffusion tensor imaging. *PLoS ONE, 8(*3), e59440.

Loewenstein, D. A., Barker, W. W., Chang, J. Y., Apicella, A., Yoshii, F. Kothari, P. … Daura, R. (1989). Predominant left hemisphere metabolic dysfunction in dementia. *Archives of Neurology, 46*(2), 146-152.

Lopez, O. L., Jagust, W. J., DeKosky, S. T., Becker, J. T., Fitzpatrick, A., Dulberg, C., … Kawas, C. (2003). Prevalence and classification of mild cognitive impairment in the Cardiovascular Health Study Cognition Study: Part 1. *Archives of Neurology, 60*(10), 1385.

Lye, T. C., & Shores, E. A. (2000). Traumatic brain injury as a risk factor for Alzheimer's disease: a review. *Neuropsychology Review, 10*(2), 115-129.

Madden, D. J., Bennett, I. J., Burzynska, A., Potter, G. G., Chen, N.-k., & Song, A. W. (2012). Diffusion tensor imaging of cerebral white matter integrity in cognitive aging. *Biochimica et Biophysica Acta (BBA)-Molecular Basis of Disease, 1822*(3), 386-400.

Maguire, E. A. (2001). Neuroimaging studies of autobiographical event memory. *Philosophical Transactions of the Royal Society B: Biological Sciences, 356*, 1441-1451.

Maslow, K. (2006). Early-onset dementia: A national challenge, a future crisis: Washington, DC: Alzheimer's Association.

Mayeux, R., Sano, M., Chen, J., Tatemichi, T., & Stern, Y. (1991). Risk of dementia in first-degree relatives of patients with Alzheimer's disease and related disorders. *Archives of Neurology, 48*(3), 269.

McDowell, I., Xi, G., Lindsay, J., & Tierney, M. (2007). Mapping the connections between education and dementia. *Journal of Clinical and Experimental Neuropsychology, 29*(2), 127-141.

McGleenon, B., Dynan, K., & Passmore, A. (1999). Acetylcholinesterase inhibitors in Alzheimer's disease. *British Journal of Clinical Pharmacology, 48,* 471-480.

McKhann, G., Drachman, D., Folstein, M., Katzman, R., Price, D., & Stadlan, E. M. (1984). Clinical diagnosis of Alzheimer's disease Report of the NINCDS-ADRDA Work Group under the auspices of Department of Health and Human Services Task Force on Alzheimer's Disease. *Neurology, 34*(7), 939-939.

McKhann, G. M., Knopman, D. S., Chertkow, H., Hyman, B. T., Jack, C. R., Kawas, C. H., . . . Mayeux, R. (2011). The diagnosis of dementia due to Alzheimer's disease: Recommendations from the National Institute on Aging-Alzheimer's Association workgroups on diagnostic guidelines for Alzheimer's disease. *Alzheimer's and Dementia, 7*(3), 263-269.

Medina, D., DeToledo-Morrell, L., Urresta, F., Gabrieli, J. D. E., Moseley, M., Fleischman, D., … Stebbins, G. T. (2006).White matter changes in mild cognitive impairment and AD: A diffusion tensor imaging study. *Neurobiology of Aging, 27,* 663-672.

Meyer, U. (2013). Developmental neuroinflammation and schizophrenia. *Progress in Neuro-psychopharmacology and Biological Psychiatry, 42,* 20-34.

Minghetti, L. (2005). Role of inflammation in neurodegenerative diseases. *Current Opinion in Neurology, 18,* 315-321.

Miniño, A., Xu, J., & Kochanek, K. (2010). Deaths: preliminary data for 2008. *National Vital Statics Report, 59*.

O'Dwyer, L., Lamberton, F., Bokde, A. L. W., Ewers, M., Faluyi, Y. O., Tanner, C., … Hampel, H. (2011). Multiple indices of diffusion identifies white matter damage in mild cognitive impairment and Alzheimer's disease. *PLoS ONE, 6*(6), e21745.

Parente, D. B., Gasparetto, E. L., Hygino da Cruz, L. C., Domingues, R. C., Baptista, A. C., Carvalho, A. C. P., & Domingues, R. C. (2008). Potential role of diffusion tensor MRI in the differential diagnosis of mild cognitive impairment and Alzheimer's disease. *American Journal of Roentgenology, 190*, 1369-1374.

Parsons, C. G., Stoffler, A., & Danysz, W. (2007). Memantine: A NMDA receptor antagonist that improves memory by restoration of homeostasis in the glutamatergic system - too little activation is bad, too much is even worse. *Neuropharmacology, 53*, 699-723.

Pendlebury, S. T., & Rothwell, P. M. (2009). Prevalence, incidence, and factors associated with pre-stroke and post-stroke dementia: A systematic review and meta-analysis. *The Lancet Neurology, 8*(11), 1006-1018.

Petersen, R. C., Smith, G. E., Waring, S. C., Ivnik, R. J., Tangalos, E. G., & Kokmen, E. (1999). Mild cognitive impairment: Clinical characterization and outcome. *Archives of Neurology, 56*(3), 303.

Plassman, B. L., Langa, K. M., Fisher, G. G., Heeringa, S. G., Weir, D. R., Ofstedal, M. B., . . . Rodgers, W. L. (2007). Prevalence of dementia in the United States: The aging, demographics, and memory study. *Neuroepidemiology, 29*(1-2), 125-132.

Plassman, B. L., Havlik, R., Steffens, D., Helms, M., Newman, T., Drosdick, D., . . . Burke, J. (2000). Documented head injury in early adulthood and risk of Alzheimer's disease and other dementias. *Neurology, 55*(8), 1158-1166.

Pooley, R. A. (2005). Fundamental physics of MR imaging. *Radiographics, 25*(4), 1087-1099.

Portet, F., Ousset, P. J., Visser, P. J., Frisoni, G. B., Nobili, F., Scheltens, Ph., …the MCI Working Group of the European Consortium on Alzheimer's Disease (EADC). (2006). Mild cognitive impairment (MCI) in medical practice: A critical review of the concept and new diagnostic procedure. Report of the MCI Working Group of the European Consortium on Alzheimer's Disease. *Journal of Neurology, Neurosurgery and Psychiatry, 77*, 714-718.

Potter, G. G., Plassman, B. L., Burke, J. R., Kabeto, M. U., Langa, K. M., Llewellyn, D. J., . . . Steffens, D. C. (2009). Cognitive performance and informant reports in the diagnosis of cognitive impairment and dementia in African Americans and whites. *Alzheimer's & Dementia: the Journal of the Alzheimer's Association, 5*(6), 445-453.

Poustchi-Amin, M., Mirowitz, S. A., Brown, J. J., McKinstry, R. C., & Li, T. (2001). Principles and applications of echo-planar imaging: A review for the general radiologist. *Radio Graphics, 21*(3), 767-779.

Reisberg, B., Franssen, E. H., Souren, L., Auer, S. R., Akram, I., & Kenowsky, S. (2002). Evidence and mechanisms of retrogenesis in Alzheimer's and other dementias: Management and treatment import. *American Journal of Alzheimer's Disease and Other Dementias, 17*, 202-212.

Raji, C. A., Ho, A. J., Parikshak, N. N., Becker, J. T., Lopez, O. L., Kuller, L. H., . . . Thompson, P. M. (2010). Brain structure and obesity. *Human Brain Mapping, 31*(3), 353-364.

Roe, C. M., Xiong, C., Miller, J. P., & Morris, J. C. (2007). Education and Alzheimer disease without dementia support for the cognitive reserve hypothesis. *Neurology, 68*(3), 223-228.

Rose, S. E., Chen, F., Chalk, J. B., Zelaya, F. O., Strugnell, W. E., Benson, M., … Doddrell, D. M. (2000). Loss of connectivity in Alzheimer's disease: An evaluation of white matter tract integrity with colour coded MR diffusion tensor imaging. *Journal of Neurology, Neurosurgery and Psychiatry, 69*(4), 528-530.

Rowe, D., Jacobson, K. C., & van den Oord, E. J. G. (1999). Genetic and environmental influences on vocabulary IQ: Parental education level as moderator. *Child Development, 70*(5), 1151-1162

Ruest, T., Holmes, W. M., Barrie, J. A., Griffiths, I. R., Anderson, T. J., Dewar, D., & Edgar, J. M. (2011). High-resolution diffusion tensor imaging of fixed brain in a mouse model of Pelizaeus–Merzbacher disease: comparison with quantitative measures of white matter pathology. *NMR in Biomedicine, 24*(10), 1369-1379.

Salat, D. H., Tuch, D. S., van der Kouwe, A. J. W., Greve, D, N., Pappu, V., Lee, S. Y., … Rosas, H. D. (2010). White matter pathology isolates the hippocampal formation in Alzheimer's disease. *Neurobiology of Aging, 31*, 244-256.

Sämann, P. G., Schlegel, J., Müller, G., Prantl, F., Emminger, C., & Auer, D. P. (2003). Serial proton MR spectroscopy and diffusion imaging findings in HIV-related herpes simplex encephalitis. *American Journal of Neuroradiology, 24,* 2015–2019.

Schulze, E. T., Geary, E. K., Susmaras, T. M., Paliga, J. T., Maki, P. M., & Little, D. M. (2011). Anatomical correlates of age-related working memory declines. *Journal of Aging Research, 2011*.

Seeley, W. W., Crawford, R. K., Zhou, J., Miller, B. L., Greicius, M. D. (2009). Neurodegenerative diseases target large-scale human brain networks. *Neuron, 62*, 42-52.

Seshadri, S., Wolf, P., Beiser, A., Au, R., McNulty, K., White, R., & D'agostino, R. (1997). Lifetime risk of dementia and Alzheimer's disease. The impact of mortality on risk estimates in the Framingham Study. *Neurology, 49*(6), 1498-1504.

Silverstein, N. M., & Maslow, K. (Eds.). (2006). Improving hospital care for persons with dementia. New York: Springer Publishing Company, Inc.

Siger, M., Schuff, N., Zhu, X., Miller, B. L., & Weiner, M. W. (2009). Regional Myo-inositol Concentration in Mild Cognitive Impairment Using 1H Magnetic Resonance Spectroscopic Imaging. *Alzheimer Disease and Associated Disorders, 23*(1), 57-62.

Solomon, A., Kivipelto, M., Wolozin, B., Zhou, J., & Whitmer, R. A. (2009). Midlife serum cholesterol and increased risk of Alzheimer's and vascular dementia three decades later. *Dementia and Geriatric Cognitive Disorders, 28*(1), 75-80.

Song, S., Sun, S., Ju, S., Lin, S., Cross, A. H., & Neufeld, A. H. (2003). Diffusion tensor imaging detects and differentiates axon and myelin degeneration in mouse optic nerve after retinal ischemia. *NeuroImage, 20*, 1714-1722.

Sperling, R. A., Aisen, P. S., Beckett, L. A., Bennett, D. A., Craft, S., Fagan, A. M., . . . Montine, T. J. (2011). Toward defining the preclinical stages of Alzheimer's disease: Recommendations from the National Institute on Aging-Alzheimer's Association workgroups on diagnostic guidelines for Alzheimer's disease. *Alzheimer's and Dementia, 7*(3), 280-292.

Stenset, V., Bjørnerud, A., Fjell, A. M., Walhovd, K. B., Hofoss, D., Due-Tønnessen, P., … Fladby, T. (2011). Cingulum fiber diffusivity and CSF T-tau in patients with subjective and mild cognitive impairment. *Neurobiology of Aging, 32*, 581-589.

Stern, Y. (2006). Cognitive reserve and Alzheimer disease. *Alzheimer Disease & Associated Disorders, 20*(2), 112-117.

Stricker, N. H., Schweinsburg, B. C., Delano-Wood, L., Wierenga, C. E., Bangen, K. J., Haaland, K, Y., … Bondi, M. W. (2009). Decreased white matter integrity in late-myelinating fiber pathways in Alzheimer's disease supports retrogenesis. *Neuroimage 45*(1), 10-16.

Sun, S., Liang, H., Cross, A. C., & Song, S. (2008). Evolving Wallerian degeneration after transient retinal ischemia in mice characterized by diffusion tensor imaging. *Neuroimage, 40*(1), 1-10.

Sun, S., Liang, H., Le, T. Q., Armstrong, R. C., Cross, A. C., & Song, S. (2006). Differential sensitivity of in vivo and ex vivo diffusion tensor imaging to evolving optic nerve injury in mice with retinal ischemia. *Neuroimage, 32*, 1195-1204.

Sun, S., Liang, H., Schmidt, R. E., Cross, A. C., & Song, S. (2007). Selective vulnerability of cerebral white matter in a murine model of multiple sclerosis detected using diffusion tensor imaging. *Neurobiology of Disease, 28*(1), 30-38.

Sun, S., Song, S. Harms, M. P., Lin, A., Holtzman, D., Merchant, K. M., & Kotyk, J. J. (2005). Detection of age-dependent brain injury in a mouse model of brain amyloidosis associated with Alzheimer's disease using magnetic resonance diffusion tensor imaging. *Neuroimage, 191*(1), 77-85.

Takahashi, S., Yonezawa, H., Takahashi, J., Kudo, M., Inoue, T., & Tohgi, H. (2002). Selective reduction of diffusion anisotropy in white matter of Alzheimer disease brains measured by 3.0 Tesla magnetic resonance imaging. *Neuroscience Letters, 332*(1), 45-48.

Thillainadesan, S., Wen, W., Zhuang, L., Crawford, J., Kochan, N., Reppermund, S., … Sachdev, P. (2012). Changes in mild cognitive impairment and its subtypes as seen on diffusion tensor imaging. *International Psychogeriatric, 24*(9), 1483-93.

Thompson, P. M., Hayashi, K. M., Zubicaray, G., Janke, A. L., Rose, S. E., Semple, J., … Toga, A. W. (2003). Dynamics of gray matter loss in Alzheimer's disease. *The Journal of Neuroscience, 23*(3), 994-1005.

Thompson, P. M., Mega, M. S., Woods, R. P., Zoumalan, C. I., Lindshield, C. J., Blanton, R. E., … Toga, A. W. (2001). Cortical change in Alzheimer's disease detected with a disease-specific population-based brain atlas. *Cerebral Cortex, 11*(1), 1-16.

Tyszka, J. M., Readhead, C., Bearer, E. L., Pautler, R. G., & Jacobs, R. E. (2006). Statistical diffusion tensor histology reveals regional dysmyelination effects in the shiverer mouse mutant. *NeuroImage, 29*(4), 1058-1065.

Wang, Y., West, J. D., Flashman, L. A., Wishart, H. A., Santulli, R. B., Rabin, L. A., . . . Saykin, A. J. (2012). Selective changes in white matter integrity in MCI and older adults with cognitive complaints. *Biochimica et Biophysica Acta (BBA)-Molecular Basis of Disease, 1822*(3), 423-430.

Westerhausen, R., Kreuder, F., Dos Santos Sequeira, S., Walter, C., Woerner, W., Wittling, R. A., … Wittling, W. (2004). Effects of handedness and gender on macro- and microstructure of the corpus callosum and its subregions: A combined high-resolution and diffusion-tensor MRI study. *Cognitive Brain Research, 21*(3), 418-426.

What is the Cingulum? Retrieved from http://www.wisegeek.com/what-is-the-cingulum.htm.

What is the External Capsule? Retrieved from http://www.wisegeek.com/what-is-the-external-capsule.htm.

Wilson, R. S., Weir, D. R., Leurgans, S. E., Evans, D. A., Hebert, L. E., Langa, K. M., … Bennett, D. A. (2011). Sources of variability in estimates of the prevalence of Alzheimer's disease in the United States. *Alzheimer's and Dementia, 7*(1), 74-79.

Yaffe, K., Lindquist, K., Schwartz, A., Vitartas, C., Vittinghoff, E., Satterfield, S., . . . Cauley, J. (2011). Advanced glycation end product level, diabetes, and accelerated cognitive aging. *Neurology, 77*(14), 1351-1356.

Żekanowski, C., Styczyńska, M., Pepłońska, B., Gabryelewicz, T., Religa, D., Ilkowski, J., . . . Pfeffer, A. (2003). Mutations in presenilin 1, presenilin 2 and amyloid precursor protein genes in patients with early-onset Alzheimer's disease in Poland. *Experimental neurology, 184*(2), 991-996.

Zhang, Y., Du, A. T., Hayasaka, S., Jahng, G. H., Hlavin, J., Zhan, W., … Schuff, N. (2008). Patterns of age-related water diffusion changes in human brain by concordance and discordance analysis. *Neurobiology of Aging, 31*(11), 1991-2001.

Zhang, Y., Schuff, N., Camacho, M., Chao, L. L., Fletcher, T. P. Yaffe, K., … Weiner, W. (2013). MRI markers for mild cognitive impairment: Comparisons between white matter integrity and gray matter volume measurements. PLoS ONE, 8(6), e66367.

Zhang, Y., Schuff, N., Du, A., Rosen, H. J., Kramer, J. H., Gorno-Tempini, M. L., … Weiner, W. (2009). White matter damage in frontotemporal dementia and Alzheimer's disease measured by diffusion MRI. *Brain, 132*, 2579-2592.

Zhang, Y., Schuff, N., Jahng, G.-H., Bayne, W., Mori, S., Schad, L., . . . Yaffe, K. (2007). Diffusion tensor imaging of cingulum fibers in mild cognitive impairment and Alzheimer disease. *Neurology, 68*(1), 13-19.